



SWEPOS data quality monitoring – GNSS Signal Disturbances Detection System

Kibrom Ebuy Abraha, Anders Frisk

Mats Westberg, Peter Wiklund

2021

LANTMÄTERIET



Copyright ©

2021-09-07

Author Kibrom Ebuy Abraha, Anders Frisk, Mats Westberg, Peter Wiklund

Typography and layout Rainer Hertel

Total number of pages 93

Lantmäterirapport 2021:1 ISSN 0280-5731

This page is intentionally left blank.

Executive Summary

This report summarizes a GNSS signal disturbance detection system that has been developed as part of the daily quality monitoring of SWEPOS data. In response to the expansion of the SWEPOS network and the increased availability and number of signals from the multi-GNSS environment, and the growing threat of GNSS signal interference, a signal-to-noise ratio (SNR) based signal interference detection system has been developed. It focuses on monitoring the quality of SWEPOS data and detecting signal disturbances that may occur due to (un)intentional interference, equipment failure and multipath.

Multi-GNSS multi-frequency signal disturbances are monitored and reported. SNR is modeled for each signal and station taking into account receiver, satellite elevation, azimuth and other dependent effects. The residuals (model minus observed data) indicate any unmodeled effects and disturbances. Disturbances can be related to (un)intentional interference (e.g., jamming).

The GNSS interference detection system focuses primarily on situational awareness, where it detects and monitors signal disturbances. Detected disturbances are characterized by periods (occurrence time), frequency and power. Persistent signal disturbances are reported to the Swedish Post and Telecom Authority (PTS) for awareness and further characterization such as geolocalization.

The report briefly summarizes the detection system and presents real signal disturbance incidents that have been detected at several stations in the SWEPOS network.

Sammanfattning

Denna rapport beskriver ett system för detektering av GNSS-signalstörningar. Systemet har utvecklats för att ingå i den dagliga kvalitetsövervakningen av SWEPOS-data. Som en följd av utbyggnaden av SWEPOS-nätet, den ökade tillgängligheten och antalet signaler från alla GNSS-system och det växande hotet från GNSS-signalstörningar har ett system utvecklats, som kan detektera signalinterferens baserat på signalbrusförhållande (SNR). Systemet är tänkt att övervaka kvaliteten på SWEPOS-data och upptäcka signalstörningar som kan uppstå på grund av avsiktlig eller oavsiktlig störning, utrustningsfel och flervägsfel. Signalstörningar för alla aktuella GNSS och frekvenser övervakas och rapporteras. SNR modelleras för varje signal och station med avseende på mottagare, satellitens elevation och azimut och andra faktorer. Residualerna (modell minus observerade data) indikerar omodellerade effekter och störningar. Detekteringssystemet är främst avsett för att ge kännedom om situationen, där signalstörningar detekteras och övervakas. Upptäckta störningar kategoriseras beroende på störningens längd, frekvens och effekt. Långvariga signalstörningar rapporteras till Post- och telestyrelsen (PTS) för kännedom och ytterligare utredning, t.ex. lokalisering. Rapporten sammanfattar kort detektionssystemet och presenterar verkliga signalstörningar som har upptäckts på flera stationer i SWEPOS-nätet.

Contents

1	Introduction	2
1.1	Background	2
1.2	SWEPOS	3
1.3	SWEPOS-QC	5
1.3.1	Motivation	5
1.3.2	Goals	10
1.4	Report structure	10
2	SWEPOS Data	12
2.1	SWEPOS Rinex Data	12
2.2	Receiver types	12
2.2.1	Trimble NetR9	13
2.2.2	Trimble Alloy	14
2.2.3	Septentrio PolaRx5	14
2.2.4	Receiver performance	14
2.3	Data processing	16
2.3.1	Anubis	16
2.3.2	In-house Developed Libraries	17
3	GNSS Signal disturbance detection in SWEPOS	18
3.1	Overview	18
3.1.1	Automatic Gain Control (AGC)	19
3.1.2	Signal-to-Noise-Ratio (SNR)	19
3.1.2.1	Elevation dependency	20
3.1.2.2	Station Equipment	21
3.1.2.3	GPS Flex Power	23
3.2	Methodology	28
3.2.1	Reference window (RW) definition	29
3.2.2	Evaluation Window (EW)	29
3.2.3	Demonstration on simulated interference waves	31
4	Real signal disturbance incidents	36
4.1	RFI related disturbances	36
4.2	Equipment related disturbances	39
4.3	Station environment related disturbances	44

5	Summary	49
	References	50
A	Appendix with more figures and tables	53
A.1	More signal disturbance incidents	53
A.1.1	Östra Frölunda (TOST)	53
A.1.2	Gällivare (0GVA)	54
A.1.3	Skövde (1SKV)	57
A.1.4	Mockfjärd (0MOC)	59
A.1.5	Örkelljunga (0ORK)	63
A.1.6	Kristianstad (0KRI)	64
A.1.7	Grisslehamn (0GIS)	67
A.2	More Tables	68
A.2.1	Monitored GNSS signals and their frequencies	68
A.2.2	More signal disturbance incidents	69
A.2.3	List of SWEPOS stations	71

List of Figures

1.1	SWEPOS GNSS observation network of ground stations. More stations which are operated by Trimble are also included. See tables 1.1 and appendix A.4 for station category and list, respectively.	4
1.2	Time-series of GPS MP1, MP2, observation rate and total number of cycle slips for station 0MOL for the period 2017.5 to 2021.5.	6
1.3	Elevation-azimuth diagram for station 0MOL for the period before the event on the 14th of July (a) – 1st of June to 10th of July, and after the event (b) – 23rd of July to 31st of August, 2021. The lines indicate satellite paths while the color-code shows the multipath values for GPS L2.	8
1.4	MP2 distribution (probability density function) for periods before (green lines) and after (red lines) the 14th of July, 2020.	8
1.5	Station 0MOL and the newly installed radio mast.	9
2.1	Receiver types in use in the SWEPOS network. Red, orange and green colors indicate stations with Trimble NetR9, Trimble Alloy, and Septentrio PolaRx5 receivers, respectively.	13
2.2	Pseudorange multipath on GPS L2 (MP2, left figure) and total number of cycle slips (right figure) plotted against latitude angles of stations of the entire SWEPOS network. Colors categorize stations by their receiver types.	15
3.1	SNR for GPS L1 C/A code plotted against elevation angle of satellites. Green dots show raw data while red indicates a polynomial fit.	21
3.2	SNR for GPS L5 Q code plotted for all GPS satellites against elevation angles. Color codes show the receiver types.	22
3.3	SNR for stations 0STR (top) and 1MAL (bottom). Red vertical dotted lines indicate antenna-splitter installation dates. At the time of antenna-splitter installation both stations were equipped with Trimble NetR9 receiver and JNSCR C146-22-1 antenna.	23
3.4	SNR plotted against elevation angle of satellites for station 0ROS. Figures top to bottom show SNR for GPS L1 C/A code (GPSS1C), encrypted P(Y)-code on L1 (GPSS1W), GPS L2C (GPSS2L), encrypted P(Y)-code on L2 (GPSS2W) and L5 Q code (GPSS5Q).	25

3.5	SNR for the encrypted P(Y)-code on GPS L2 (GPSS2W) for BLOCK IIF and IIR-M (top), and BLOCK IIR-A, IIR-B and IIIA (bottom) for station OROS.	26
3.6	As in figure 3.5 but plotted against azimuth angles of the satellites.	27
3.7	Elevation-azimuth diagram of SNR for the encrypted P(Y)-code on GPS L2 (GPSS2W) for BLOCK IIF and IIR-M satellites stacked over the entire SWEPOS network of 500+ stations.	28
3.8	Flow diagram of the SNR-based GNSS disturbance detection system.	31
3.9	SNR time series for GPS L1 C/A code for station FOI1. The lower figure shows the mean value of all tracked satellites for the days of January 20-21, 2021. The upper figure shows the PRN05 GPS for January 20, 2021. Regions highlighted with dotted boxes indicate interference signals generated by the GNSS simulator conducted by FOI. The red dotted boxes indicate AWGN with a 20 MHz bandwidth, the brown dotted boxes indicate AWGN with a 2 MHz bandwidth, the orange dotted boxes show the unmodulated CW carrier, and the green dotted boxes show the frequency modulated waveform.	33
3.10	Time series of SNR residuals for GPS L1 C/A for GPS PRN05 (top) and mean from all GPS satellites (bottom).	34
3.11	A demonstration of the SNR-based GNSS signal disturbance detection system. See text for details.	35
4.1	SNR residuals for GPS L5 (top figure) and GAL L5a (middle figure) and BDS B2b (bottom figure) for station OGIS. Green dots indicate SNR residuals with no disturbances while orange and red dots indicate moderate and major disturbances, respectively.	37
4.2	A fast Fourier transform spectrum and waterfall displays sample of the interference at OGIS as recorded by software defined radio (SDR).	38
4.3	Spectrum from the Septentrio PolaRx5 receiver for the detected disturbances at OGIS on May 15, 2021.	39
4.4	Top figure shows a picture of Norrköping (ONOR) station. The station is equipped with Septentrio PolaRx5 receiver and ASH700936A_M antenna. Middle figure shows SNR for GPS L5 from all tracked satellites for April 27, 2021. Bottom figure shows elevation angles of the satellites.	40
4.5	As in figure 4.4 but for Jönköping (OJON). The station is equipped with Septentrio PolaRx5 receiver and JNSCR_C146-22-1 antenna	41

4.6	SNR residuals for GPS L1, GLO G2, GAL E5a, BDS B2b signals for station 1STV.	43
4.7	Station performance in the network-RTK system for 1STV. The blue line shows the total number of GPS, GLO and GAL satellites tracked, while the orange line shows how many have been resolved from the tracked satellites. The vertical dotted line shows the epoch when the antenna is changed from JNSCR_C146-22-1 to LEIAR20.	44
4.8	SNR residuals for GAL E6 signal for station 0TIV. The upper figure shows the residuals for the entire horizon of the station, while the lower figure shows the residuals for azimuth from 50 to 290 degrees. The different colors are as in figure 4.1.	46
4.9	Elevation-azimuth diagram of SNR for GAL E6 signal for station 0TIV. Colors show SNR values.	47
A.1	SNR residuals for GPS L1 (upper figure) and L2 (lower figure) signals for station TOST. Green dots indicate SNR residuals with no disturbances while orange and red dots indicate moderate and major disturbances, respectively.	54
A.2	SNR residuals for GPS L1 (top) and GAL E1 (bottom) signals for station 0GVA. The different colors are as in figure A.1.	55
A.3	SNR residuals for GLO G1 (top) and BDS B1-2 (bottom) signals for station 0GVA.	56
A.4	Waterfall format spectrum plot – time-versus-frequency for station 0GVA. Colors indicate the power of the signal. Figure (a) shows spectrum for the frequency range 1565 - 1615 MHz, which covers GPS L1, GAL E1 and GLO G1 frequencies. Spectrum for the frequency range 1215 - 1265 MHz, which covers GPS L2 and GLO G2 frequencies, is included in (b) for comparison.	57
A.5	SNR residuals for GPS L1 (top) and GAL E1 (bottom) signals for station 1SKV. The different colors are as in figure A.1	58
A.6	SNR residuals on GLO G1 (top) for station 1SKV. SNR residuals for BDS B1-2 (bottom) is included for comparison but hasn't been affected by the disturbances.	59
A.7	SNR residuals for GPS L2C (top) and GLO G2 (bottom) signals for station 0MOC. The different colors are as in figure A.1	60

A.8	SNR residuals for GPS L5, GAL E5a, and BDS B2a (from top to bottom, respectively) signals for station 0MOC.	61
A.9	SNR residuals for GAL E6, GAL E5b, BDS B2b, and BDS B3 (from top to bottom, respectively) signals for station 0MOC.	62
A.10	SNR residuals for GPS L5, GAL E5a, and BDS B2a (from top to bottom, respectively) signals for station 0ORK. The different colors are as in figure A.1	63
A.11	Waterfall format spectrum plot – time-versus-frequency for station 0ORK. Colors indicate the power of the signal. The figure shows spectrum for the L5 frequency band.	64
A.12	SNR residuals for GPS L1 signal for station 0KRI. The different colors are as in figure A.1.	65
A.13	Station performance in the network-RTK system for 0KRI for day 243, 2021. Dark to light magenta colors show the total number of tracked, processed and solved satellites, respectively.	65
A.14	Spectrum from the Septentrio PolaRx5 receiver a) during the interference b) when there was no interference for station 0KRI.	66
A.15	Continued figure from figure 4.1. SNR residuals for GAL E5b (top) and GAL E5a + E5b signals for station 0GIS.	67

List of Tables

1.1	Catagories of stations in figure 1.1. The network RTK, class A and monitoring categories of stations are owned and operated by SWEPOS. See Appendix Table A.4 for a complete list and more information.	5
A.1	GNSS signals and frequencies monitored by the SWEPOS disturbance detection system.	68
A.2	Real signal disturbance incidents detected at SWEPOS stations. The reported disturbances are for the period doy 103, 2021 to the time of writing the report.	69
A.3	Table A.2 continued	70
A.4	List of SWEPOS stations (see map in Figure 1.1). Twenty-three more stations in Sweden which are owned by Trimble are also included.	71
A.5	Table A.4 continued	72
A.6	Table A.4 continued	73
A.7	Table A.4 continued	74
A.8	Table A.4 continued	75
A.9	Table A.4 continued	76
A.10	Table A.4 continued	77
A.11	Table A.4 continued	78
A.12	Table A.4 continued	79
A.13	Table A.4 continued	80
A.14	Table A.4 continued	81

Chapter 1

Introduction

1.1 Background

The day-to-day activities of our society are highly linked to the use of Global Navigation Satellite Systems (GNSS). It is unthinkable to find yourself in a situation where GNSS positioning systems would not work. The US Global Positioning System (GPS), the first GNSS that revolutionized the technology-driven society, the Russian Global'naya Navigatsionnaya Sputnikovaya Sistema (GLONASS – GLO), now fully operational, the almost complete European GNSS (Galileo – GAL) and the Chinese BeiDou System (BDS) bring an era of multi-GNSS. As most of these systems have already matured, the dependency on a single system will decrease. The use of multiple GNSS provides diversity and redundancy which, in turn, offers significant improvements for many applications.

A geodetic infrastructure like the Continuously Operating Reference Stations (CORS) is fundamentally important to greatly benefit the GNSS dependent society. CORS networks provide GNSS data that support a wide range of applications, such as real-time positioning, geoscientific applications, meteorological and space meteorological studies. SWEPOS¹ is the Swedish CORS network operated by Lantmäteriet (Swedish Mapping, Cadastral and Land Registration Authority). The performance of a well-functioning geodetic service like SWEPOS could well be measured by the quality, resiliency, integrity, and continuity of its service. Monitoring and verifying the quality of the GNSS data provided by the CORS network is key and a primary focus of any geodetic infrastructure striving to improve the quality of its service.

Lantmäteriet, in collaboration with other research institutes, Chalmers University of Technology, Onsala Observatory and the Research Institutes of Sweden (RISE), has implemented projects and conducted studies to improve the performance of the SWEPOS service. Three CLOSE (**C**halmers, **L**antmäteriet, **O**nsala, **R**ISE) Real Time Kinematic (RTK) effort projects have been conducted since 2008. Close-RTK I was run during 2008-2009, the objective of which was to investigate the main sources of errors in the SWEPOS network (Emardson et al, 2009). CLOSE-RTK II, which was carried out in 2010-2011, investigated the effects of the ionosphere for the SWEPOS

¹<https://www.lantmateriet.se/swepos>

network-RTK service (Emardson et al, 2011). The third CLOSE-RTK project has been running during 2014-2017 and mainly focused on investigating station-specific errors, such as the effects of monument (in)stability (Johansson et al, 2019). The project has also investigated station-dependent antenna calibration methods and the ongoing developments of Precise Point Positioning (PPP) and PPP-RTK real-time methods.

These projects played an important role in investigating various aspects that influence the performance of a CORS network and in building the perfect site for a GNSS reference station. In addition, they have developed tools for real-time monitoring of error sources such as the ionosphere (Emardson et al, 2011). A recent evaluation of GNSS data characteristics, such as the number of cycle slips, code multipath and the signal-to-noise ratio (SNR), has also been carried out at selected SWEPOS stations to monitor the quality of the SWEPOS data and the possible detection of problematic data (Nilsson and Ning, 2019). SWEPOS-QC (SWEPOS Quality Check) is a continuation of those efforts. It is an effort to contribute to Lantmäteriet's goal of ensuring the resilience and integrity of the SWEPOS service. Its goal is to improve the quality control of the SWEPOS data using Receiver INdependent EXchange (RINEX, Gurtner (1994)) data to monitor GNSS signal disturbances and in return for early detection of station anomalies.

1.2 SWEPOS

SWEPOS offers a wide range of services, from providing dual-frequency data to PPP and relative positioning to geoscientific and meteorological research, to providing DGNSS and RTK corrections for real-time applications. Furthermore, SWEPOS is the foundation and backbone of SWEREF 99 (Jivall and Lidberg, 2000), which is the Swedish national geodetic reference frame.

At the time of writing this report, SWEPOS operates around 500 stations (see figure 1.1 and table A.4). Figure 1.1 shows 500 ground stations operated by SWEPOS and 23 more stations operated by Trimble. Almost 450 of the stations are part of the network-RTK.

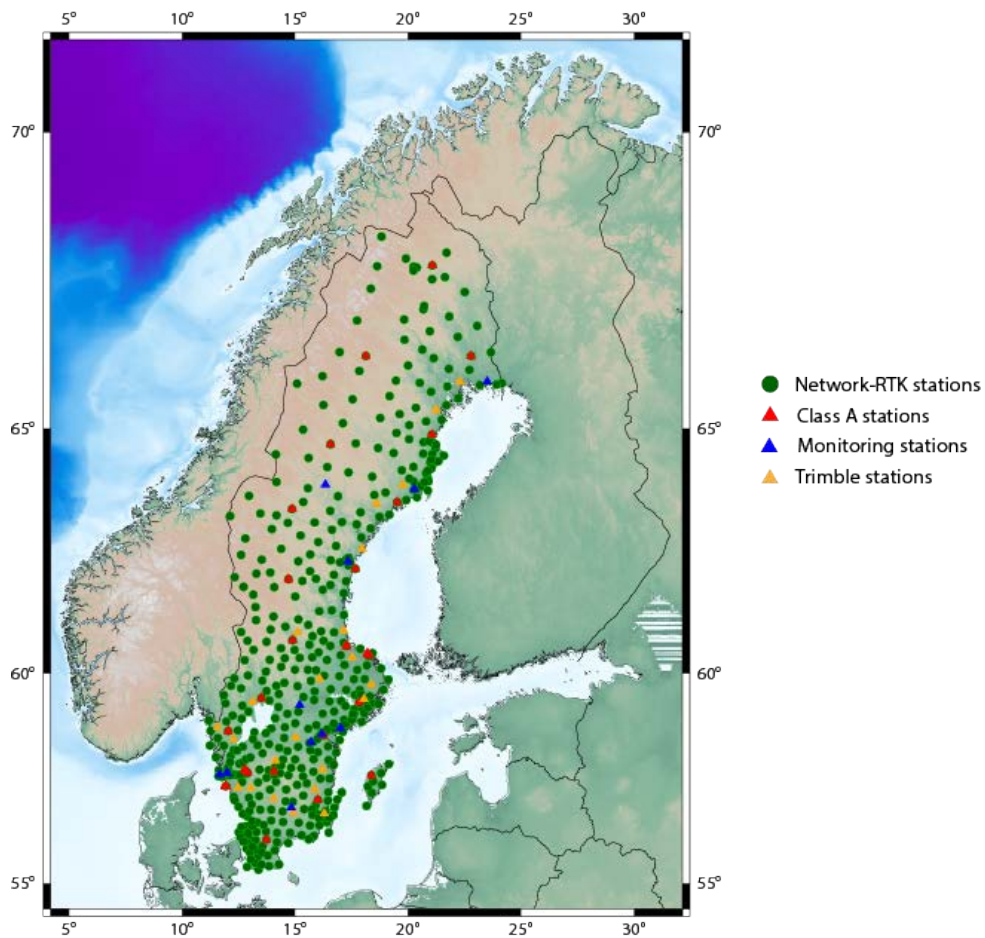


Figure 1.1: SWEPOS GNSS observation network of ground stations. More stations which are operated by Trimble are also included. See tables 1.1 and appendix A.4 for station category and list, respectively.

Classes A and B are the SWEPOS station classification according to how they are established (Norin et al, 2008). Class A stations are mounted on stable foundations (either a concrete pillar or steel grid mast), while Class B stations are built on buildings for network-RTK purposes. Most of the network-RTK stations are classified as class B. The monitoring and some class A stations are used to provide real-time status of the SWEPOS RTK service to users². Some monitoring stations are also established within infrastructure projects in collaboration with the Swedish Transport Administration (Trafikverket) to monitor project-adapted network-RTK solutions.

SWEPOS has constantly developed in terms of size and quality of its service. Since

²<https://swepos.lantmateriet.se/services/realtimemonitors.aspx>

2010, when the SWEPOS network-RTK service has achieved national coverage, the number of stations increased from 170+ to 500+ in 2021. In addition, the antennas and receivers of all stations have been improved, allowing the network to track modernized GPS signals and all GLO, GAL and BDS signals. It has upgraded its service from GPS + GLO only to GPS + GLO + GAL since February 2018. Work is underway to provide real time corrections based on combined GPS, GLO, GAL and BDS observations.

Table 1.1: Categories of stations in figure 1.1. The network RTK, class A and monitoring categories of stations are owned and operated by SWEPOS. See Appendix Table A.4 for a complete list and more information.

Type	Owner	Total Number of Stations
Network RTK stations	SWEPOS	450
Class A stations	SWEPOS	35
Monitoring stations	SWEPOS	13
Trimble stations	Trimble	23

1.3 SWEPOS-QC

SWEPOS-QC is a quality monitoring of GNSS observations of SWEPOS data. It uses daily and hourly RINEX files to assess overall data quality, monitor, detect and alarm signal disturbances, and early detection of anomalous stations.

1.3.1 Motivation

From satellite-based errors such as unmodeled clocks and orbits to atmospheric refraction and station-specific errors, GNSS observations and derived products are affected by errors from various sources. GNSS observing geometry plays an important role in how these unmodeled errors propagate to derived products. There are many factors that compromise the GNSS observing geometry. These include changes in satellite constellations as well as natural and man-made obstruction objects. In addition to compromising the geometry of the observation, obstructions cause signal distortion, signal attenuation and signal reflection (known as multipath). To avoid these effects, the International GNSS Service (IGS³) recommends GNSS antennas to be installed in environmentally friendly areas, that is, away from natural and man-made obstructions⁴. Consequently, the GNSS stations in the SWEPOS network are established in

³<https://igs.org/>

⁴<http://kb.igs.org/hc/en-us/articles/202011433-Current-IGS-Site-Guidelines>

a clear sky with a low multipath environment and minimal signal obstructions.

However, stations are still subject to station-specific errors that can be due to new structures built near stations after they are established, which could cause signal obstructions and multipath. Furthermore, they are subject to unintentional interferences, for example to ionospheric scintillation and radio frequency interference (RFI), and intentional interferences, for example jamming and spoofing.

Figure 1.2 shows a time series of pseudorange multipath at the GPS signals L1 (MP1) and L2 (MP2) (left figure), observation rate (ratio of recorded observations to expected observations, right top figure) and total number of cycle slips (lower left figure) for the period 2017.5 to 2021.5 for the Mollösund station (0MOL). The station is located in the municipality of Orust, Västra Götaland county, Sweden. The red vertical dotted lines in the figure indicate receiver, antenna, radom, and firmware upgrades, if any. The breaks in the time series indicate how changes and/or upgrades in the station equipment (mainly the receiver) affect the GNSS observation characterization parameters mentioned above. This is related to the receiver algorithms and the way they mitigate errors. See the 2.2.4 section for more details on how receivers mitigate errors differently.

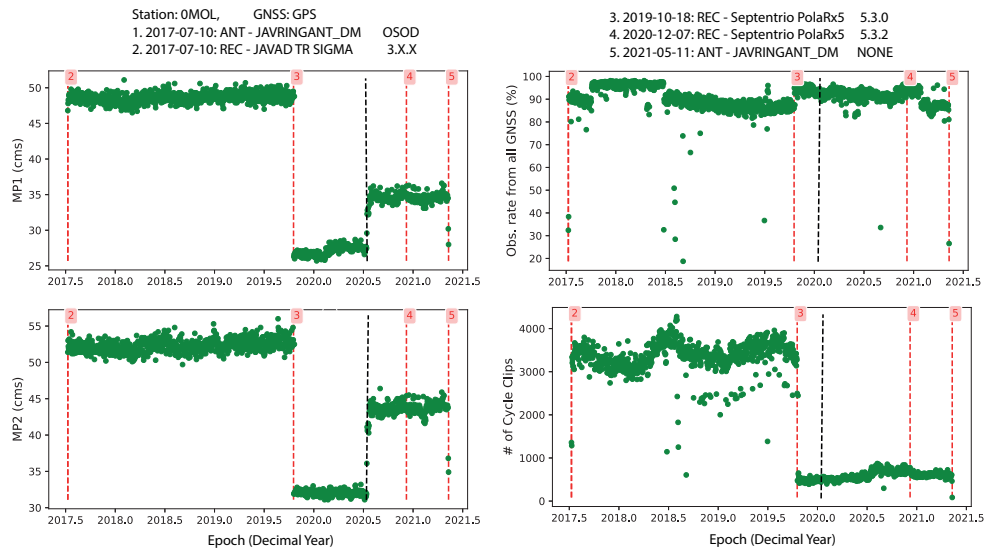


Figure 1.2: Time-series of GPS MP1, MP2, observation rate and total number of cycle slips for station 0MOL for the period 2017.5 to 2021.5.

The black vertical dotted lines in Figure 1.2 indicate a day, July 14, 2020, which

is an interruption of unknown origin in the time series. The data break is not linked to any equipment change or firmware upgrade registered for the station. Since the specified date, the multipath has increased by 30 to 40 percent. On January 10, 2021, poor performance was noticed on the SWEPOS network-RTK system (result not shown here) for the station. The station showed poor performance in resolving tracked satellites for all GNSS, more clearly for GPS and GLONASS than for Galileo. However, a detailed analysis of the historical data from the station could clearly show that the station problem started back in time, on July 14, 2020. As there was no equipment change, the problem could only be related to an equipment failure or a change in the station's environment.

Figures 1.3a and 1.3b show elevation-azimuth diagrams of the station for GPS L2 (color-codes with blue and red indicating low and high multipath cases, respectively) for 0MOL. Multipath values are stacked over 40 days for clarity in the periods before and after July 14, 2020, respectively. Comparing the two figures indicates that below 30 degrees elevation, the multipath increases across the horizon (0-360 degrees azimuth). However, at higher elevation angles, the multipath increase occurs for 50-100 and 175-225 degrees azimuth. A significant increase in the multipath could be seen even up to 70 degrees elevation for the latter azimuth range (figure 1.4). Figure 1.4 shows how the multipath was distributed before and after July 14, 2020, at different elevation angles. The general analysis could infer that something has changed near the station, in a southwesterly or southeasterly direction. Multipath at higher elevation angles could infer that the multipath causing object could be higher than the station antenna.

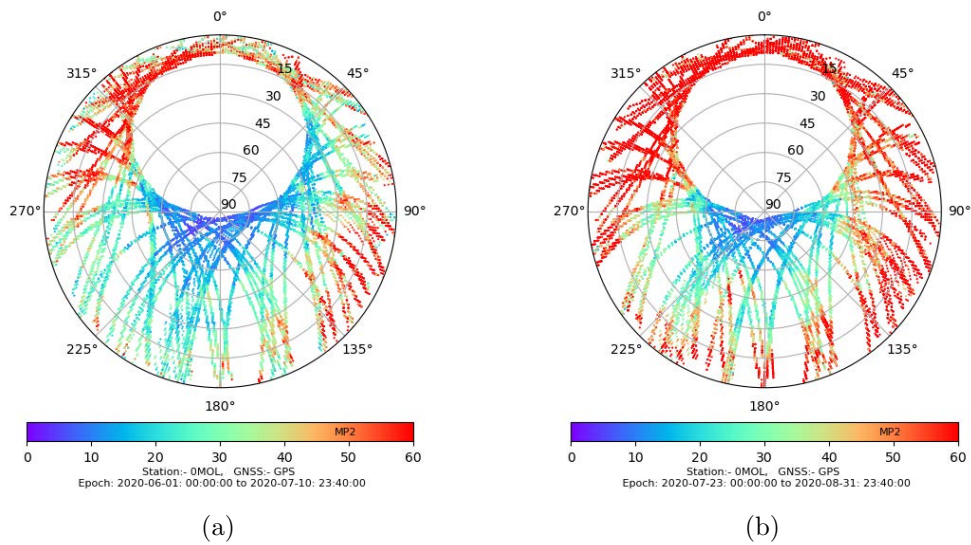


Figure 1.3: Elevation-azimuth diagram for station 0MOL for the period before the event on the 14th of July (a) – 1st of June to 10th of July, and after the event (b) – 23rd of July to 31st of August, 2021. The lines indicate satellite paths while the color-code shows the multipath values for GPS L2.

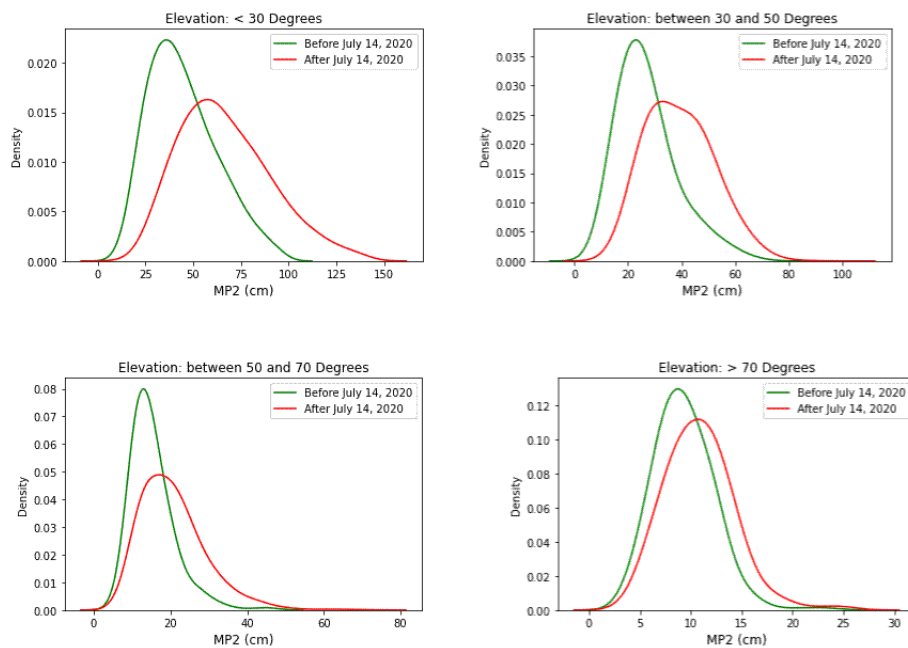


Figure 1.4: MP2 distribution (probability density function) for periods before (green lines) and after (red lines) the 14th of July, 2020.

After the complete analysis and hypothesizing the causes, the station was visited on February 10, 2021. A new telephone mast was found to be about ten meters from the antenna in a southwesterly direction (see figure 1.5). During the visit, we were informed that the telephone mast was installed in July 2020. The station was then flagged off from the network-RTK as of February 12, 2021. On May 10, 2021, the station was moved to a new location and its name has been changed to 1MOL.



Figure 1.5: Station 0MOL and the newly installed radio mast.

Due to the extended number of stations and the workload in the SWEPOS operations center, problems such as the 0MOL station problem could take a long time to detect. The problem in 0MOL was detected six months after the construction of the telephone mast and began to cause disturbances in the observations of the stations. SWEPOS-QC aims to use improved quality control of RINEX data to detect similar problems as soon as possible. RINEX files contain useful parameters that can be used to characterize the GNSS data to verify the quality of the observation, which, in turn, can infer serious problems with the station equipment and/or its environment. These include the code multipath, the number of cycle slips, the phase SNR, the observation rate, and the history of the number of satellites. As part of the daily quality control of SWEPOS operations, an SNR-based signal disturbance detection system has been developed that monitors all signals from all GNSS listed in table A.1 across the entire SWEPOS network and alarms of possible signal disturbances.

1.3.2 Goals

SWEPOS-QC is an extension of Lantmäteriet's effort to maintain the quality of SWEPOS data and is an enhanced quality control of RINEX-based GNSS data. Its main objective is to check the signal quality of the SWEPOS network based on single GNSS and multi-GNSS observations. Table A.1 lists the signals and their respective frequencies that are monitored by SWEPOS-QC.

By checking the quality of the signals, the project aims to detect signal disturbances and station anomalies as early as possible. The causes of signal disturbances can be:

- Intentional and unintentional interferences such as jamming
- Hardware failures
- Signal obstructions which may cause cycle slips and multipath e.g., new buildings, snow accumulation, tree foliage and/or vegetation

Situational awareness of the signal disturbances is the primary focus of SWEPOS-QC. When disturbances in the signal are detected, a data quality focus group within SWEPOS is informed. The data quality focus group then monitors and characterizes the disturbances. The cause of signal disturbances is further investigated to identify whether they occur due to equipment failure, multipath, or (un)intentional RFI. Persistent (un)intentional RFI-related disturbances are reported to the Swedish Post and Telecom Authority (PTS) for further awareness and characterization, such as geolocalization of the cause.

1.4 Report structure

The report is divided into five main sections (Introduction, SWEPOS Data, GNSS Signal Disturbance Detection in SWEPOS, Real signal disturbance incidents, Summary, and Appendix).

Introduction

This section introduces the report and contains general information about GNSS and SWEPOS. In addition, it describes the objectives and motivations of SWEPOS-QC.

SWEPOS Data

General information on SWEPOS data, the different types of receivers within the SWEPOS network and RINEX data processing are included in chapter 2.

GNSS signal disturbance detection in SWEPOS

The SNR-based GNSS signal disturbance system in SWEPOS is described and demonstrated using real GNSS observations with simulated interference waves in chapter 3.

Real signal disturbance incidents

Real GNSS signal disturbances of different causes detected using the method described in chapter 3 are presented in chapter 4.

Summary

Chapter 5 summarizes the report and recommends further work to improve the detection system.

Appendix

Appendix A includes more real GNSS signal disturbance incidents, figures, and tables.

Chapter 2

SWEPOS Data

2.1 SWEPOS Rinex Data

Data streamed from SWEPOS stations is used in the RTK service of the SWEPOS network, where the corrections of this service allow users to obtain a centimeter level of precision in real time. GNSS observations and navigation messages are also stored in RINEX format for post-processing related applications such as geophysical surveys and definitions of terrestrial reference frames. The RINEX files are also used for daily monitoring of the stability of SWEPOS stations. SWEPOS also contributes RINEX data from a number of Class A stations to international initiatives and organizations such as IGS and EUREF Permanent Network (EPN¹).

In addition, RINEX files are used for daily quality control purposes such as data gaps, signal obstructions, and multipath in the station environment. Both RINEX 2.0X² (RINEX2³) and RINEX 3.0X (RINEX3⁴) versions are stored. SWEPOS-QC performs an extended quality analysis of RINEX3 files to monitor signal disturbances from any cause. Currently, it is a post-processing mode that checks the quality of daily and hourly files. The RINEX data flow within SWEPOS operations prepares the RINEX3 observation and navigation files for the entire SWEPOS network, which are the main input formats for the daily SWEPOS-QC routines. The SWEPOS network is equipped with three different types of receivers (see section 2.2). While most RINEX files are generated from the network-RTK software, Trimble Pivot Platform (TPP⁵), which is a Trimble program used for SWEPOS network-RTK service, some receivers also generate RINEX files.

2.2 Receiver types

SWEPOS stations are equipped with three types of receivers, namely Trimble NetR9, Trimble Alloy, and Septentrio PolaRx5. Figure 2.1 shows map of the SWEPOS stations

¹<https://www.epncb.oma.be/>

²X represents different versions

³<https://files.igsb.org/pub/data/format/rinex210.txt>

⁴<https://kb.igs.org/hc/en-us/articles/115003980248-RINEX-3-00>

⁵<https://www.trimble.com/Real-Time-Networks/Trimble-Pivot-Platform.aspx>

color-coded with the receiver types. Red, orange, and green indicate stations with NetR9, Alloy, and PolaRx5 receivers, respectively.

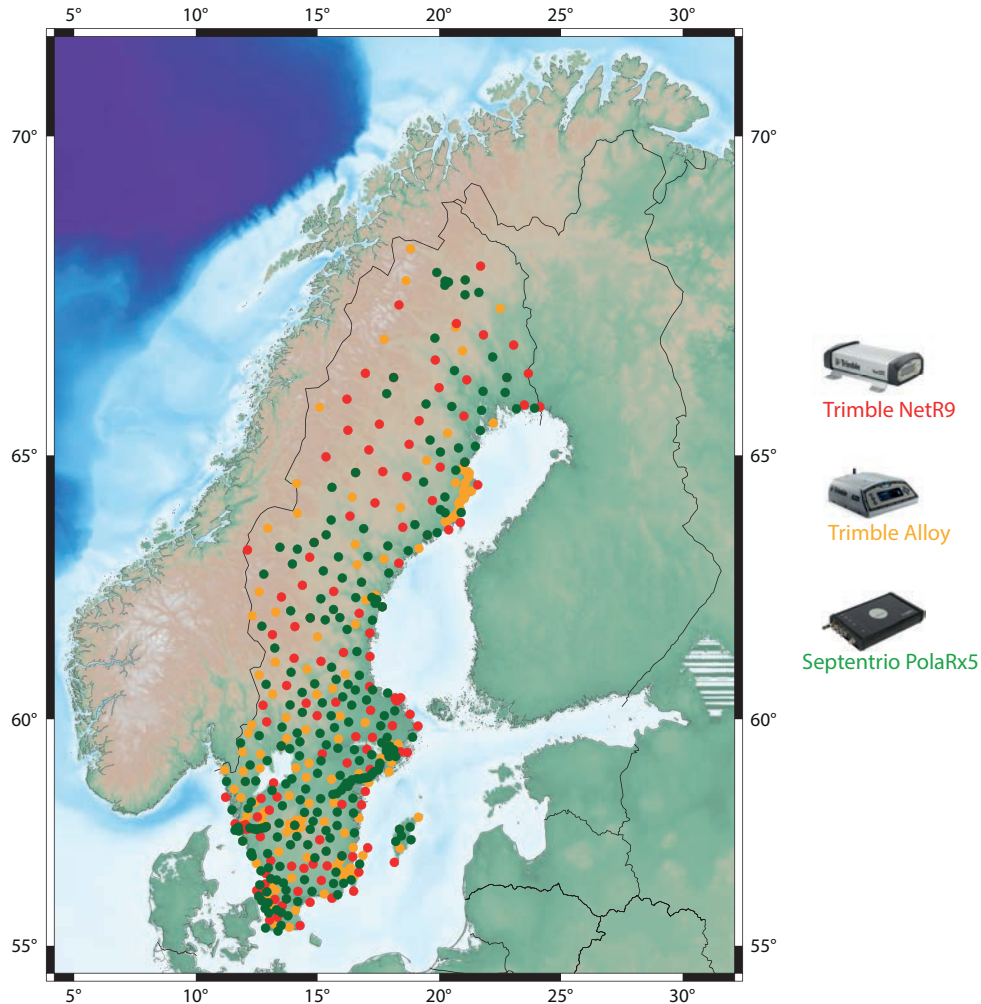


Figure 2.1: Receiver types in use in the SWEPOS network. Red, orange and green colors indicate stations with Trimble NetR9, Trimble Alloy, and Septentrio PolaRx5 receivers, respectively.

2.2.1 Trimble NetR9

Trimble NetR9⁶ is one of the generations of Trimble 360 receiver technologies offering approximately 440 channels with multi-GNSS tracking capability. It is capable of tracking all GPS, GLO, GAL and BDS signals and other regional constellations. The

⁶<https://monitoring.trimble.com/products-and-solutions/netr9-ti-m-gnss-receiver>

receiver includes Trimble’s Everest multipath rejection algorithm and low elevation tracking technology. In addition, it includes a Proprietary Receiver Autonomous Integrity Monitor (RAIM) system that allows detecting and rejecting degraded signals. At the time of writing this report, 26 percent of SWEPOS stations are equipped with this receiver.

2.2.2 Trimble Alloy

Trimble Alloy⁷ is Trimble’s next-generation receiver launched in 2018 and is suitable for real-time network applications. It includes most of the latest Trimble technologies described in the 2.2.1 section. In addition, it provides 672 channels with multi-GNSS multi-signal tracking capabilities. The receiver has wind and dust protection technology that makes it suitable for harsh environments. The receiver includes an enhanced multipath rejection technology, called Everest plus⁸, which uses a neural network to derive an improved multipath estimate. The receiver also includes a web-based user interface spectrum analyzer, Trimble’s Maxwell7 interference detection technology, which makes it easy to troubleshoot GNSS signal disturbances from different sources. Twenty-six percent of SWEPOS stations are equipped with a Trimble Alloy receiver.

2.2.3 Septentrio PolaRx5

Septentrio PolaRx5⁹ is a high precision multi-GNSS multi-frequency GNSS reference receiver that includes 544 channels. The receiver provides low-noise measurements with a patented multipath mitigation technology, called APME +, which works well in protecting against short-delay multipaths. In addition, it has the Advanced Interference monitoring and mitigation (AIM+) feature that works well to mitigate and filter interference of different kinds. It also includes an intuitive web usage interface that makes monitoring and operations easy. Forty-five percent of SWEPOS stations were equipped with this receiver at the time of writing this report.

2.2.4 Receiver performance

GNSS receivers are the backbone for delivering high-precision GNSS positioning and other derivative products. The way in which sources of GNSS errors are compensated for is key for GNSS receivers to achieve the expected level of accuracy in a short period

⁷<https://www.trimble.com/Real-Time-Networks/Trimble-Alloy.aspx>

⁸<https://oemgnss.trimble.com/technologies/advanced-multipath-mitigation/>

⁹<https://www.septentrio.com/en/products/gnss-receivers/reference-receivers/polarx-5>

of time. Receivers rely on accurate external models to correct errors related to satellite orbits and atmospheric effects. However, errors related to the environment and station equipment are difficult to correct and model. These include, but are not limited to, multipath, signal attenuation, and RFI. Those sources of errors can only be partially managed and how the receivers handle them depends on which type of robust receiver technology the receivers are equipped with.

SWEPOS stations are equipped with three different types of receivers (see section 2.2). As shown in figure 1.2, changing the receiver or upgrading the firmware changes the multipath values. Figure 2.2 shows the pseudorange multipath for GPS L2 and the number of cycle slips for all stations in the SWEPOS network. Values are based on performance for two weeks in 2021 from January 1 to January 15 and are plotted against the latitude of the stations. There are differences between the receivers (see colors) in the multipath values and the number of cycle slips. However, there is no clear latitude dependence that infer that the differences are linked to how the receivers manage to reduce and mitigate errors.

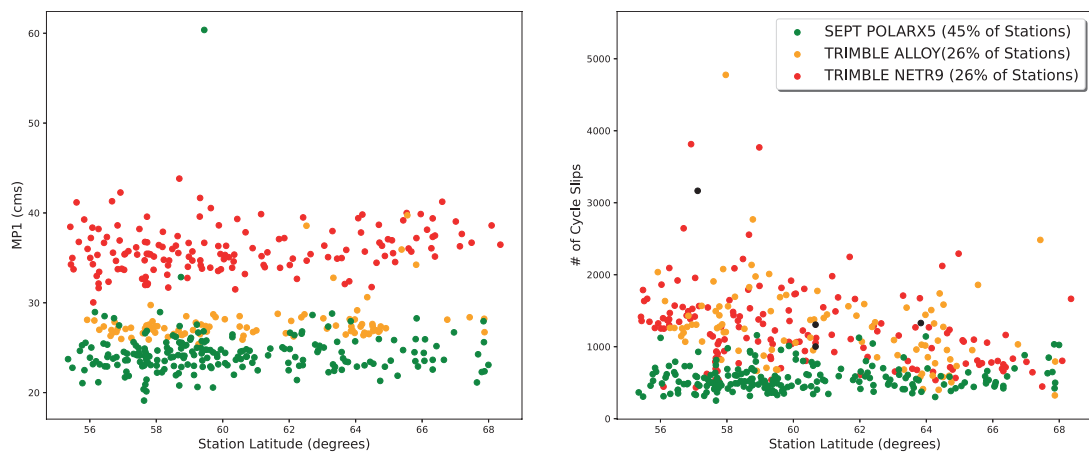


Figure 2.2: Pseudorange multipath on GPS L2 (MP2, left figure) and total number of cycle slips (right figure) plotted against latitude angles of stations of the entire SWEPOS network. Colors categorize stations by their receiver types.

Stations with the Septentrio PolaRx5 receiver (green dots) perform well in terms of multipath mitigation and recording fewer cycle slips. The Septentrio PolaRx5 receiver's performance compared to others is likely tied to the APME+ technology, which better mitigates short-delay multipaths. Trimble Alloy performs better than NetR9 in mitigating multipath. However, its performance in the number of cycle slips is similar.

Trimble Alloy's better performance over NetR9 can be related to the Everest plus, which is an improved neural network based multipath rejection technology.

Figure 2.2 at a glance shows how receivers perform differently in mitigating errors and this, in turn, would affect delivery of accurate positioning and initialization time. Changing the Trimble NetR9 receivers to receivers with improved error mitigation features could significantly reduce systematic errors such as multipath. This, in turn, would improve the overall performance of the SWEPOS network and service. There is already a plan to phase out Trimble NetR9 receivers within SWEPOS in the near future.

2.3 Data processing

RINEX observation and navigation data obtained from TPP or station receivers are the main inputs of the GNSS interference detection system. Anubis (see section below) is used to primarily process RINEX data, where GNSS observation statistics and data characterization parameters are generated. Python libraries that were developed as part of SWEPOS daily data quality monitoring are used to automate Anubis processing, extract Anubis outputs, quality monitoring, signal disturbance detection and alarm problematic stations.

2.3.1 Anubis

G-Nut/Anubis¹⁰ is an open source command line tool for qualitative and quantitative monitoring of GNSS RINEX files. It can handle multi-GNSS multi-frequency data. It provides observation statistics and characterizes GNSS data in terms of, among others, number of cycle slips, observation rate, code multipath, and SNR. It takes RINEX2.0X or RINEX3.0X as input to provide those GNSS data characteristics. In addition, it supports GNSS navigation messages and in return provides elevation and azimuth dependent parameters. G-Nut/Anubis also supports other input formats such as Radio Technical Commission for Maritime Services (RTCM) and provides other operating modes for more complex data handling and quality control. More information can be found here¹¹ (Vaclavovic and Dousa, 2016).

¹⁰<https://www.pecny.cz/Joomla25/index.php/gnss/sw/anubis>

¹¹<https://gnutsoftware.com/gnss-and-data-quality>

2.3.2 In-house Developed Libraries

Anubis is used to generate the GNSS data characteristics that are used to monitor the quality of RINEX files. In-house developed libraries are then used to extract Anubis results, for detailed data quality analysis, and to generate alarms at problematic stations. The prototype is written in Python libraries and runs on a Red Hat Enterprise Linux 8.3 server.

Chapter 3

GNSS Signal disturbance detection in SWEPOS

3.1 Overview

GNSS provides a positioning, navigation and timing (PNT) service 24 hours a day, 7 days a week with global coverage. However, by going through all sources of errors, GNSS signals are underpowered when received by terrestrial receivers, making GNSS signals vulnerable to (un)intentional RFI. The sources of GNSS signal disturbances can generally be classified as unintentional and intentional. Ionospheric scintillations, other systems with frequencies similar to GNSS, broadcasting and communications emitters are examples of unintentional interference sources. GNSS signal disturbance can also be an intentionally created situation, which can be due to jamming, where GNSS signals are deliberately interrupted with a stronger signal, or spoofing, where one's position is deliberately falsified.

In GNSS reference stations such as SWEPOS, signal disturbances can occur due to, among others, antenna/equipment failures, signal obstructions such as trees, antenna splitters/cables, multipath and RFI. The detection of these disturbances of any cause is a priority objective of SWEPOS-QC. This is called situational awareness. Once disturbances are detected, they can be characterized in terms of cause, time of occurrence, frequency, power, and location.

In the case of GNSS reference stations, the detection of disturbances in the signals can be carried out by an external interference monitoring system, in which a detection system is installed near or at the reference stations. However, this is not feasible in terms of cost and scalability. These types of systems are more suitable for sensitive infrastructures like airports, not for a wide area and network like SWEPOS. The GNSS Interference Detection and Analysis System (GIDAS)¹, which is a project supported by the European Space Agency (ESA), is an example that passed airport tests. Another example is the interference detection system of the Swedish Defence Research Agency (FOI), called RF-Oculus (Linder et al, 2019), which is an interference detection focused on the L1 frequency of GPS.

¹<https://www.ohb-digital.at/en/research/gidas>

As an external monitoring system is not feasible for SWEPOS stations, it is more practical to develop methods that monitor GNSS pre- or post-correlation observables, which is data already available from receivers. Various detection methods are discussed and proposed in the literature. The most common are Automatic Gain Control (AGC) and SNR-based detection systems.

3.1.1 Automatic Gain Control (AGC)

GNSS receivers contain an AGC, which allows them to maintain a slow variation in the power of the received signals. If interference appears, it affects the way the AGC operates, which in turn can be used to monitor and detect interference signals (Bastide et al, 2003; Akos, 2012). The nominal voltage of the AGC increases or decreases, where monitoring the standard deviations of these variations compared to a defined threshold can be used to determine the change in receiver power and, in turn, detect interference. AGC-based jamming detection is reported to be sensitive to pulsed signals (Ndili and Enge, 1998). A challenge of using AGC to detect interference is setting thresholds.

Although AGC measurements may be available on most modern receivers, these measurements are not included in the RINEX3 data and there is a lack of tools to extract the information from the receivers' binary file formats. Consequently, it may not be convenient to use this measure for an automatic interference detection system for the SWEPOS network. However, an AGC-based detection system as a complement to other methods will be used once other tools are developed to extract the information internally or within the GNSS community.

3.1.2 Signal-to-Noise-Ratio (SNR)

SNRs have also been widely used to monitor GNSS signal interference and detect RFI (Calcagno et al, 2010; Borio and Gioia, 2015; Balaei et al, 2006; Axell, 2014; Axell et al, 2015). In the presence of RFI, for example, when a jammer is close to a GNSS receiver, the noise level of GNSS measurements increases, causing a drop in SNR values. The reduction of SNR values can be monitored and used to detect disturbances in the signal. However, unpredictable events in SNR can occur due to factors other than RFI. These include equipment failures and signal obstructions and multipath induced by the station environment. Changes in the station environment can be unpredictable for a rover, for example, if the receiver moves in an urban environment. However, this is not the case for reference stations, such as the SWEPOS network, as their environments can be partially monitored for blocking objects and multipaths. Since the purpose of

this work is to detect disturbances of any cause, unpredictable drops in SNR remain of interest to detect and investigate their cause. SNR values are easily accessible from all commercial GNSS receivers and are included in RINEX files. Consequently, an SNR-based GNSS signal disturbance detection system has been developed as part of the daily quality control of SWEPOS data. SNR values in RINEX files are standardized to be expressed in units of dBHz and the same units are used throughout the report unless otherwise noted.

Emissions near or in the GNSS frequency band are restricted, as they would otherwise interfere with GNSS measurements. Therefore, unless an object that can cause RFI is (un)intentionally close to the GNSS receiver, RFI-free GNSS measurements are expected as a norm. Unless an interfering signal appears, the SNR values change very slowly and can be treated as a stationary process for a short period of time (Calcagno et al, 2010). However, there are other factors that affect SNR variations. Known factors include multipath, signal obstructions, elevation angle of satellites, GNSS receiver, antenna and antenna splitter cables, and GNSS power flex. SNR drops due to these factors should be monitored and modeled (if possible) to improve and reduce false alarms from a SNR-based detection system. Some of the factors that affect SNR variations are described in the following subsections.

3.1.2.1 Elevation dependency

SNR values change slowly over time and are highly dependent on the elevation angle of the satellites. SNR variations with satellite elevation angles are primarily related to antenna gain patterns. Figure 3.1 shows the SNR values for the GPS L1 C/A code for a station over a period of one day for all satellites plotted against elevation angles. Green points indicate raw data, while red points show a polynomial fit model of the SNR. Low SNR values are expected at low satellite elevation angles. Furthermore, low elevation SNRs are more susceptible to multipath.

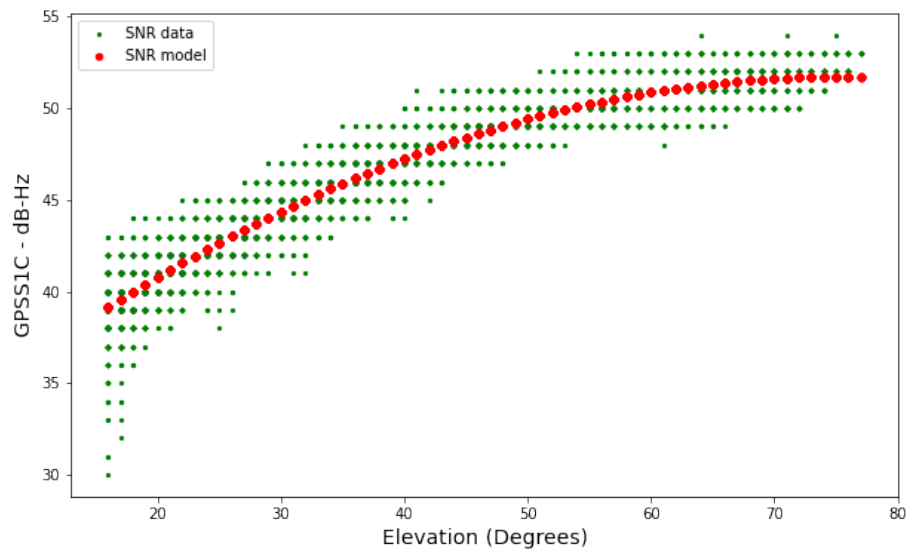


Figure 3.1: SNR for GPS L1 C/A code plotted against elevation angle of satellites. Green dots show raw data while red indicates a polynomial fit.

Modern commercial receivers handle long delay multipath well. However, short delay multipath affects GNSS measurements and causes quasi-periodic oscillations in SNR (Benton and Mitchell, 2011). Filtering the effects of multipath is essential for a detection system that aims to monitor SNR drops caused by interference. In this work, SNR values below 20 degrees elevation are discarded to reduce multipath effects. Since discarding low elevation data removes a subtle amount of data, multipath filtering, for example, as in Benton and Mitchell (2011); Bilich et al (2008) could reduce the amount of data to discard and improve the performance of a detection system.

3.1.2.2 Station Equipment

In addition to factors such as multipath, station equipment such as receiver and antenna splitters influence the GNSS SNR. These factors should also be taken into account when establishing a SNR-based detection system. The architecture and characteristics of the receiver have an impact on the SNR. Figure 3.2 shows the SNR for the GPS L5 Q code of three different receivers. The figure emphasizes SNR variations between receivers. However, it should be noted that since the receivers are installed different station environments, other effects, such as multipath, may also have con-

tributed to the variations.

SNR is also affected by the type of antenna. Inside SWEPOS there are different antennas with different amounts of signal amplification, such as 30, 40 or 50 dB of gain. Furthermore, antenna splitters also have an impact on SNR. Two types of antenna splitters are commonly used in SWEPOS. The first amplifies the signal strength while the other reduces it. Figure 3.3 shows the SNR for stations OSTR (upper figure) and 1MAL (lower figure). The red vertical dotted lines in both figures indicate the dates the antenna splitters were installed. The SNR values for OSTR increased after the antenna splitter was installed, while the values decreased for station 1MAL. Records within the SWEPOS database indicated that a splitter amplifier was installed on station OSTR while the splitter on 1MAL is an attenuator.

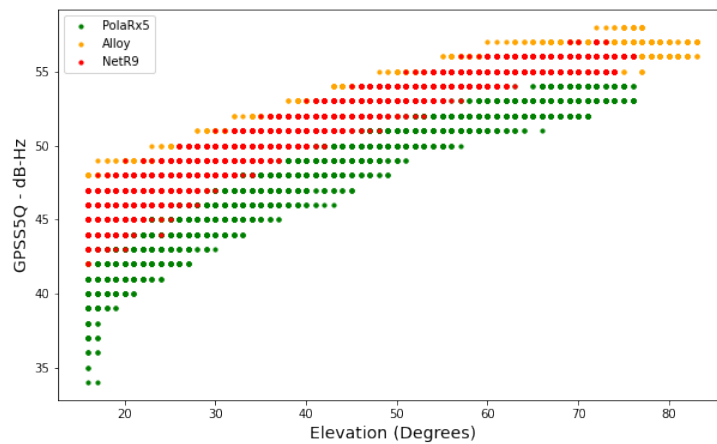


Figure 3.2: SNR for GPS L5 Q code plotted for all GPS satellites against elevation angles. Color codes show the receiver types.

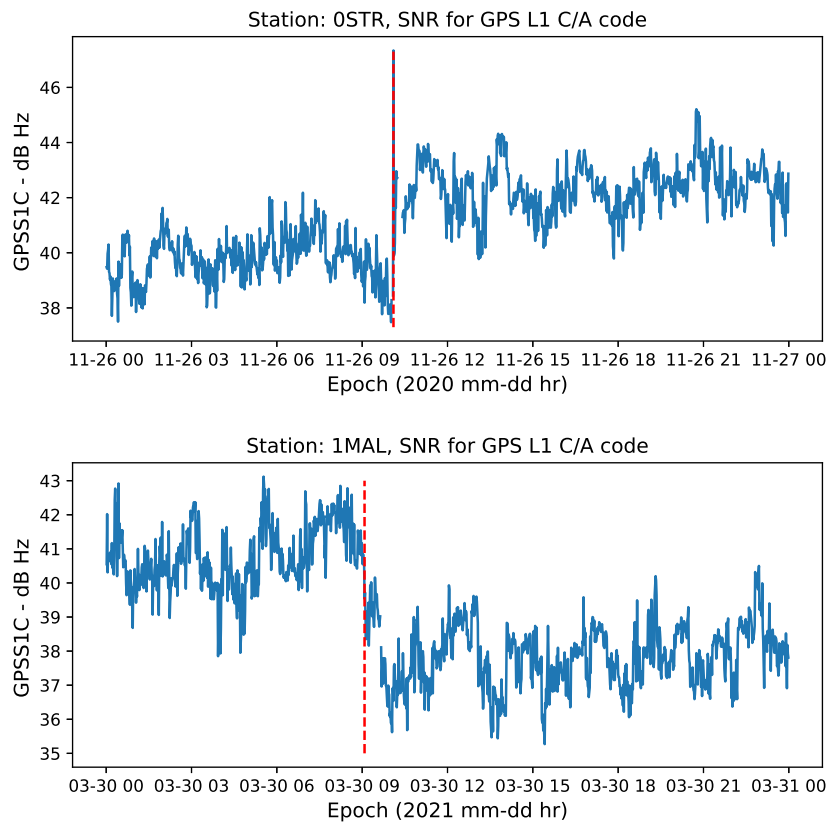


Figure 3.3: SNR for stations OSTR (top) and 1MAL (bottom). Red vertical dotted lines indicate antenna-splitter installation dates. At the time of antenna-splitter installation both stations were equipped with Trimble NetR9 receiver and JNSCR C146-22-1 antenna.

3.1.2.3 GPS Flex Power

GNSS satellites transmit signals with constant power. However, the GPS BLOCKs IIF and IIR-M satellites redistribute power over individual signals, which is called flex power (Steigenberger et al, 2019; Esenbuğa and Hauschild, 2020). The GPS flex power is realized for better protection of signals against interference. Different types of flex power campaigns have been carried out at different times. An example is the four-day flex power campaign on the GPS BLOCK IIR-M and IIF satellites in

2017. Additionally, geographically driven flex power was permanently activated since January 2017 on the IIR-M and IIF BLOCKS. The flex power causes drops in SNR and affects the estimation of GPS-derived products, such as the differential code bias estimation (Esenbuğa and Hauschild, 2020). Flex power changes must be located, monitored, and modeled to avoid false alarms from flex power induced SNR drops.

Figure 3.4 shows the SNR for the GPS frequencies L1, L2 and L5 for the station OROS. The second and fourth rows of figure 3.4, SNR for the L1 and L2 encrypted P(Y)-code, respectively, are identical. This is due to a semi-codeless technique used by geodetic GNSS receivers for the encrypted P(Y)-code of the L1 and L2 frequencies (Steigenberger et al, 2019). In figure 3.4, there are two different patterns that can be clearly seen in the SNRs of the encrypted P(Y)-code of the L1 and L2 frequencies (GPSS1W/GPSS2W) as opposed to the SNRs of the other signals. This is due to the flex power of the GPS BLOCK IIR-M and IIF satellites.

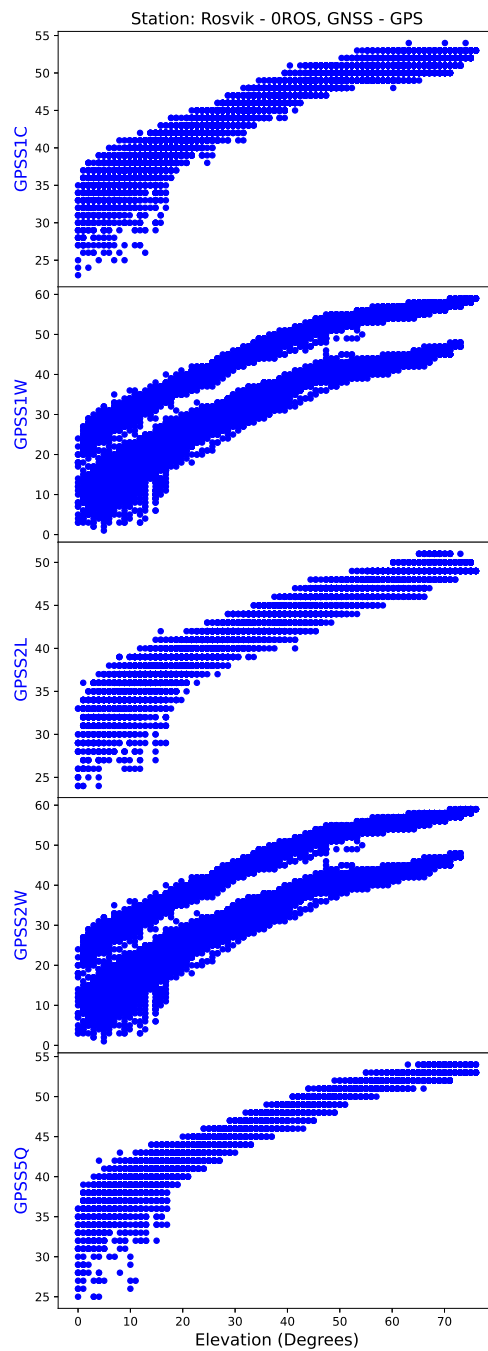


Figure 3.4: SNR plotted against elevation angle of satellites for station 0ROS. Figures top to bottom show SNR for GPS L1 C/A code (GPSS1C), encrypted P(Y)-code on L1 (GPSS1W), GPS L2C (GPSS2L), encrypted P(Y)-code on L2 (GPSS2W) and L5 Q code (GPSS5Q).

Figure 3.5 shows GPSS2W categorized by satellite BLOCKS. The upper figure shows GPSS2W for BLOCK IIR-M and IIF, while the lower figure is for BLOCK IIR-A, IIR-B, and IIIA. Figures 3.6a and 3.6b show GPSS2W plotted against the azimuthal angle of the satellites for BLOCK IIR-M and IIF, and BLOCK IIR-II, IIR-B, and IIIA respectively. The two different patterns in figure 3.5 for BLOCK IIR-M and IIF are the SNR drops which can also be seen in figure 3.6a. The SNR drops are due to the geographically driven flex power that was permanently activated in 2017. As can be seen from figure 3.6a, SNR changes due to flex power are evident when satellites reach certain degrees of azimuth.

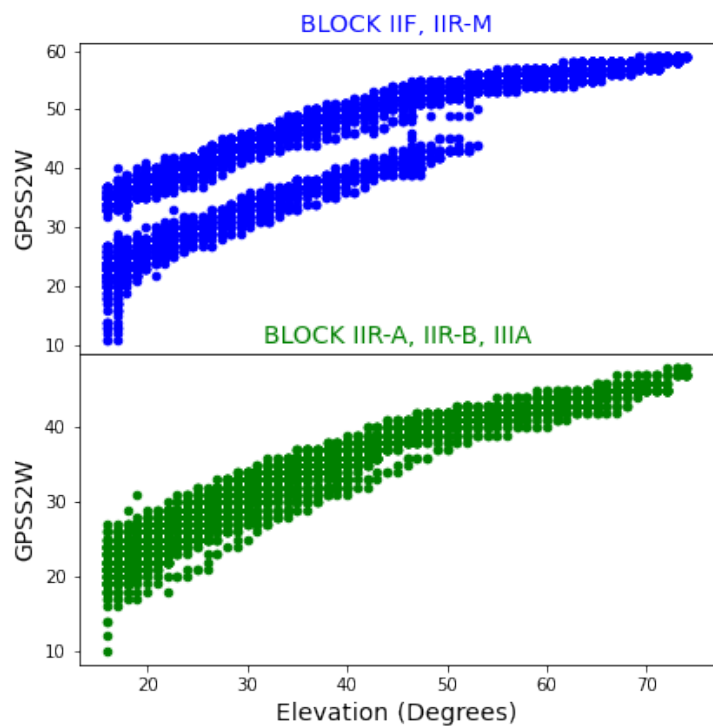
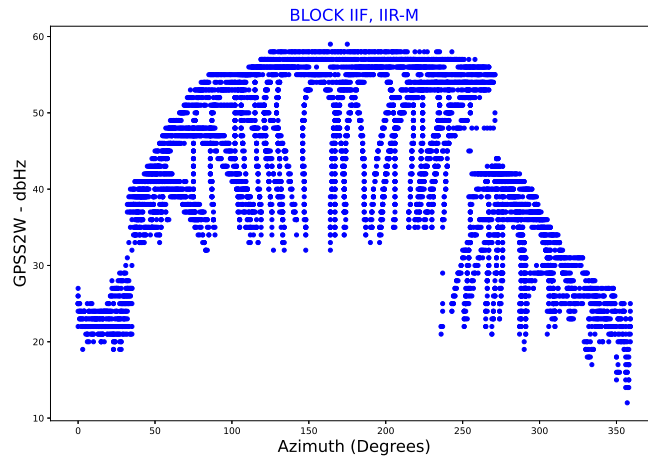
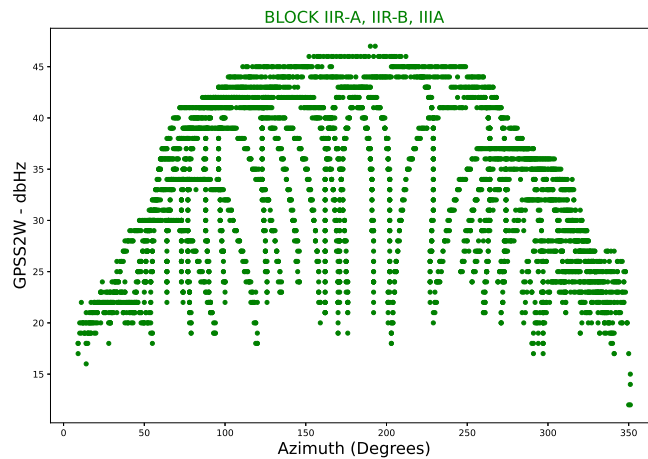


Figure 3.5: SNR for the encrypted P(Y)-code on GPS L2 (GPSS2W) for BLOCK IIF and IIR-M (top), and BLOCK IIR-A, IIR-B and IIIA (bottom) for station OROS.



(a)



(b)

Figure 3.6: As in figure 3.5 but plotted against azimuth angles of the satellites.

Figure 3.7 shows the elevation-azimuth diagram BLOCK IIR-M and IIF satellites for GPSS2W stacked over all SWEPOS stations. Color code infers SNR values. It can be seen that, for ground stations within Sweden, the SNR drops due to the flex power changes occur when the satellites reach 225-360 degrees and 0-30 degrees azimuth. Although most SNR changes occur at lower elevation angles (<30 degrees), SNR drops occur at elevation angles up to 55 degrees for azimuths 250-290 degrees.

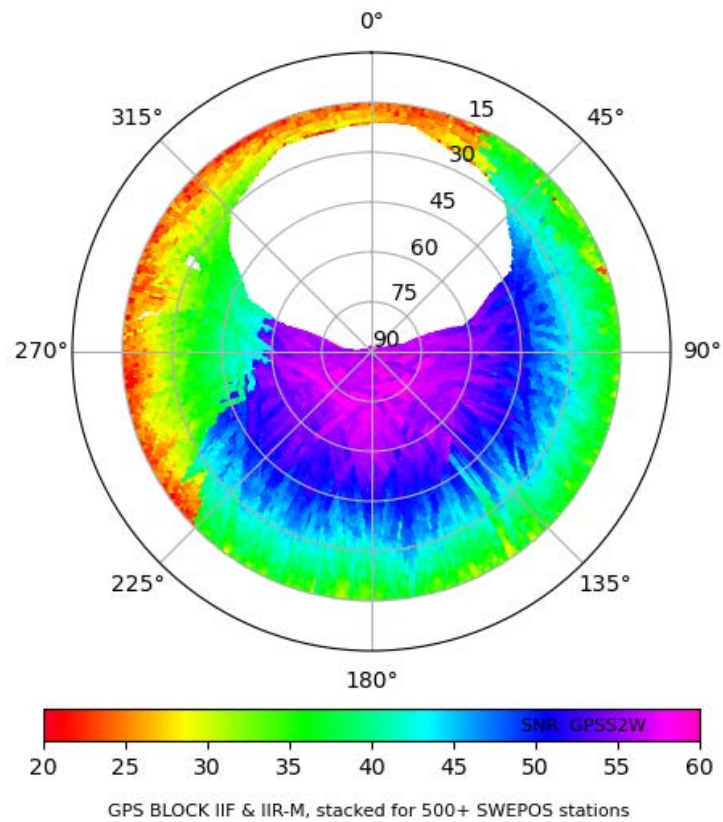


Figure 3.7: Elevation-azimuth diagram of SNR for the encrypted P(Y)-code on GPS L2 (GPSS2W) for BLOCK IIF and IIR-M satellites stacked over the entire SWEPOS network of 500+ stations.

3.2 Methodology

The suitable GNSS disturbance detection method that can be implemented for the GNSS network of reference stations like SWEPOS would be an SNR-based method. This can be established by monitoring unexpected drops in SNR values against a predetermined reference. This can be supported by comparing different frequency bands and GNSS, monitoring the number of reachable satellites for a given receiver, and comparing between different receivers. This SNR-based detection system can be consolidated with AGC-based monitoring if available for a given receiver. A SNR-

based GNSS disturbance detection prototype has been developed in SWEPOS. The method takes advantage of historical SNR measurements to predetermine the SNR characteristics of all GNSS signals from a given receiver and uses them as a reference window (RW) to detect disturbances in the signals from any source. Defining the RW involves taking several days of data that is not subject to interference and considering other factors that can cause SNR drops (see section 3.1.2). Evaluation windows (EW) are then configured to compare their distributions with the RW distribution. Signal disturbances are then reported if the comparisons meet a set of threshold values.

3.2.1 Reference window (RW) definition

The definition of an RW is the backbone of the detection system. This is determined by forming an RW for each station and each GNSS frequency listed in the table A.1 from multi-day data that are not affected by any interference. The receivers' integrated spectrum analyzer and intensive manual intervention and visualization were involved in the identification of interference-free data for all SWEPOS stations. Next, the SNR is modeled for each frequency and each station. This is determined by a second order polynomial best fit regression model that takes into account the dependence of the SNR on the elevation angle of the satellites and other factors described in section 3.1.2. The coefficients from the derived regression model are then used to calculate SNR residuals (model minus measured) for all satellites tracked. The mean value of the residuals of all satellites is calculated and defined as a RW.

3.2.2 Evaluation Window (EW)

Once an RW is established, an evaluation window (EW) is defined that slides over time. The coefficients from the RW model are used to fit the EWs and the residuals are calculated. The distribution of the EW residuals is then compared to the RWs and disturbances are reported according to predefined threshold values (null (H0) and alternative (H1) hypotheses) as follows:

- H0 : if $(\text{Mean SNR residuals} = \text{Mean of EW residuals} - \text{Mean of RW residuals}) \geq -2 \text{ dBHz}$, no signal disturbances are reported.
- H1 : if $\text{Mean SNR residuals} < -2 \text{ dBHz}$, disturbances are reported as:
 - $-4 \text{ dBHz} \leq \text{Mean SNR residuals} < -2 \text{ dBHz}$, disturbances reported but no alarm is generated.

- $-6 \text{ dBHz} < \text{Mean SNR residuals} < -4 \text{ dBHz}$, moderate signal disturbance alarm generated
- $\text{Mean SNR residuals} \leq -6 \text{ dBHz}$, major signal disturbance alarm generated

Signal disturbances are reported if the mean difference between EW and RW residuals is larger than 2 dBHz. If mean difference larger than 4 and 6 dBHz are reported, alarms are generated as moderate and major signal disturbances, respectively. Since strong interfering signals can cause complete signal loss, the algorithm compares data gaps in SNRs for all signals, and signal disturbance is reported if data gaps occur only in certain signals. As data gaps in all signals can be related to power outages, they are not reported as disturbances, although strong interfering signals which cover all frequency bands can also cause the same problem.

The choice of EW length depends on many factors. An important factor is whether it is required to detect short duration pulses. The EW length is defined as 10 seconds for 1 second sampled RINEX3 files and 10 minutes for 30 second sampled RINEX3 files.

Figure 3.8 shows the flow diagram of the detection system. Once RW is formed for a station, it is stored and used to compare it to any new incoming data for that station. Daily, new coming RINEX files are processed with Anubis and sent to Python libraries for additional basic quality control. The RW availability is then checked for a given station. If previously formed RW is available, EWs are formed and compared. If RW is not available, for example, for a new station which hasn't been processed before, further evaluation is required as in section 3.2.1 to define an RW. In addition, a new RW is defined for a station if an equipment change or firmware upgrade is detected. This is to avoid equipment related SNR discrepancies as described in section 3.1.2.2.

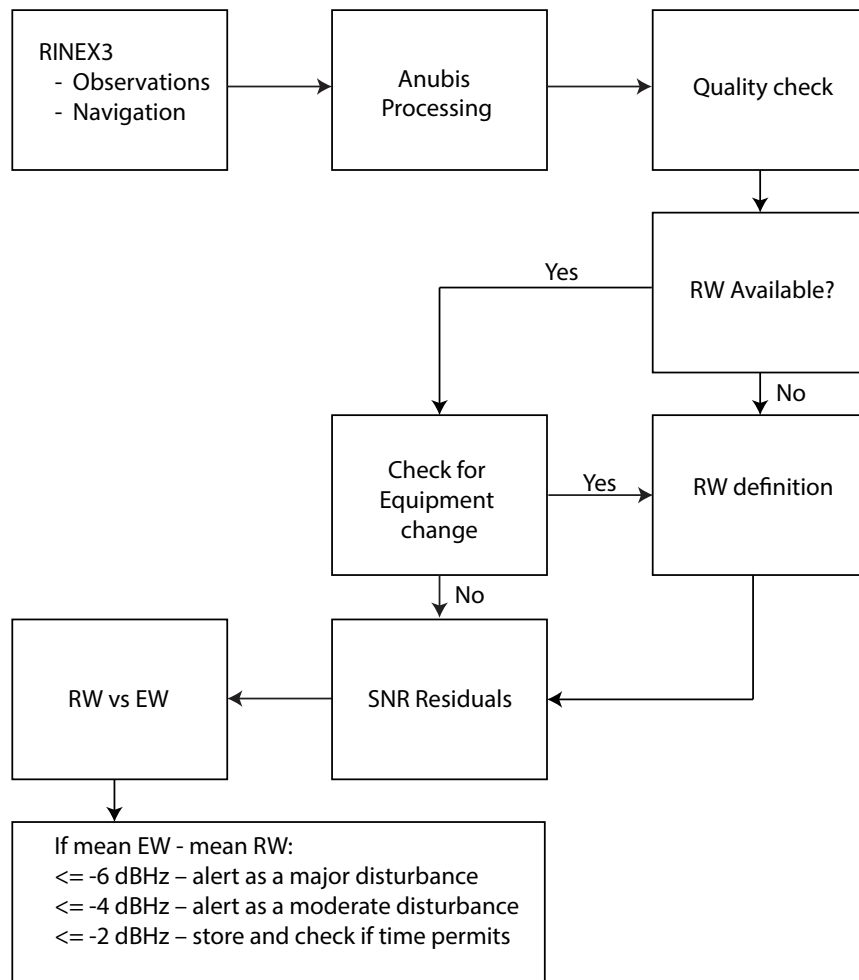


Figure 3.8: Flow diagram of the SNR-based GNSS disturbance detection system.

3.2.3 Demonstration on simulated interference waves

The SNR-based detection system has been tested and demonstrated on real GNSS data with simulated interference waves. The interference waves were simulated in FOI GNSS-lab using GSS9000 Series GNSS Simulator². The details of the simulation and the overall impact assessment have been demonstrated and reported in [Alexandersson et al \(2021\)](#).

Figure 3.9 shows raw SNR data for the GPS L1 C/A (GPSS1C) code in dBHz for a station named FOI1. FOI1 is an experimental FOI station and is not part of the

²<https://www.spirent.com/products/gnss-simulator-gss9000>

SWEPOS network. The lower figure shows the mean SNR value of all tracked GPS satellites for the days of January 20-21, 2021. The upper figure shows the SNR for PRN G05 for January 20, 2021 for 06-12 hours in UTC. Dotted boxes highlight regions where interference waves were simulated. Four different types of interference waves centered on the GPS L1 frequency were simulated. The first wave was an Additive white Gaussian noise (AWGN) with a 20 MHz bandwidth (red dotted box). The second simulated wave was an AWGN with a 2 MHz bandwidth (brown dotted box). In addition, two more waves were simulated, which are continuous wave unmodulated carrier (orange dotted box) and frequency modulated wave (green dotted box). A five minute interval was maintained before and after each simulated wave. The interference waves were simulated on January 20 and 21 with the same configuration.

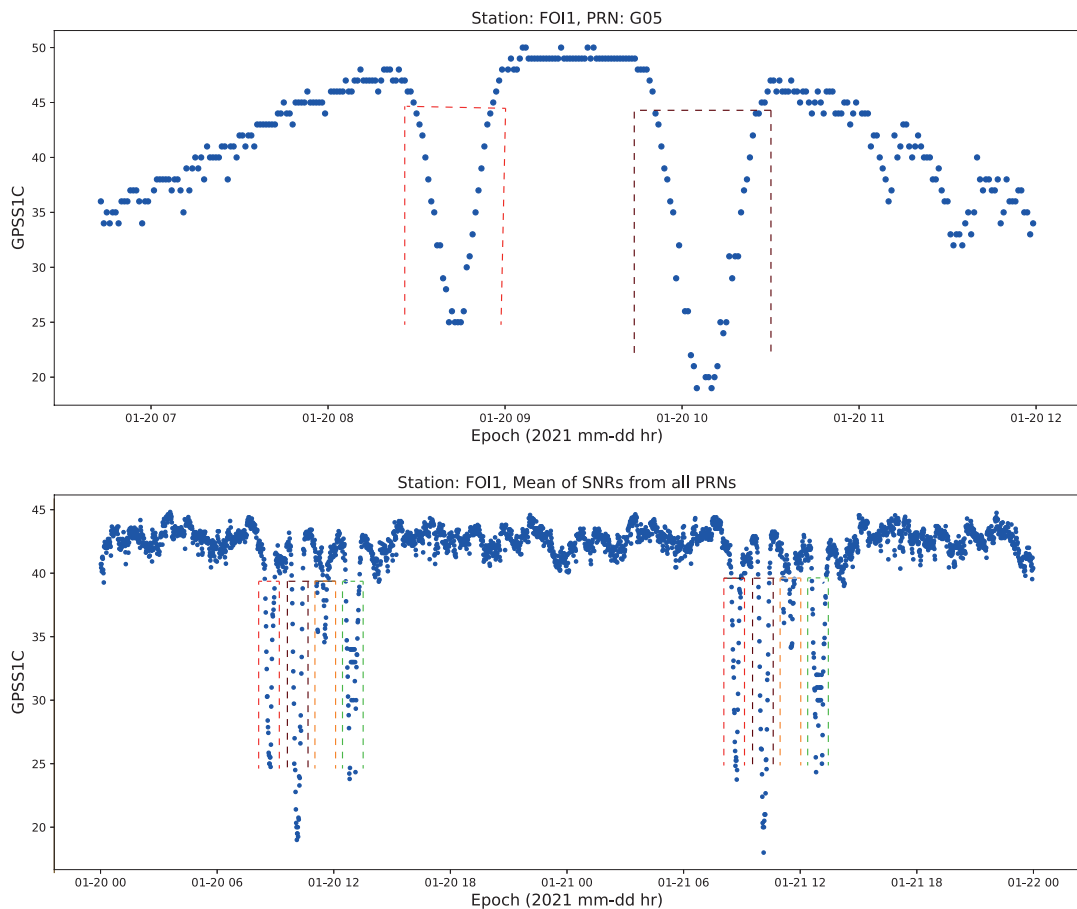


Figure 3.9: SNR time series for GPS L1 C/A code for station FOI1. The lower figure shows the mean value of all tracked satellites for the days of January 20-21, 2021. The upper figure shows the PRN05 GPS for January 20, 2021. Regions highlighted with dotted boxes indicate interference signals generated by the GNSS simulator conducted by FOI. The red dotted boxes indicate AWGN with a 20 MHz bandwidth, the brown dotted boxes indicate AWGN with a 2 MHz bandwidth, the orange dotted boxes show the unmodulated CW carrier, and the green dotted boxes show the frequency modulated waveform.

Since this is a simulated environment, the interference-free section of the data is known, that is, the data section in which interference is not simulated. RW is defined as described in section 3.2.1 using the interference free data. Using the RW model, SNR residuals are calculated for figure 3.9 and plotted in figure 3.10. Figure 3.10 shows the SNR residuals for PRN G05 (top) and the mean of all GPS PRNs (bottom). The figure shows much cleaner data compared to the raw data in figure 3.9. Modeling and

elimination of factors affecting SNR would reduce false alarms that would be mistaken for actual interference.

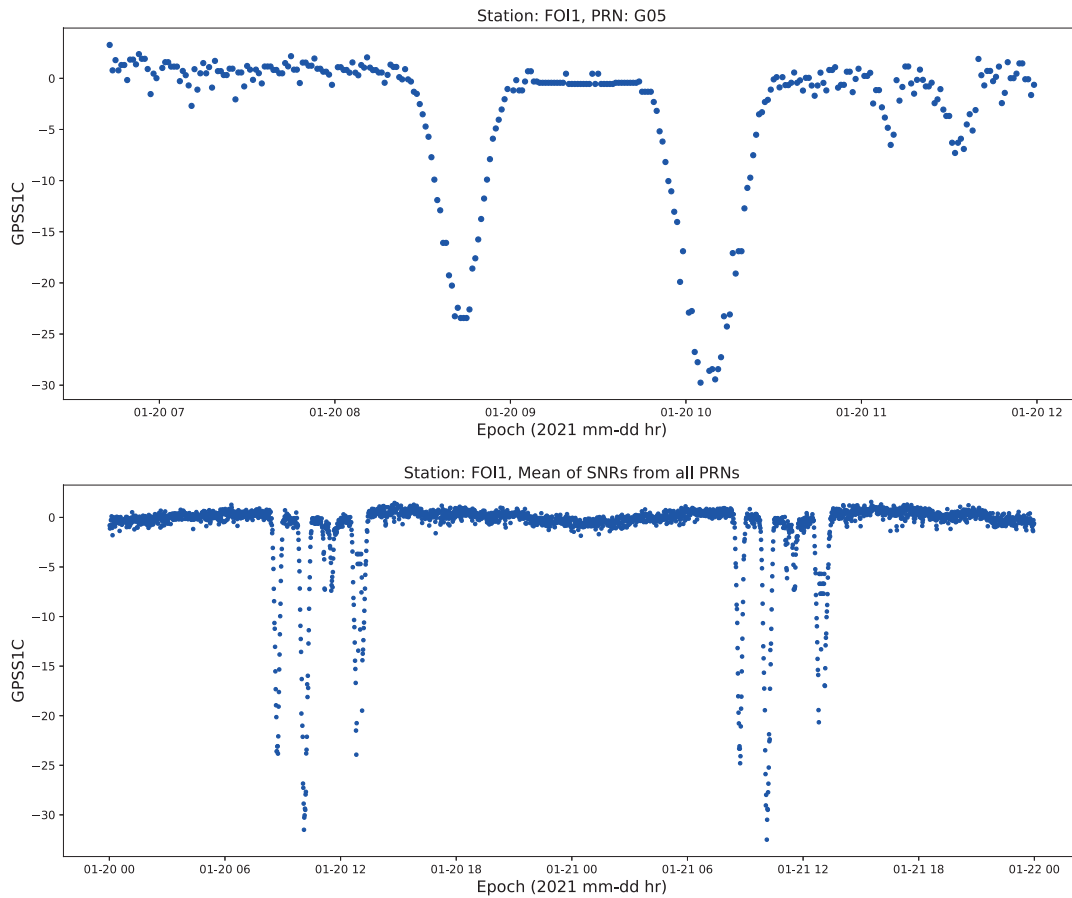


Figure 3.10: Time series of SNR residuals for GPS L1 C/A for GPS PRN05 (top) and mean from all GPS satellites (bottom).

Figure 3.11 is a plot of the SNR residuals and shows how the reference and evaluation windows are formed and compared. The green dots show the SNR residuals of the RW that are from the interference-free section of the data. The rest of the data shows the SNR residuals when the RW model is fitted. EWs of a size of 10 seconds are formed (blue boxes) that slide in time. The distributions of the EWs are compared to the RWs. A disturbance (red dots) is reported if an EW is not comparable to a RW according to the thresholds described in section 3.2.2. The red dots in the figure show that the four types of simulated interference waves have been detected. If ten consecutive EWs pass the disturbance test, which means that if no disturbances are

detected, a new RW is defined with a duration of 100 seconds, which the following data (EW) will be compared with (green points at the end of time series in figure 3.11). Creating the new RW from interference-free consecutive EWs allows monitoring of SNR drops in a short period of time, since the SNR is stationary for a short period of time and RW then would avoid long-term trends and variations.

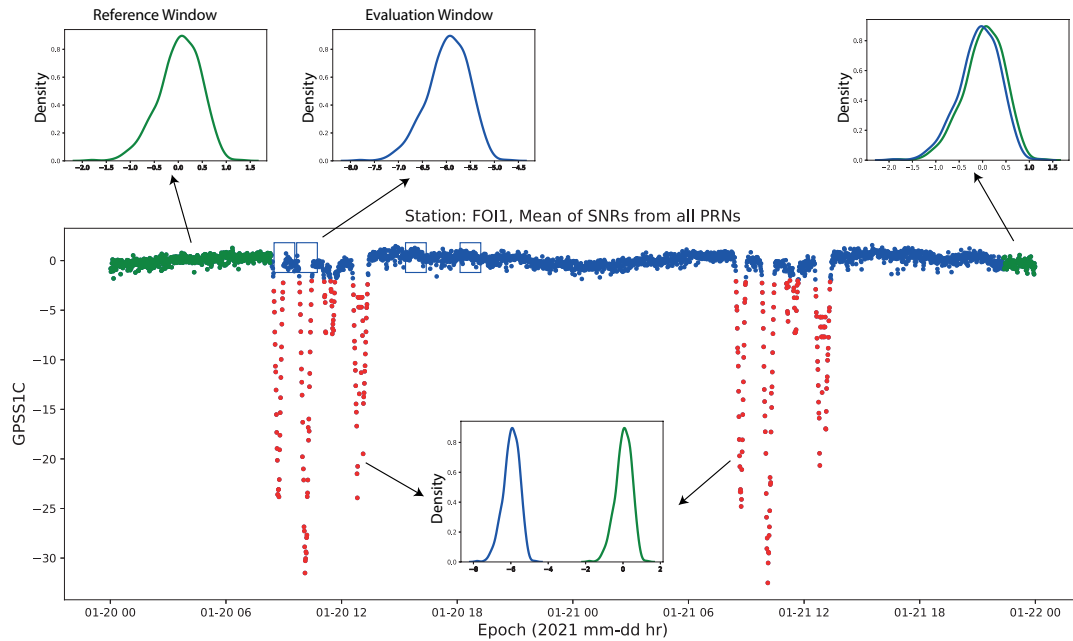


Figure 3.11: A demonstration of the SNR-based GNSS signal disturbance detection system. See text for details.

Furthermore, it can be seen from figure 3.11 that the method used here successfully detected the simulated intentional interference waves (red dots). It shows that SNR-based interference detection can detect all kinds of interfering signals as long as they are sufficiently powerful to degrade the GNSS signal power. However, the use of SNR-only-based disturbance detection would work poorly in identifying (un)intentional interference caused by jamming. This is due to the fact that other factors, such as degradation of satellite visibility, multipath and equipment failures, could also cause degradation of the GNSS signal strength. The SNR-based detection system would work well to detect signal interference of any source, but it may not be the sole means of classifying the types of interference and identifying the sources.

Chapter 4

Real signal disturbance incidents

This chapter presents actual signal interference incidents that have been detected using the SNR-based signal disturbance detection system described in chapter 3. More signal disturbance incidents detected at multiple stations from the SWEPOS network is presented in Appendix A.

4.1 RFI related disturbances

RFI detection is crucial for monitoring the quality of GNSS data and for national awareness and security. SWEPOS stations are built and located in a quiet environment and may not be optimal for detecting interference in sensitive infrastructure such as airports and military bases. However, the monitoring, detection and alerting RFIs using the SWEPOS network would continue to play an important role in raising awareness of the situation and national security needs.

RFI-related signal disturbances have been detected at several SWEPOS stations. Signal disturbances have been detected on the GPS L5, GAL E5 and BDS B2b frequencies for the Grisslehamn station (0GIS) on May 15, 2021 at 15:50 local time using the the SNR-based detection system. The station is part of the SWEPOS network-RTK service and is located in the port of Grisslehamn, Norrtälje Municipality, Stockholm County, Sweden. At the time of detection, the station was equipped with a Trimble NetR9 receiver and a JAVRINGANT_DM antenna.

Figure 4.1 shows the SNR residuals for the GPS L5 (top), GAL E5a (middle) and BDS B2b (bottom) signals. Green dots in the figures indicate undisturbed data, while orange and red dots indicate moderate and major disturbances, respectively. The interference causes the SNR values for these signals to drop by as much as 20 dBHz. After the incident, the network-RTK software showed poor performance in solving GAL satellites. A Septentrio PolaRx5 receiver was sent to the station and installed in parallel on May 20, 2021. During the visit, no changes were noted in the station environment that could cause interference. However, the port near the station is full of small and large vessels.

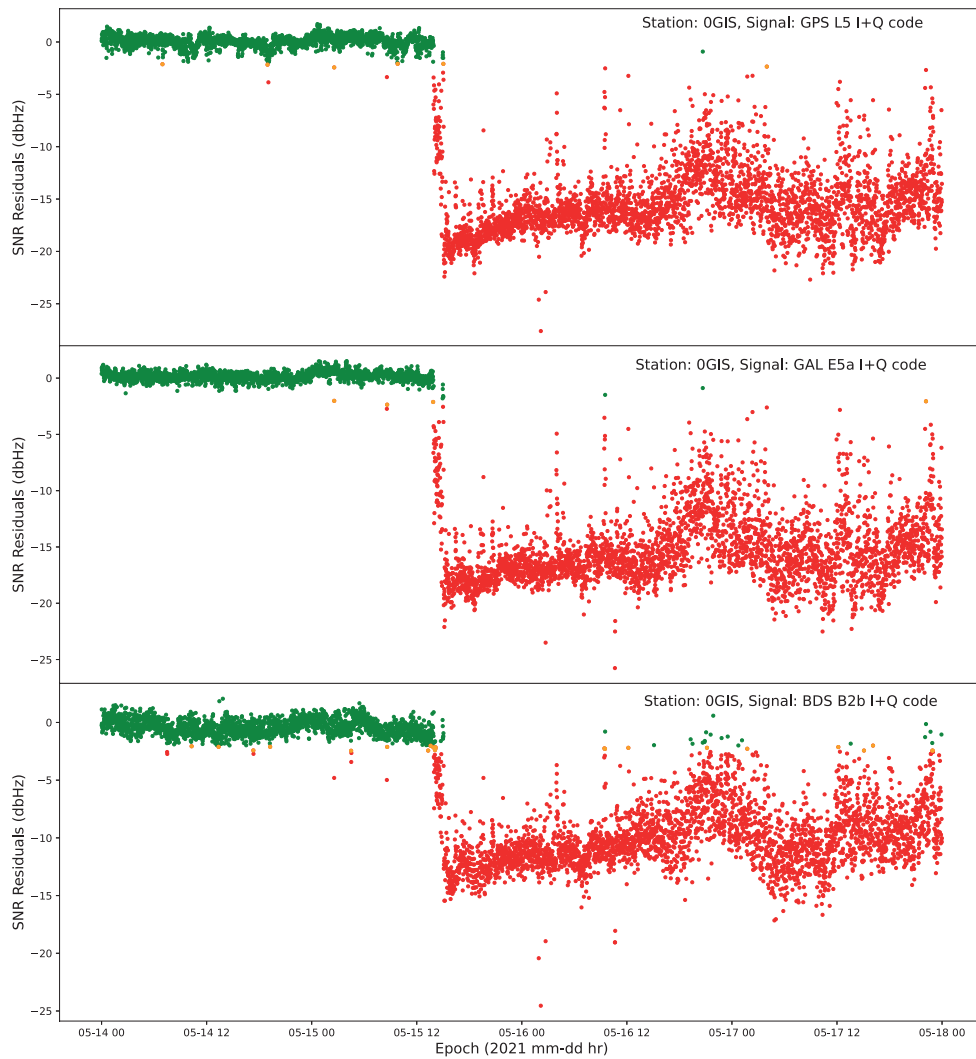


Figure 4.1: SNR residuals for GPS L5 (top figure) and GAL L5a (middle figure) and BDS B2b (bottom figure) for station 0GIS. Green dots indicate SNR residuals with no disturbances while orange and red dots indicate moderate and major disturbances, respectively.

A software-defined radio (SDR)¹ installed on a computer and used during the visit showed a strong signal centered at 1181.03 MHz. Figure 4.2 shows the RF spectrum (upper graph) and the waterfall display (lower graph) of what the SDR has recorded during the visit to the station. The scale in the top graph is the full decibel scale (dBFS). Zero dBFS represents a maximum possible signal level and the weakest signals

¹<https://www.rtl-sdr.com/>

are represented in negative dBFS numbers. The vertical red line in the RF spectrum shows the frequency to which the SDR is tuned and more information such as the dBFS values of the peak signal centered at 1181.03 MHz and the noise floor. The RF waterfall display (lower graph) shows the intensity of the signals (red represents high intensity signals). The horizontal axis of the waterfall display shows frequency, while the vertical axis is time.

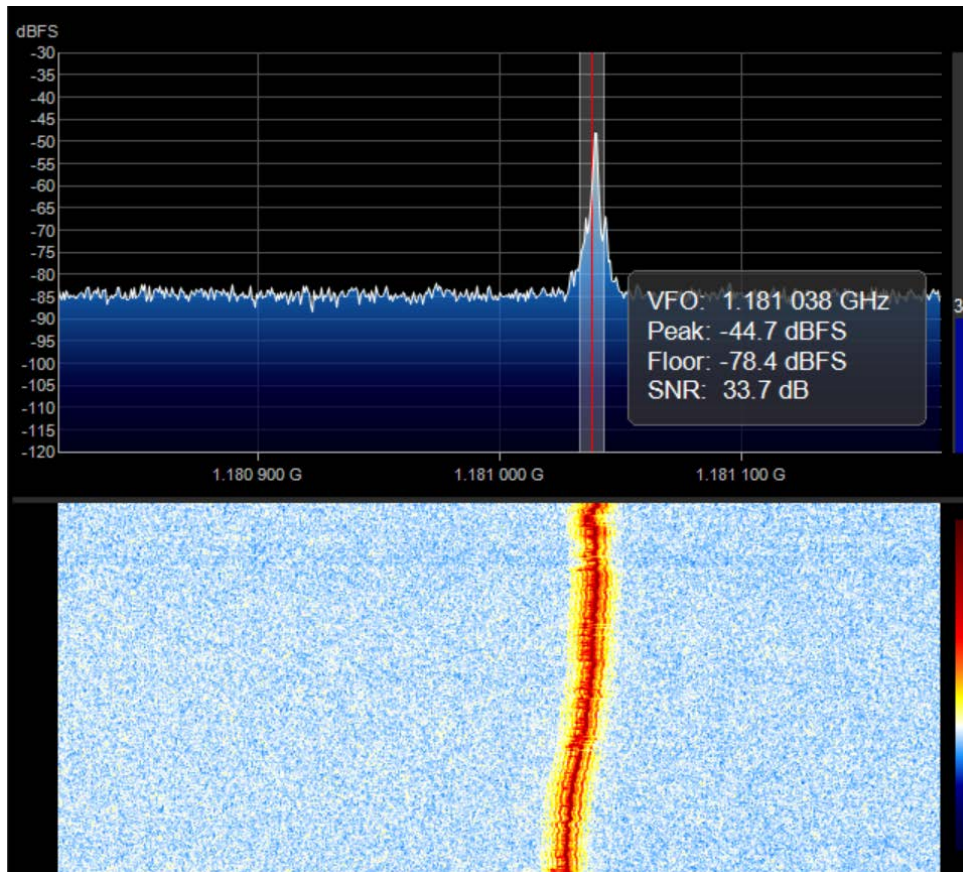


Figure 4.2: A fast Fourier transform spectrum and waterfall displays sample of the interference at OGIS as recorded by software defined radio (SDR).

Figure 4.3 shows a spectrum diagram of the spectral analyzer of the Septentrio PolaRx5 receiver indicating that the interference signal is a narrow band interference centered at 1181.67 MHz with a power of nearly 90 db. It has been observed that the center frequency of the interfering signal changes slightly with time, sometimes reaching 1182.8 MHz and the power ranging 90–100 db. Although the interfering signal is characterized by a narrow band, it affects a wider band of signals from 1176.45 MHz

(GPS L5, GAL E5a and BDS B2a signals) to 1207.14 MHz (GAL E5b and BDS B2b signals, see figure A.15). The effect of the interference has also been noticed in the TPP program where the L5 signal was lost for tracked GPS satellites and the program was unable to solve the GAL satellites.

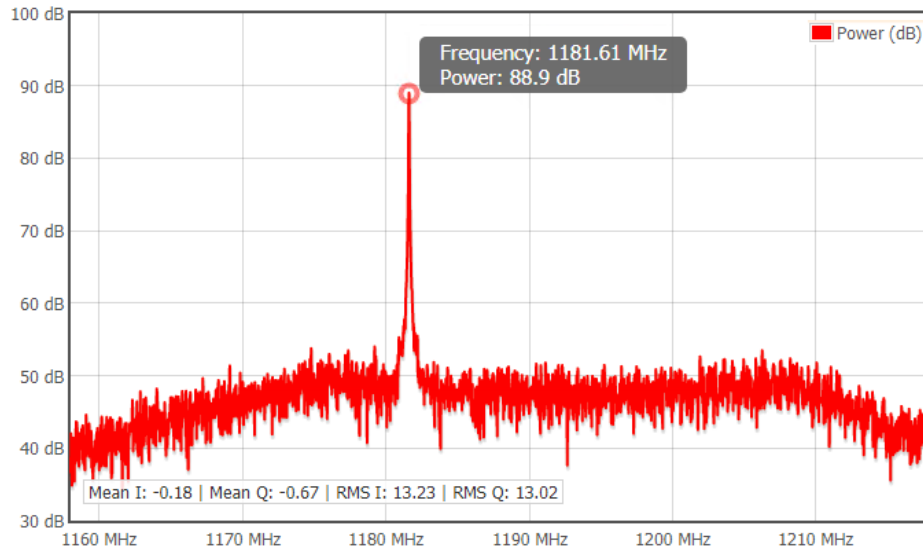


Figure 4.3: Spectrum from the Septentrio PolaRx5 receiver for the detected disturbances at OGIS on May 15, 2021.

SWEPOS is closely monitoring the situation and has reported the case to PTS on May 24, 2021. PTS visited the station on June 6, 2021 and confirmed the presence of the disturbance, its frequency and power, and attempted to locate the source. They suspected that the source could be a boat with a GPS tracker. However, the owner of the suspected boat took the boat on a trip the next day, but the disturbance continued to exist. At the time of writing, the disturbance has been active for 91 days and the source has not been found. PTS is still monitoring the situation and regularly visits the station to geolocate the source.

4.2 Equipment related disturbances

In addition to RFI, issues related to station equipment, such as antenna failure, could lead to SNR drops. This, in turn, would cause signal disturbance alarms. For a detection program that aims to detect RFI-related disturbances, such as jamming, signal disturbance alarms related to equipment failure are considered false alarms.

However, for the purpose of this work, it is necessary to detect signal disturbances from any source.

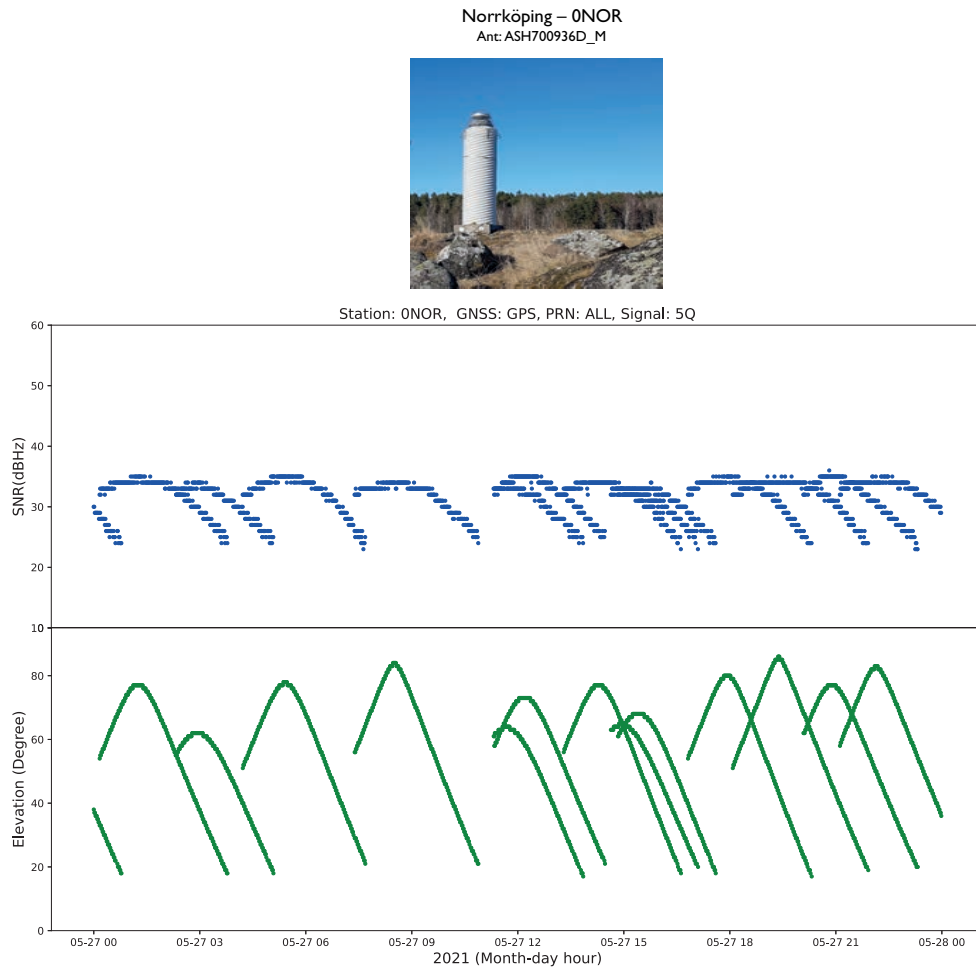


Figure 4.4: Top figure shows a picture of Norrköping (0NOR) station. The station is equipped with Septentrio PolaRx5 receiver and ASH700936A_M antenna. Middle figure shows SNR for GPS L5 from all tracked satellites for April 27, 2021. Bottom figure shows elevation angles of the satellites.

Signal disturbances have been detected in GPS L5, GAL E5a, E5b, E5 and BDS B2a, BDS B2b signals at stations 0LEK, 0LOV, 0NOR, 00SK, 0OVE, 0SKE, 0SVE, 0VIL. These stations are some of the old SWEPOS pillar stations and are not part of the network-RTK. All are equipped with Septentrio PolaRx5 receiver. The spectrum graphs of the receiver analyzer show a clean spectrum. Compared to other pillar stations like 0JON, the above-mentioned stations are equipped with old Ashtech an-

tennas. Figure 4.4 shows the SNR for GPS L5 for all tracked satellites (middle figure) and the elevation angles of the satellites (bottom figure) for 0NOR station - one of the pillar stations with disturbance of signal L5. The upper image of figure 4.4 shows an image of the station.

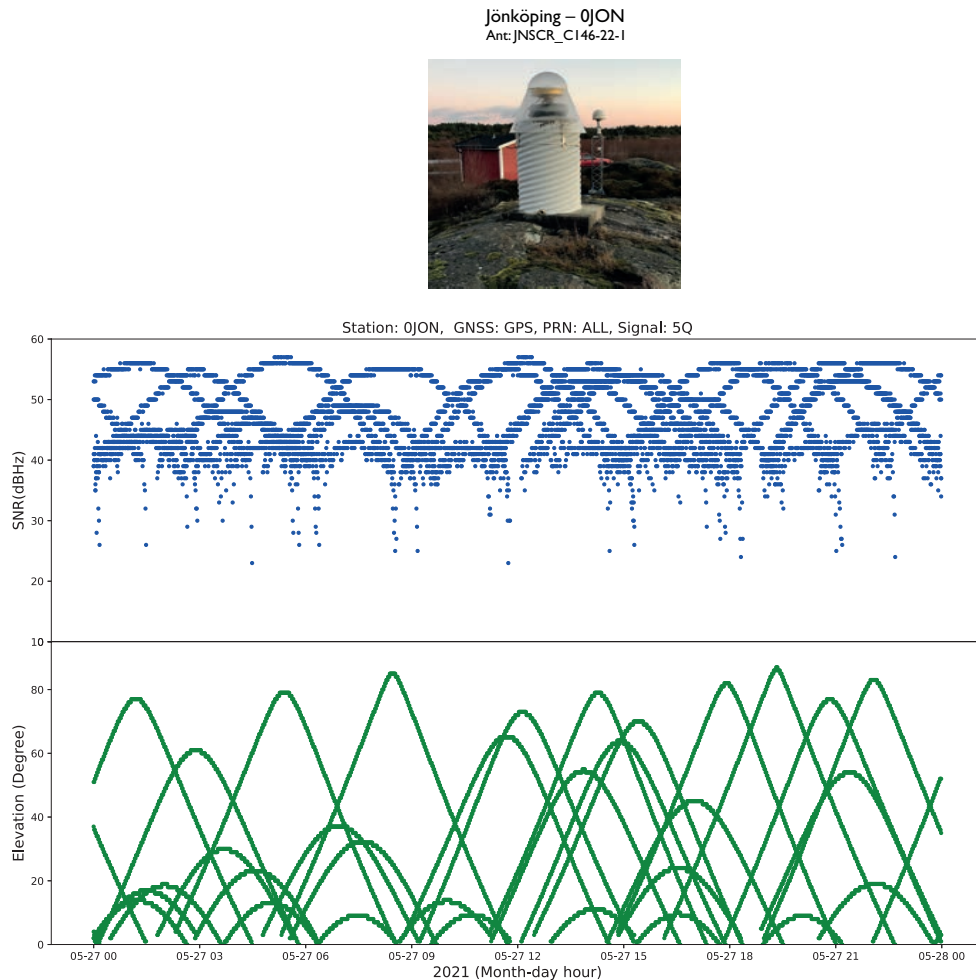


Figure 4.5: As in figure 4.4 but for Jönköping (0JON). The station is equipped with Septentrio PolaRx5 receiver and JNSCR.C146-22-1 antenna

For comparison, figure 4.5 shows the same figure as in 4.4 for 0JON, where no disturbances were observed at the same frequency. When comparing the two figures, it can be seen that the signal power is approximately 20 dBHz lower for 0NOR. Moreover, the receiver does not track the satellites until they reach a higher elevation. The same problem was observed for all pillar stations with ASH700936D_M OSOD antennas and

it was confirmed that the antenna type is not capable of handling the L5 signal. It is recommended to change the antenna for these stations if it is necessary to use them for any application in which all frequencies need to be used.

Another case of antenna failure-induced signal disturbances have been detected for station 1STV on July 25, 2021. The station was equipped with a Septentrio PolaRx5 receiver and a JNSCR_C146-22-1 OSOP antenna. The signal disturbance alarm for the station indicated that all signals, but those in the GPS L1 band were affected. Figure 4.6 shows SNR residuals for GPS L1, which was not affected by the disturbance, and GLO G2, GAL E5a, and BDS B2b signals, which were affected by the disturbance. The signal strength of all frequencies except the L1 band has started to decline.

As of July 26, the disturbances were persistent and lasted 24 hours every day. However, there were no signs of disturbance in the spectral analysis of the receiver. Also, AGC values reported from the receiver do not show any problem. The TPP performance report for the station, however, showed that some signals such as GPS L2 were lost and the number of resolved satellites decreased significantly. We suspected that the problem could be related to the antenna. The station has been flagged off from the network-RTK service on the 4th of August, 2021 until it is possible to identify the problem. The antenna was changed to LEIAR20 OSOP on the 10th of August, around 12:50 UTC and the problem has since been resolved.

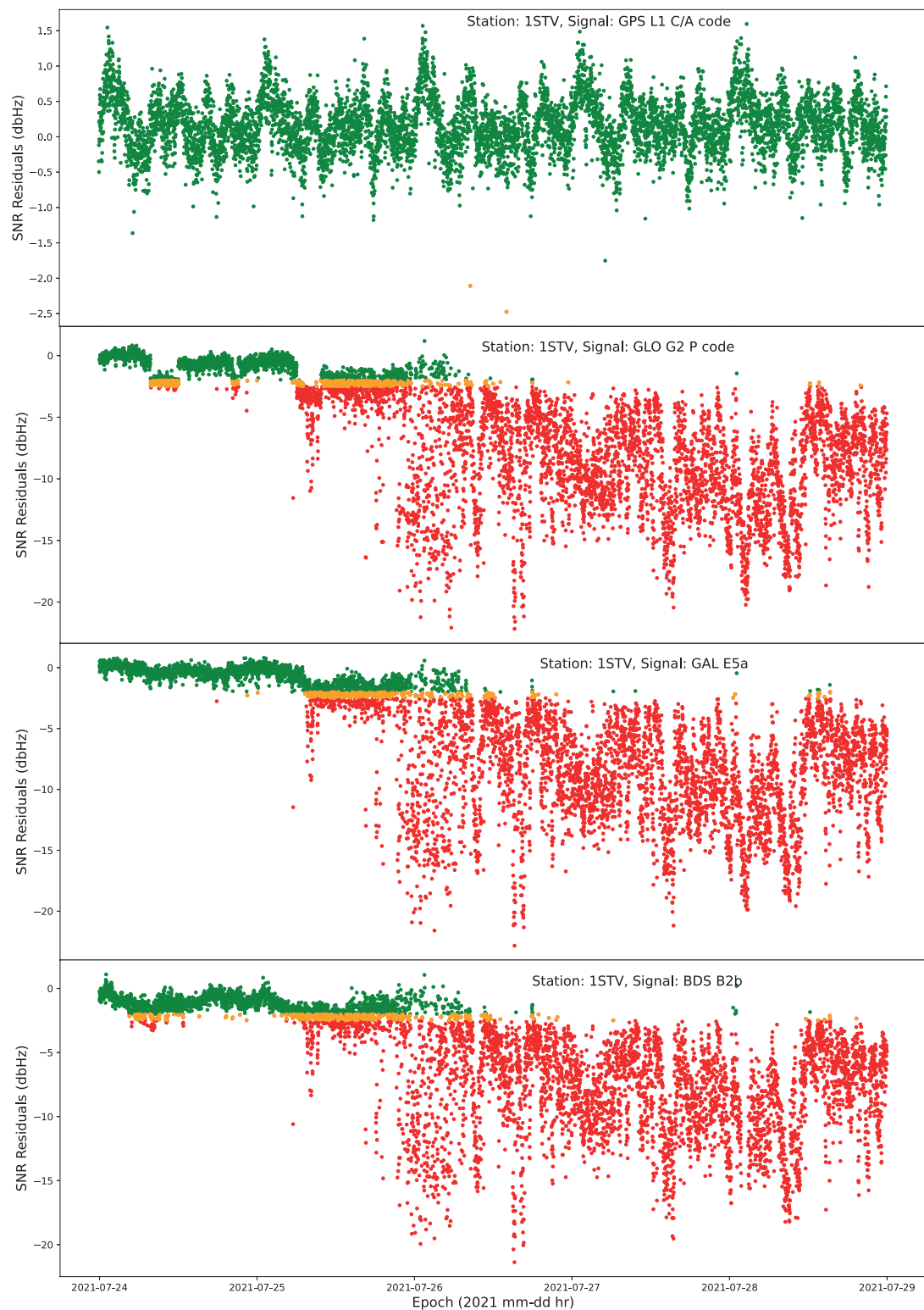


Figure 4.6: SNR residuals for GPS L1, GLO G2, GAL E5a, BDS B2b signals for station 1STV.

Figure 4.7 shows station performance in terms of the number of tracked and solved satellites. Since the problem started and before the antenna change, both the number of satellites tracked and those solved by the network-RTK system were low, only 10-40 percent of the satellites tracked were solved, sometimes even zero. After the antenna change (vertical dotted line), 80-95 percent of the tracked satellites were resolved. The station was flagged back on to the network-RTK system on the 16th of August, 2021, as it performed well within the next five days after the antenna change.

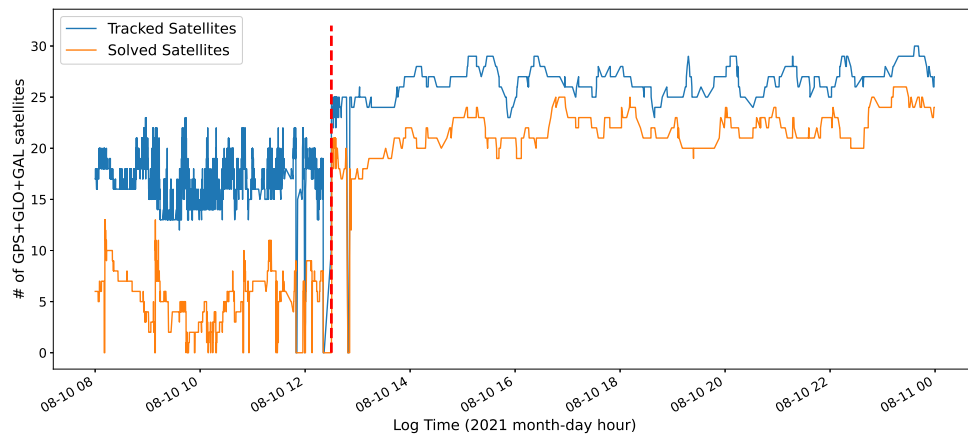


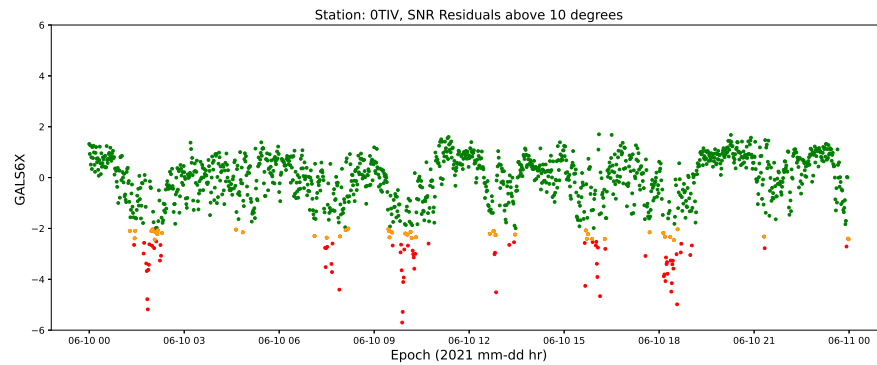
Figure 4.7: Station performance in the network-RTK system for 1STV. The blue line shows the total number of GPS, GLO and GAL satellites tracked, while the orange line shows how many have been resolved from the tracked satellites. The vertical dotted line shows the epoch when the antenna is changed from JNSCR_C146-22-1 to LEIAR20.

4.3 Station environment related disturbances

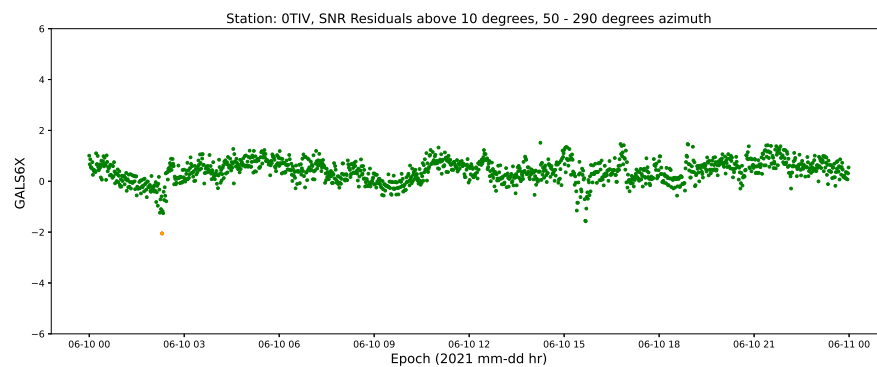
SWEPOS stations are established in a relatively quiet environment with minimal signal obstructions and multipath, so unpredictable SNR drops that are not related to RFI are minimal. However, SNR drops can still occur due to, for example, antenna failures (see section 4.2), new structures built near stations, birds perched on the antenna, snow covering the antenna or trees growing nearby and compromising the station's sky-view. These factors cannot be modeled because they are unpredictable. Signal disturbance due to these factors is likely to cause false alarms and lead to less accurate RF-related

interference detection systems. However, non-RFI-related disturbances also interests SWEPOS to be detected. They must be detected so that a measure can be taken to reduce the effect, which could be the felling of trees, the removal of snow from the antenna or the transfer of the station to a new location if necessary (see section 1.3.1 as an example).

GNSS signal disturbances were detected at station OTIV. The disturbances occurred on all GNSS frequencies. Spectral analysis from the station's receiver, however, shows a clean spectrum with no signs of interference. Figure 4.8a shows SNR residuals for GAL E6 signal for June 10, 2021. SNR residuals from satellite elevation angles below 10 degrees are discarded. The residual SNR pattern in figure 4.8a was also clearly visible at all other frequencies. However, a detailed analysis shows that disturbances occur only in certain azimuth directions.



(a)



(b)

Figure 4.8: SNR residuals for GAL E6 signal for station 0TIV. The upper figure shows the residuals for the entire horizon of the station, while the lower figure shows the residuals for azimuth from 50 to 290 degrees. The different colors are as in figure 4.1.

Figure 4.8b shows the SNR residuals as in figure 4.8a but for azimuth from 50 to 290 degrees. By discarding the data from 0 to 50 degrees and 290 to 360 degrees of azimuth, the disturbances in figure 4.8a (red dots) disappeared. This indicates that the disturbances (SNR drops) were located in a certain direction.

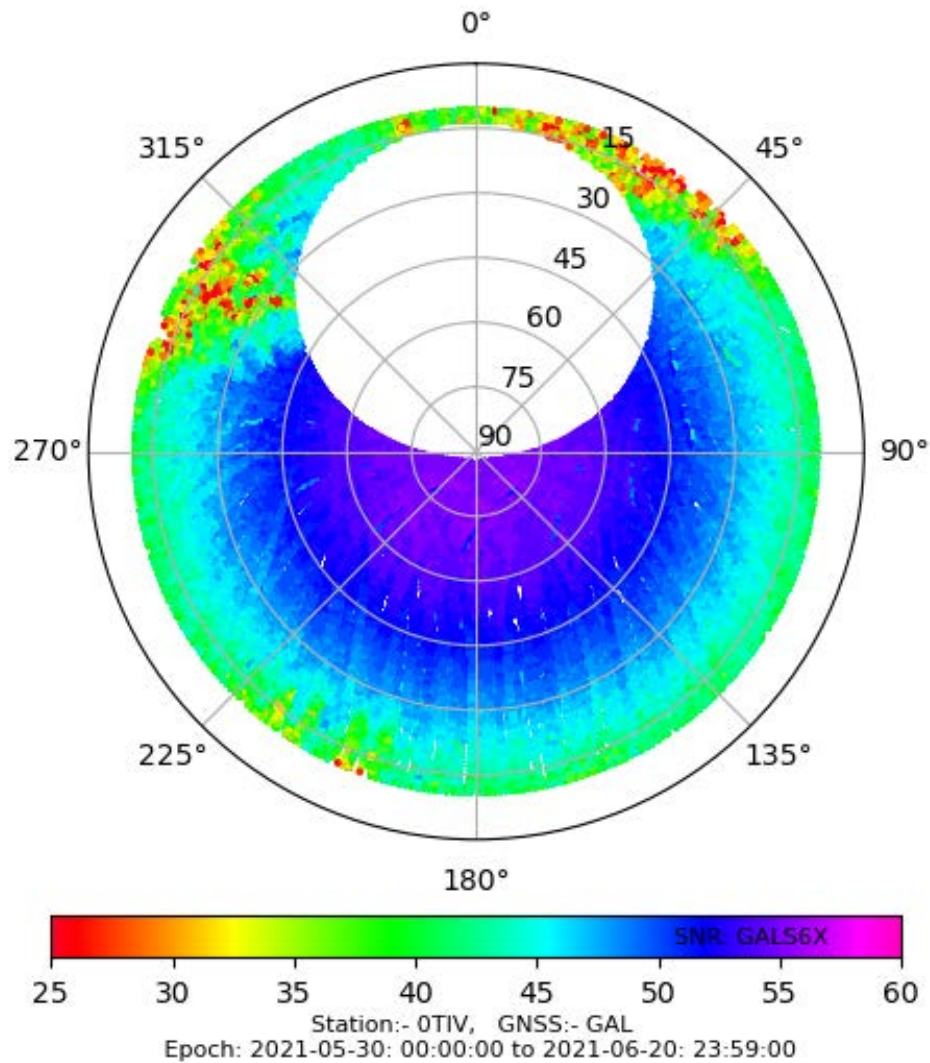


Figure 4.9: Elevation-azimuth diagram of SNR for GAL E6 signal for station 0TIV. Colors show SNR values.

Figure 4.9 shows the elevation-azimuth diagram of the tracked GAL satellites for the SNR (color-coded) of the E6 signal stacked over three weeks of data. The figure shows a clearer picture of the localized nature of the disturbances. SNR values are low, reaching less than 30 dBHz at 0–50 and 290–360 degrees of azimuth. When signals are affected only in certain directions, the effect is unlikely to be RFI, as otherwise the interference would cause the SNR to decrease in all directions. Actual images of the station environment show large trees blocking the northern and northwestern regions

of the station horizon, which are the likely cause of the SNR drops in that direction. Also, the station reportedly performs poorly on the TPP system. It is recommended to cut down the trees or find a new location for the station.

Chapter 5

Summary

SWEPOS evaluates its service performance and verifies the quality of its data on a daily basis. This report is part of that and evaluating and monitoring the quality of the SWEPOS data has been the main focus. Its objective is to monitor the signal strength of multi-frequency and multi-GNSS observations from the entire SWEPOS network and detect problematic stations early.

A prototype system for GNSS signal disturbance detection has been developed based on monitoring SNR properties in a post-processing mode with RINEX files. It models the SNR for each GNSS signal and SWEPOS station, monitors its variation, and alerts SNR drops of any cause. Unwanted reductions in SNR values are of interest to the detection system. The GNSS signal strength may decrease in the presence of RFI, e.g. when a jammer is close to the receiver, or due to equipment failure, or multipath. For an application that is intended to detect RFI-related signal disturbances, for example due to jamming, SNR drops caused by degraded satellite visibility, multipath or equipment failures can lead to misjudgment of the drops, for example as jamming. The goal of the prototype developed here, however, is a situational awareness of signal disturbances of any cause. Detected disturbances are then further investigated to identify the cause. Consequently, GNSS signal interference caused by RFI, antenna failure, and station environment, such trees, has been detected at several SWEPOS stations, characterized, and reported to authorized bodies such as PTS for awareness and geo-locating the source.

More work is required and is in progress to improve the system. Future work includes extending the prototype for real-time applications, comparing the method with other detection methods, complementing SNR measurements with other pre- and post correlation measurements such as AGC. Moreover, to reduce the multipath effect, SNRs below 20 degrees elevation are discarded. This discards a subtle amount of data. The use of multipath filtering techniques could reduce the effect and improve the overall performance of the system in detecting disturbances.

Bibliography

- Akos D (2012) Who's Afraid of the Spoofer? GPS/GNSS Spoofing Detection via Automatic Gain Control (AGC). *J Inst Navig* pp 281–290
- Alexandersson M, Fors K, Stenberg N, Frisk A, Nilsson JT, Wiklund P, Abraha KE (2021) Robust Satellitnavigering med SWEPOS – Kan SWEPOS användas för att detektera störning i GNSS-banden? FOI-R-5187-SE
- Axell E (2014) GNSS interference detection. FOI URL <https://www.foi.se/rest-api/report/FOI-R--3839--SE>
- Axell E, Eklöf FM, Johansson P, Alexandersson M, Akos DM (2015) Jamming Detection in GNSS Receivers: Performance Evaluation of Field Trials. *NAVIGATION* 62(1):73–82, DOI <https://doi.org/10.1002/navi.74>, URL <https://onlinelibrary.wiley.com/doi/abs/10.1002/navi.74>, <https://onlinelibrary.wiley.com/doi/pdf/10.1002/navi.74>
- Balaei A, Dempster A, Barnes J (2006) A Novel Approach in Detection and Characterization of CW Interference of GPS Signal Using Receiver Estimation of C/No. In: 2006 IEEE/ION Position, Location, And Navigation Symposium, pp 1120–1126, DOI 10.1109/PLANS.2006.1650719
- Bastide F, Akos D, Macabiau C, Roturier B (2003) Automatic gain control (AGC) as an interference assessment tool. *ION GPS/GNSS* pp 2042 – 2053, DOI 16thInternationalTechnicalMeetingoftheSatelliteDivisionofTheInstituteofNavigation, Portland,UnitedStates
- Benton CJ, Mitchell CN (2011) Isolating the multipath component in GNSS signal-to-noise data and locating reflecting objects. *Radio Science* 46(6), DOI <https://doi.org/10.1029/2011RS004767>, URL <https://agupubs.onlinelibrary.wiley.com/doi/abs/10.1029/2011RS004767>
- Bilich A, Larson KM, Axelrad P (2008) Modeling GPS phase multipath with SNR: Case study from the Salar de Uyuni, Bolivia. *Journal of Geophysical Research: Solid Earth* 113(B4), DOI <https://doi.org/10.1029/2007JB005194>, URL <https://agupubs.onlinelibrary.wiley.com/doi/abs/10.1029/2007JB005194>
- Borio D, Gioia C (2015) Real-time jamming detection using the sum-of-squares paradigm. In: 2015 International Conference on Localization and GNSS (ICL-GNSS), pp 1–6, DOI 10.1109/ICL-GNSS.2015.7217161

- Calcagno R, Fazio S, Savasta S, Dovis F (2010) An interference detection algorithm for COTS GNSS receivers. In: 2010 5th ESA Workshop on Satellite Navigation Technologies and European Workshop on GNSS Signals and Signal Processing (NAVITEC), pp 1–8, DOI 10.1109/NAVITEC.2010.5708008
- Emardson R, Jarlemark P, Bergstrand S, Nilsson T, Johansson J (2009) Measurement accuracy in Network-RTK. SP Report 2009:23, SP Technical Research Institute of Sweden URL <https://www.lantmateriet.se/globalassets/kartor-och-geografisk-information/gps-och-geodetisk-matning/publikationer/measurement-accuracy-in-network-rtk.pdf>
- Emardson R, Jarlemark P, Johansson J, Bergstrand S (2011) Ionospheric Effects on Network-RTK. SP Report 2011:80, SP Technical Research Institute of Sweden URL <https://www.lantmateriet.se/globalassets/kartor-och-geografisk-information/gps-och-geodetisk-matning/publikationer/ionospheric-effects-on-network-rtk.pdf>
- Esenbuğa G, Hauschild A (2020) Flex power on GPS Block IIR-M and IIF. GPS Solut 24(91), DOI <https://doi.org/10.1007/s10291-020-00996-x>
- Gurtner W (1994) RINEX: The Receiver-Independent Exchange Format. GPS World, Volume 5, Number 7 URL <http://www2.unb.ca/gge/Resources/gpsworld.july94.pdf>
- Jivall L, Lidberg M (2000) SWEREF 99 - an Updated EUREF Realisation for Sweden. EUREF symposium in Tromsø, 2000-06, 22-24 URL https://www.lantmateriet.se/contentassets/0ffb8deacf654776956dc5a3a1bedbbe/etrs89_proceed.pdf
- Johansson J, Lidberg M, Jarlemark P, Ohlsson K, Löfgren J, Jivall L, Ning T (2019) CLOSE-RTK 3: High-performance Real-Time GNSS Services. RISE Report 2019:101 URL https://www.lantmateriet.se/globalassets/kartor-och-geografisk-information/gps-och-geodetisk-matning/publikationer/close-rtk_3.pdf
- Linder S, Fors K, Stenumgaard P, Hedström J, Eliardsson P, Ranström T, Axell E, Mörnstedt F (2019) Telekonflikt - Sammanfattning 2018-2019. FOI-R-4832-SE. FOI
- Ndili A, Enge P (1998) GPS receiver autonomous interference detection. In: IEEE 1998

Position Location and Navigation Symposium (Cat. No.98CH36153), pp 123–130, DOI 10.1109/PLANS.1998.670032

Nilsson T, Ning T (2019) Anubis assessment. internal PM, Lantmäteriet

Norin D, Jonsson B, Wiklund P (2008) SWEPOS™ and its GNSS-based Positioning Services. Integrating the Generations, FIG Working Week, Stockholm, Sweden 14-19 June 2008 URL https://www.lantmateriet.se/globalassets/kartor-och-geografisk-information/gps-och-geodetisk-matning/publikationer/fig2008_norin_et_al.pdf

Steigenberger P, Thölert S, Montenbruck O (2019) Flex power on GPS Block IIR-M and IIF. GPS Solut 23(8), DOI <https://doi.org/10.1007/s10291-018-0797-8>

Vaclavovic P, Dousa J (2016) G-Nut/Anubis: Open-Source Tool for Multi-GNSS Data Monitoring with a Multipath Detection for New Signals, Frequencies and Constellations. In: IAG 150 Years, pp 775–782, URL https://link.springer.com/chapter/10.1007/1345_2015_97

Appendix A

Appendix with more figures and tables

A.1 More signal disturbance incidents

A.1.1 Östra Frölunda (TOST)

Signal disturbances have been detected on the GPS L2 and GLO G2 frequencies for the TOST station. The station is located in Östra Frölunda, Sweden, and was equipped with a Trimble NetR9 receiver and TRM55971.00 antenna without radome. Figure A.1 shows the SNR residuals for GPS L1 C/A code (upper figure) and mixed GPS L2C M+L codes (lower figure). Although no disturbances are detected on the L1 frequency, the upper part of the figure is included for comparison. The data of the figures are for the period of May 17 to June 2, 2021. However, signal disturbances have been detected in the GPS L2 signal for this station in more days since doy (day-of-year) 103, 2021 (see table A.2).

The disturbances occur mainly in the GPS L2 signal and that they appear and disappear in certain periods with variable intensity. During the strongest periods, disturbances in the GLO G2 frequency have also been observed. The strength, starting time, and duration of disturbances vary. The disturbances only occurred on weekdays. There have been no reported disturbances on weekends. During most days, disturbances begin in the morning between 8:20 and 10:00 local time (CEST). On some days it starts in the afternoon. The duration varies from day to day. This station is managed by Trimble and they have been informed on the case for awareness and further investigations.

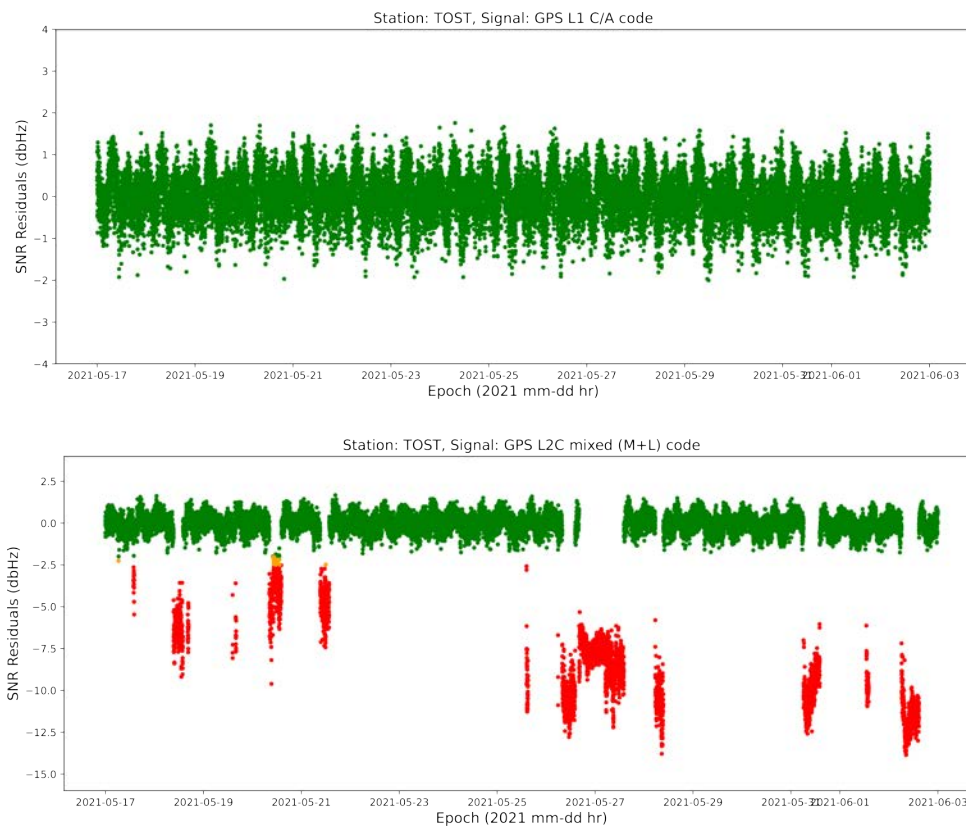


Figure A.1: SNR residuals for GPS L1 (upper figure) and L2 (lower figure) signals for station TOST. Green dots indicate SNR residuals with no disturbances while orange and red dots indicate moderate and major disturbances, respectively.

A.1.2 Gällivare (0GVA)

Signal disturbances have been detected in the 0GVA station, mainly affecting the GPS L1, GAL E1 and BDS B1-2 signals. Figures A.2 and A.3 show the SNR residuals of the affected signals for days 103-109, 2021. The station was equipped with a Trimble NetR9 receiver and JNSCR_C146-22-1 OSOD antenna. The receiver was changed to Trimble Alloy on day 138, 2021. More days with signal disturbances can be seen in table A.2. Figure A.4b shows a spectrum diagram of the affected signal spectrum (upper figure). The graph in figure A.4b is included to indicate what the spectrum would look like when there are no disturbances. Poor performance, where a drop in the number of satellites resolved for GPS and GLO, has been reported by TPP in those specific periods for the station.

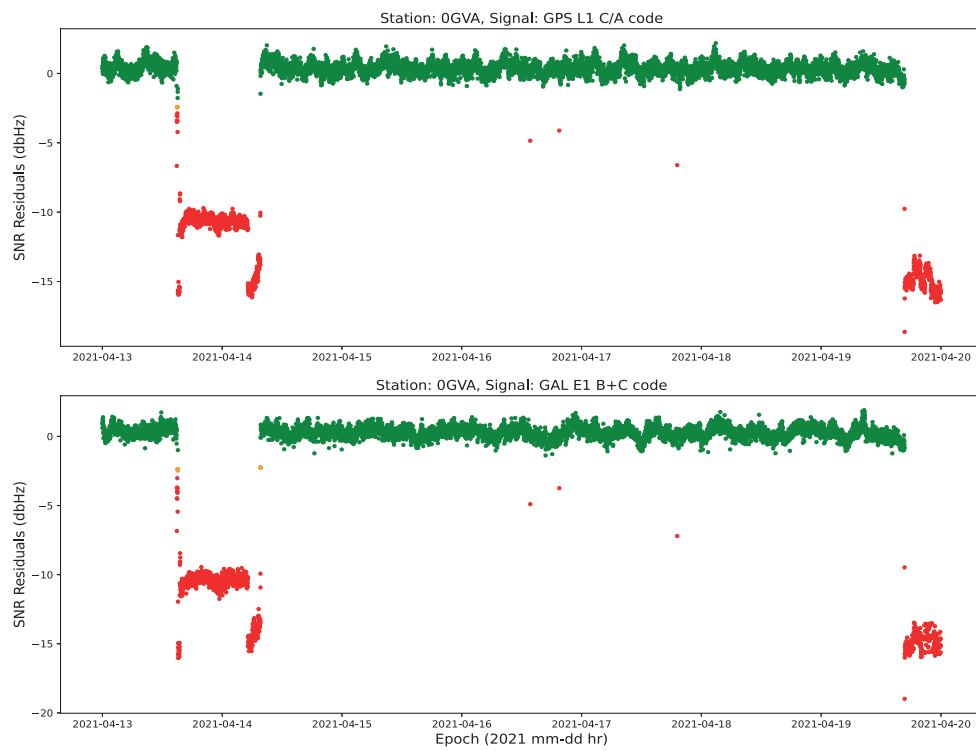


Figure A.2: SNR residuals for GPS L1 (top) and GAL E1 (bottom) signals for station OGVA. The different colors are as in figure A.1.

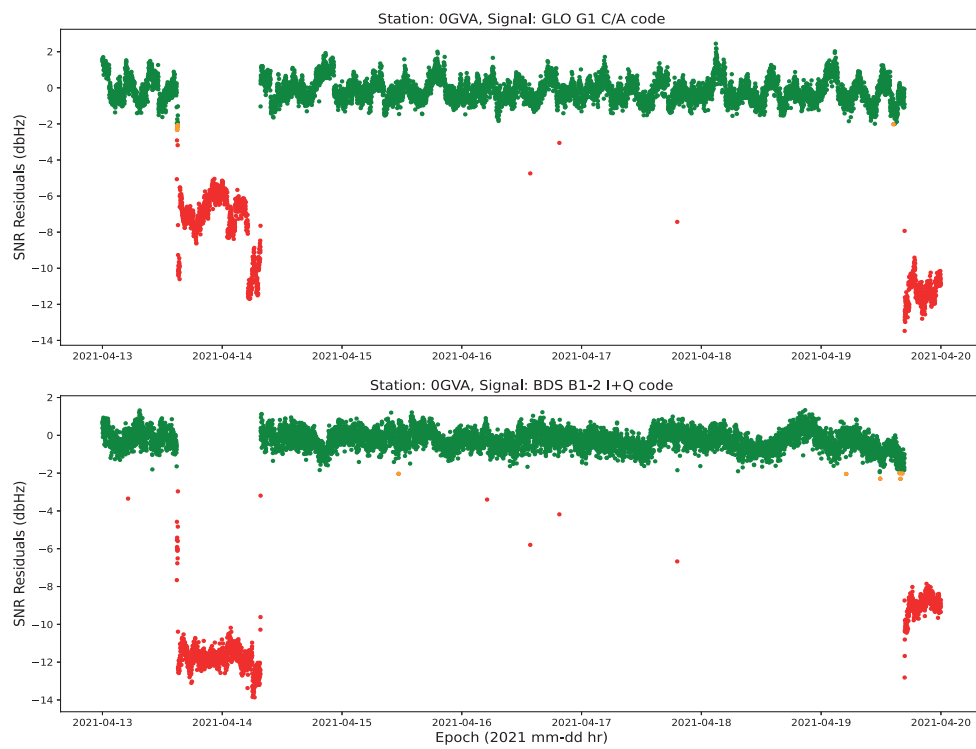
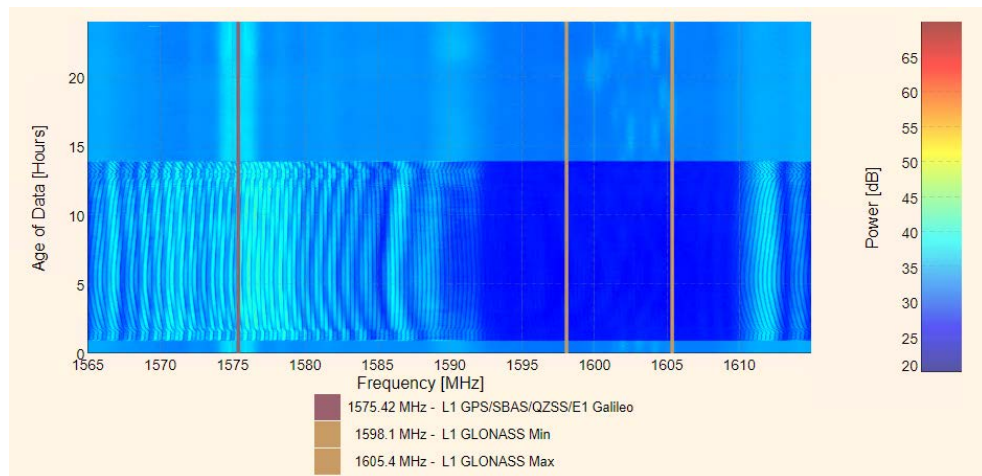
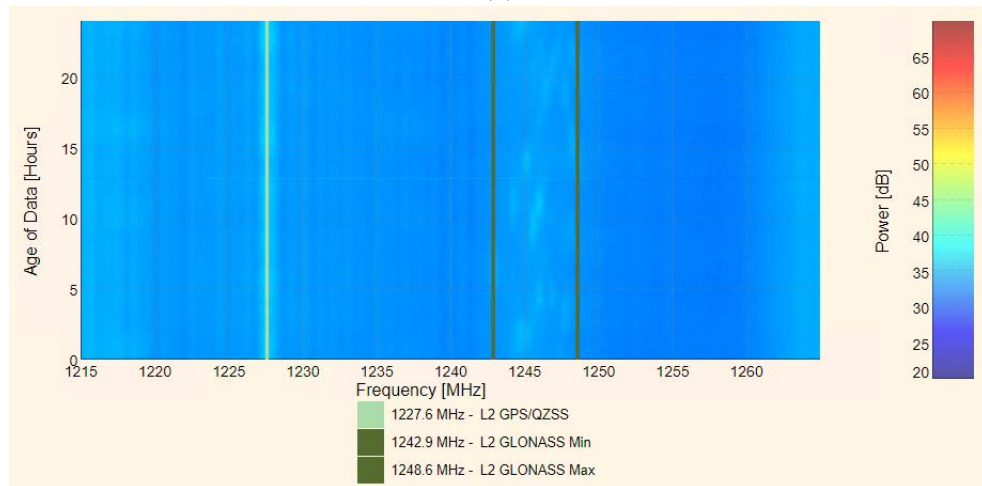


Figure A.3: SNR residuals for GLO G1 (top) and BDS B1-2 (bottom) signals for station 0GVA.



(a)



(b)

Figure A.4: Waterfall format spectrum plot – time-versus-frequency for station 0GVA. Colors indicate the power of the signal. Figure (a) shows spectrum for the frequency range 1565 - 1615 MHz, which covers GPS L1, GAL E1 and GLO G1 frequencies. Spectrum for the frequency range 1215 - 1265 MHz, which covers GPS L2 and GLO G2 frequencies, is included in (b) for comparison.

A.1.3 Skövde (1SKV)

A signal disturbance has been detected for the 1SKV station that affected the GPS L1, GAL E1 and GLO G1 signals. The station had a Trimble Alloy receiver and a JNSCR_C146-22-1 OSOD antenna at the time of detection. Figures A.5 and A.6 show SNR residuals of affected signals for days 104-106, 2021. Personal communication with

SWEPOS data quality focus group confirmed similar but short-term disturbances have been reported during the same month in 2017 and 2018. Disturbances were observed on day 115, 2017 and days 112-114, 2018. The source of the disturbances is still unknown as the nature of its short period does not allow enough time for further investigation.

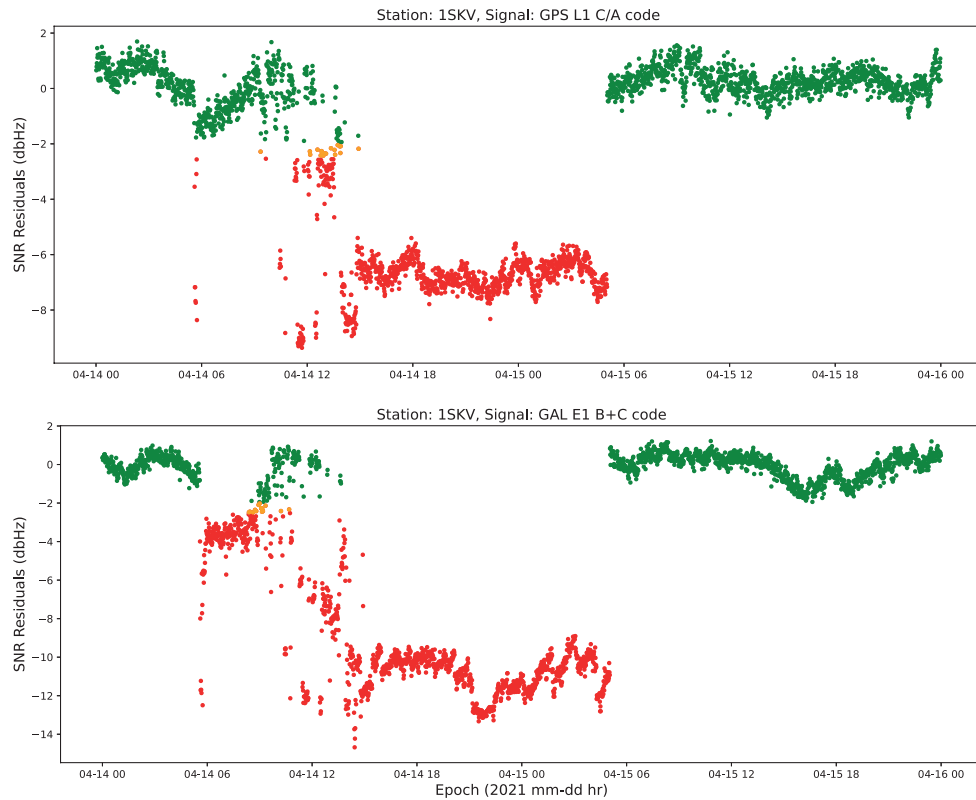


Figure A.5: SNR residuals for GPS L1 (top) and GAL E1 (bottom) signals for station 1SKV. The different colors are as in figure A.1

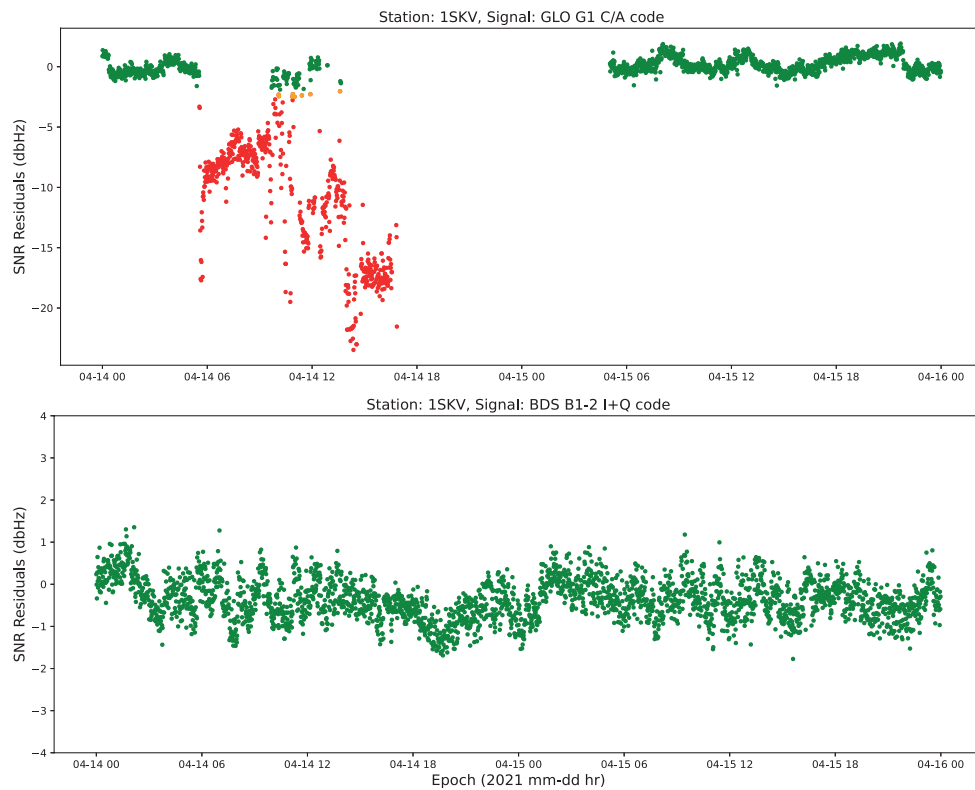


Figure A.6: SNR residuals on GLO G1 (top) for station 1SKV. SNR residuals for BDS B1-2 (bottom) is included for comparison but hasn't been affected by the disturbances.

A.1.4 Mockfjård (0MOC)

A major disturbance has been detected that lasted for more than 14 hours from doy 193 21:20 UTC to doy 194 11:39 UTC, 2021 for station 0MOC. The station is equipped with a Trimble Alloy receiver and a JNSCR_C146-22-1 OSOD antenna. The disturbance affected all signals except those in the L1 frequency range. Figures A.7, A.8, and A.9 show the SNR residuals for the affected signals for doys 193-194, 2021. The disturbances have not returned since then and the sources have not been known.

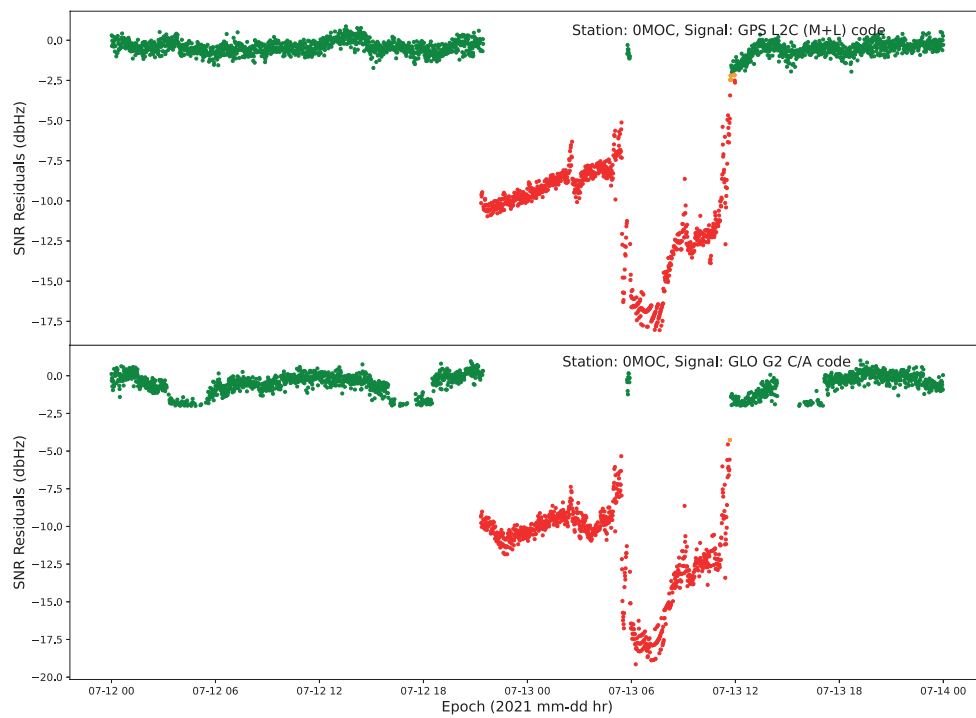


Figure A.7: SNR residuals for GPS L2C (top) and GLO G2 (bottom) signals for station 0MOC. The different colors are as in figure A.1

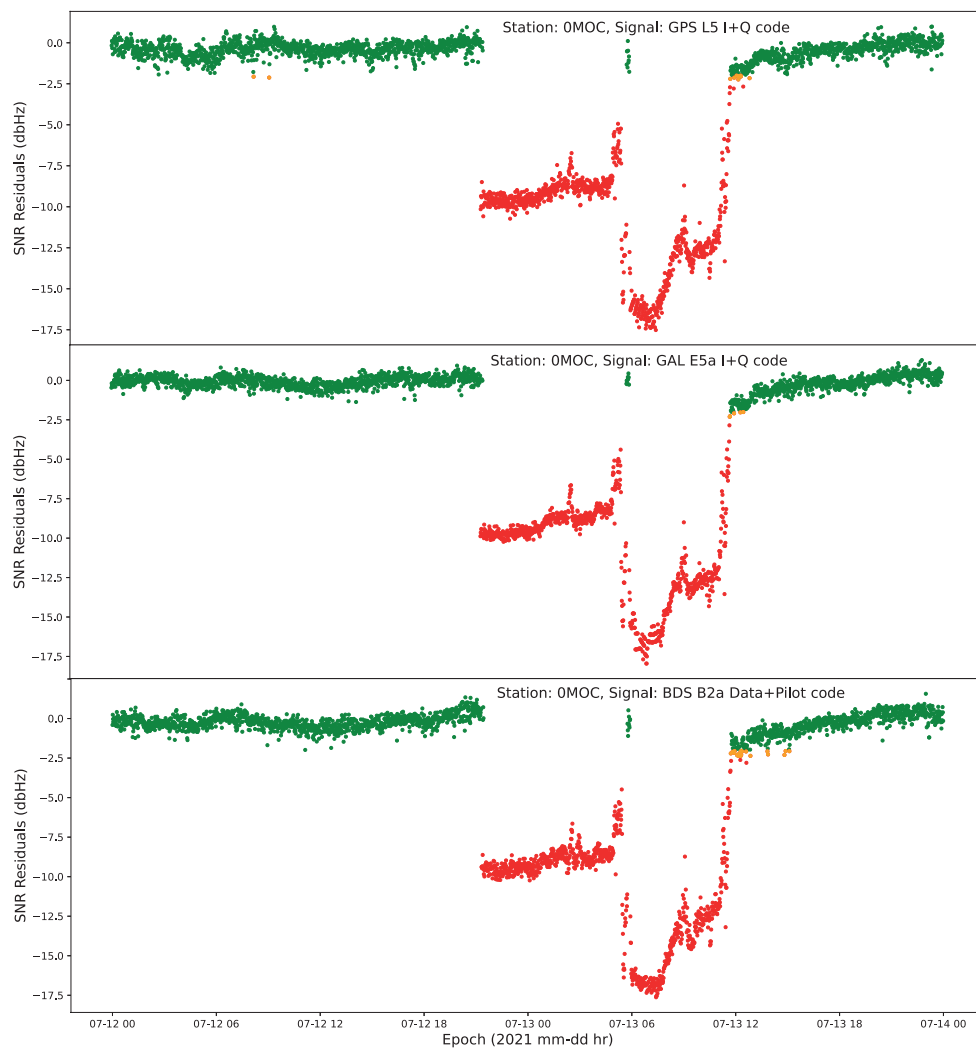


Figure A.8: SNR residuals for GPS L5, GAL E5a, and BDS B2a (from top to bottom, respectively) signals for station 0MOC.

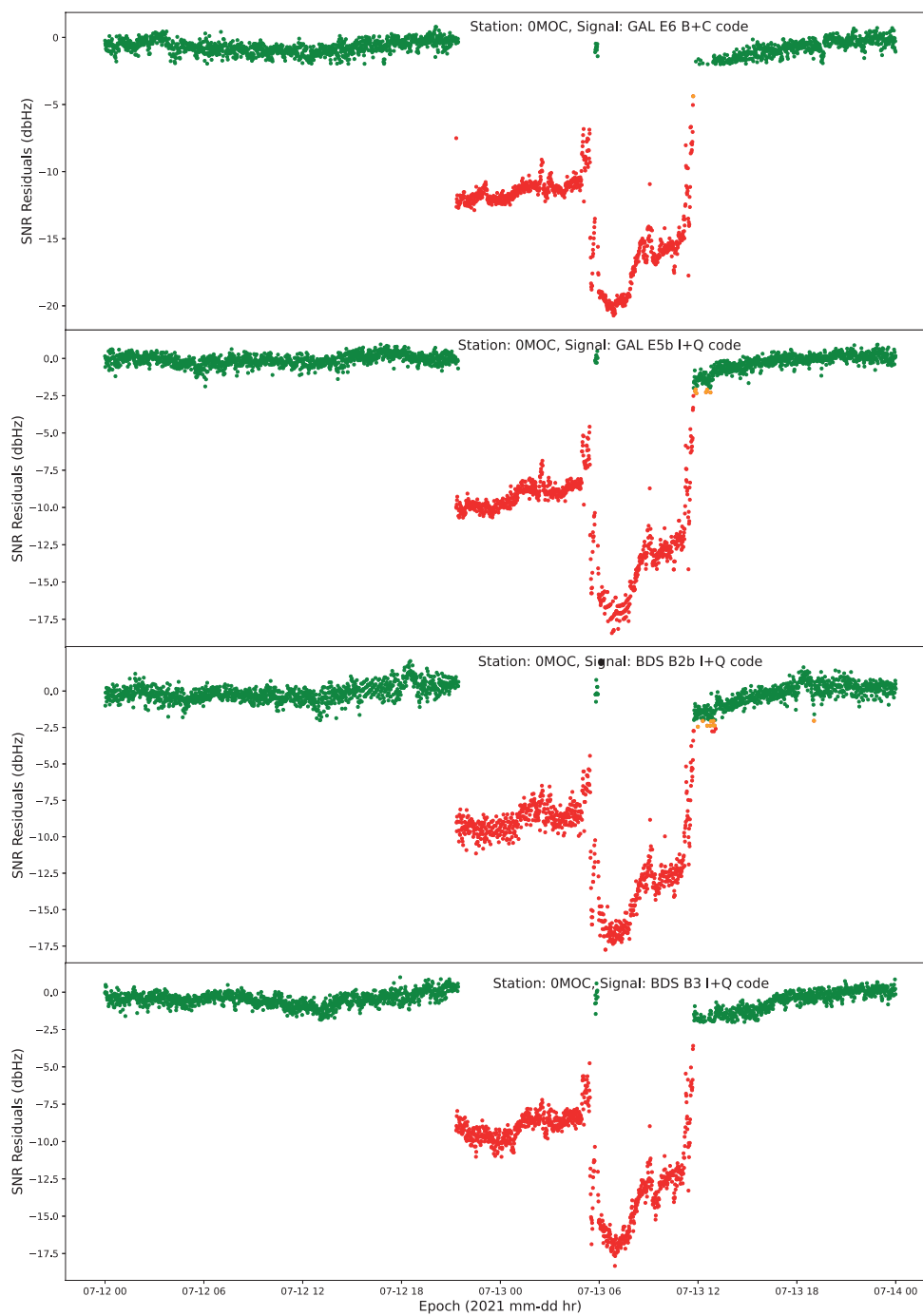


Figure A.9: SNR residuals for GAL E6, GAL E5b, BDS B2b, and BDS B3 (from top to bottom, respectively) signals for station 0MOC.

A.1.5 Örkelljunga (0ORK)

Signal disturbances have been detected affecting the GPS L5, GAL E5a and BDS B2a signals for the 0ORK station. The station was equipped with a Trimble Alloy receiver and a TRM59800.00 OSOD antenna. The SNR residuals for the affected signals are depicted in figure A.10. Figure A.11 shows a spectrum diagram from the station's receiver. The spectrum graph shows an interference signal with a center frequency slightly outside of the L5 band.

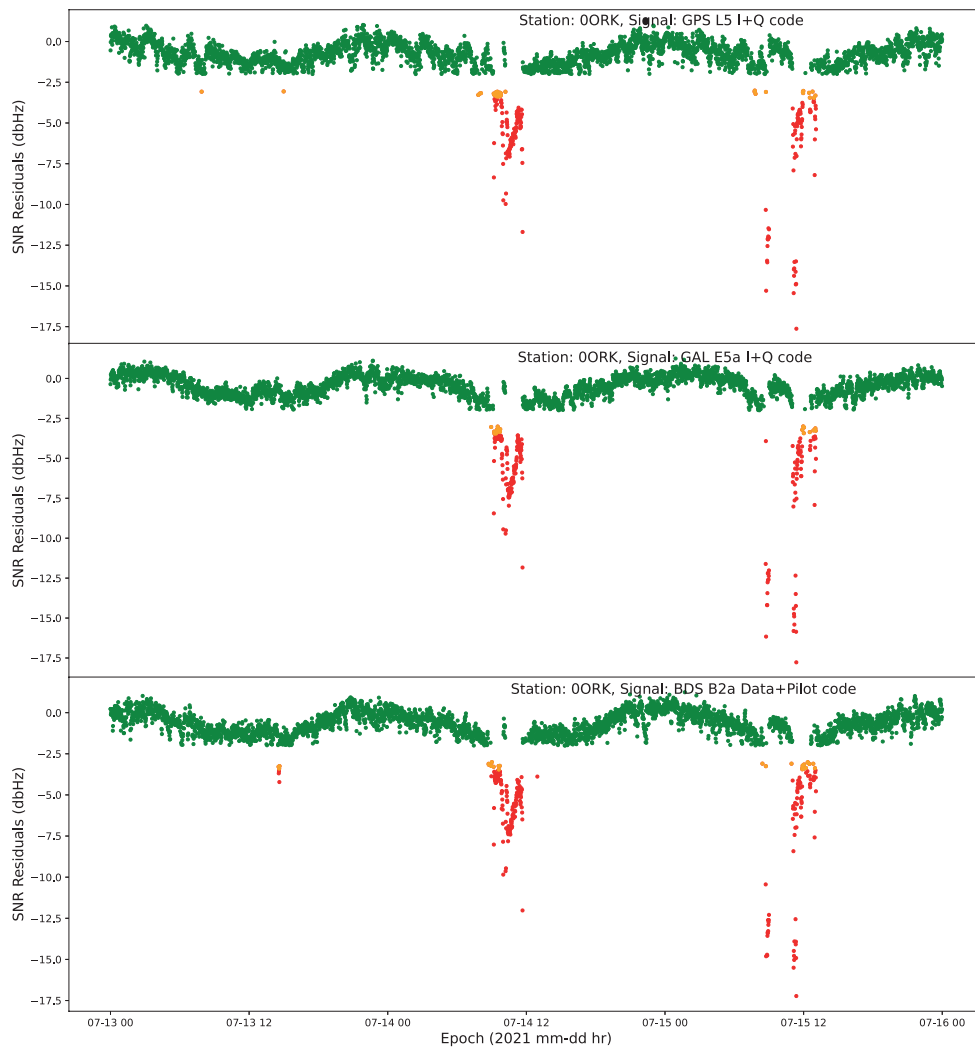


Figure A.10: SNR residuals for GPS L5, GAL E5a, and BDS B2a (from top to bottom, respectively) signals for station 0ORK. The different colors are as in figure A.1

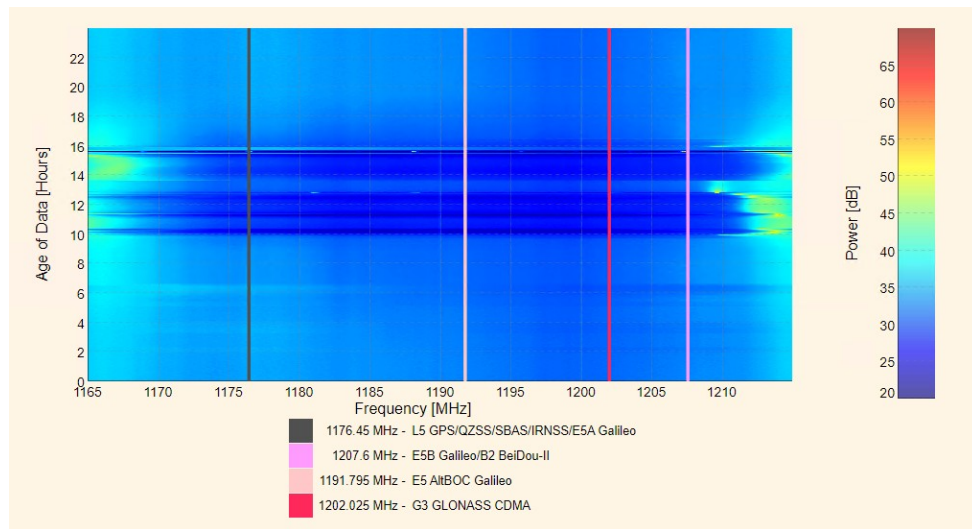


Figure A.11: Waterfall format spectrum plot – time-versus-frequency for station 0ORK. Colors indicate the power of the signal. The figure shows spectrum for the L5 frequency band.

A.1.6 Kristianstad (0KRI)

A disturbance that lasted for more than seven hours (from 6:40 to 13:49 UTC) has been detected on day 243, 2021 for station 0KRI. The station is equipped with a Septentrio PolaRx5 receiver and a JNSCR_C146-22-1 NONE antenna. The disturbance affected GPS L1, GLO G1, GAL E1 and BDS B1-2 signals. Figure A.12 shows the SNR residuals for GPS L1 for day 243, 2021. Figure A.13 shows the station's performance in the network-RTK system in terms of tracked and resolved satellites. During the disturbance, the number of resolved satellites dropped by more than 30 percent. The spectrum of the disturbance can also be seen from figure A.14a. Figure A.14b is included for comparison showing a clean spectrum before the disturbance. The disturbances have not recurred since then and the sources have not been known.

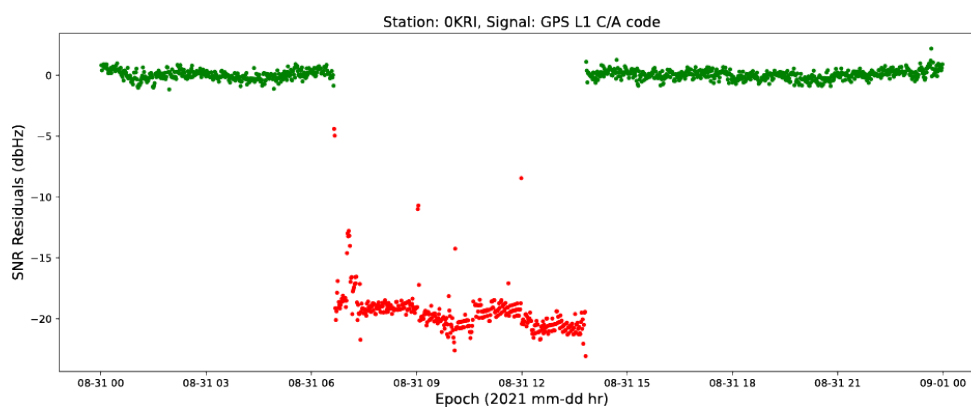


Figure A.12: SNR residuals for GPS L1 signal for station OKRI. The different colors are as in figure A.1.

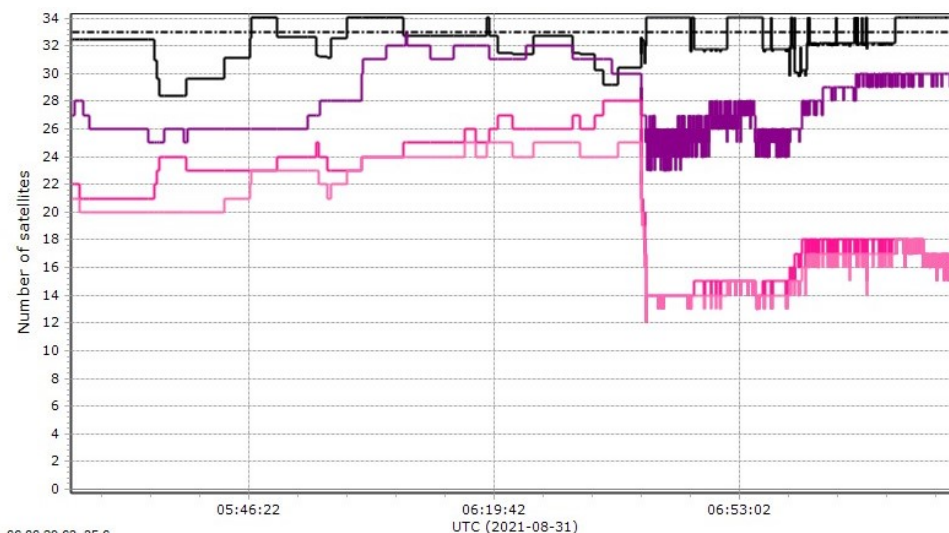
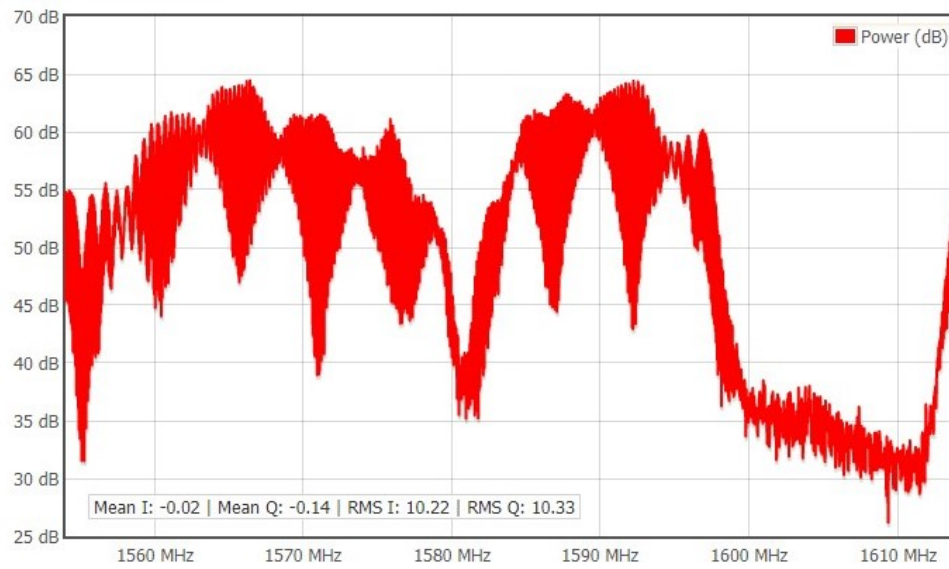
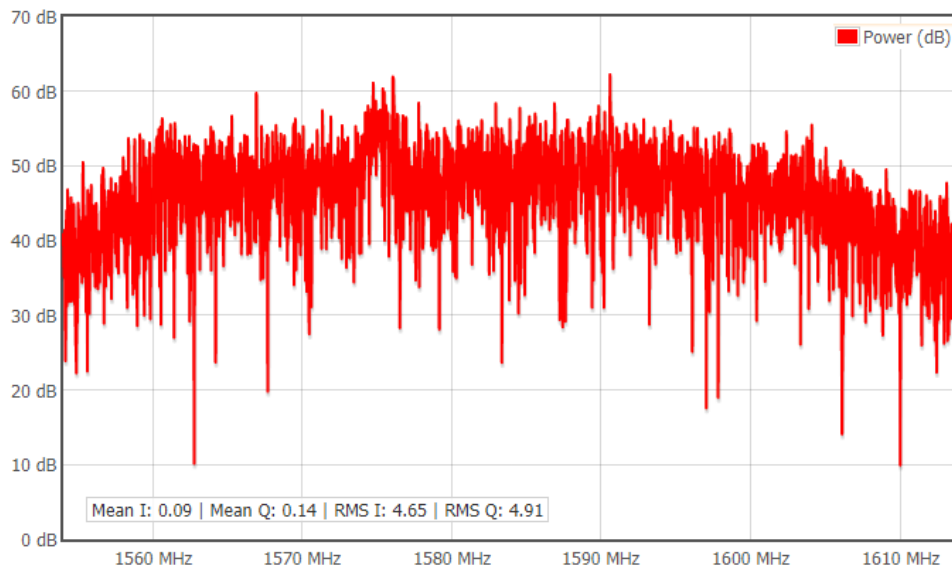


Figure A.13: Station performance in the network-RTK system for OKRI for day 243, 2021. Dark to light magenta colors show the total number of tracked, processed and solved satellites, respectively.



(a)



(b)

Figure A.14: Spectrum from the Septentrio PolaRx5 receiver a) during the interference b) when there was no interference for station 0KRI.

A.1.7 Grisslehamn (0GIS)

This section shows more figures continuing from section 4.1 for station 0GIS. Figure A.15 shows the SNR residuals for the GAL E5b and GAL E5a + E5b signals.

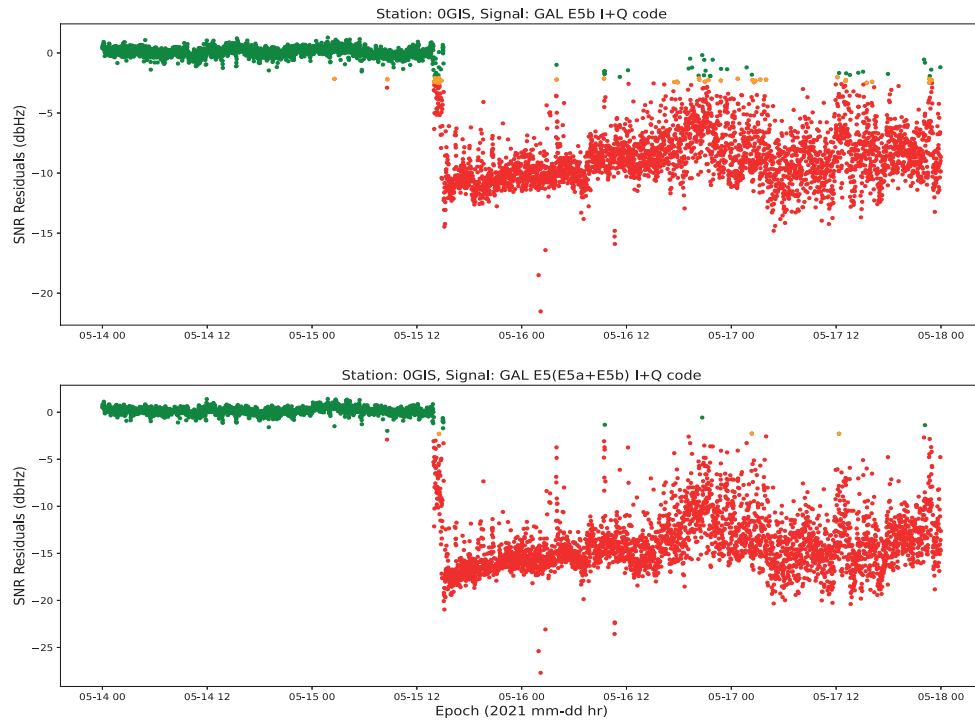


Figure A.15: Continued figure from figure 4.1. SNR residuals for GAL E5b (top) and GAL E5a + E5b signals for station 0GIS.

A.2 More Tables

A.2.1 Monitored GNSS signals and their frequencies

Table A.1: GNSS signals and frequencies monitored by the SWEPOS disturbance detection system.

GNSS	Signal	Frequency (MHz)
GPS	L1	1575.420
	L2	1227.600
	L5	1176.450
GAL	E1	1575.420
	E5a	1176.450
	E5b	1207.140
	E5 (E5a + E5b)	1191.795
	E6	1278.750
GLO	G1	1598.063 - 1608.750
	G2	1242.063 - 1252.750
	G3	1202.025
BDS	B1-2	1561.098
	B1	1575.420
	B2a	1176.450
	B2b	1207.140
	B2(B2a+B2b)	1191.795
	B3	1268.520

A.2.2 More signal disturbance incidents

Table A.2: Real signal disturbance incidents detected at SWEPOS stations. The reported disturbances are for the period doys 103, 2021 to the time of writing the report.

Station	Affected Signals	doys since 103, 2021.	Remark
0GIS	GPS L5, GAL E5, GAL E5a, GAL E5b, BDS B2b	doy 135 - Current.	The disturbance is still active. PTS is monitoring the situation. See section 4.1 for more details.
0ROS	GPS L5, GAL E5, GAL E5a, GAL E5b, BDS B2b	104-108, 117-118, 120-122, 124-125, 128	The doys presented here are only since 103. The disturbances begun in February, 2021. PTS visited the station. The source hasn't been located but the disturbance has disappeared.
1SKV	GPS L1, GAL E1, GLO G1	104-105, 123	See section A.1.3 for more details.
1STV	GPS L2, GPS L5, GAL E1, GAL E5, GAL E5a, GAL E5b, BDS B2b, BDS B3	206 – 222	See section 4.2 for more details.
0GVA	GPS L1, GLO G1, GAL E1, BDS B1-2	103-104, 109-110, 116-118, 137-138, 158, 164-166, 185-186, 188-189	See section A.1.2 for more details.
TOST	GPS L2, GLO G2	111-112, 116-118, 124-125, 130-132, 138, 140-141, 145-148, 151-153, 158-159, 161, 166-168, 173-175, 179-183, 194, 196, 215-216, 221, 225, 229-231, 237-239, 242-243, 246	See section A.1.1 for more details.
0OST	GPS L1, GLO G1, GAL E1, BDS B1-2	136-140, 148, 173	AXIS P1435-LE camera seemed to be causing the disturbances. Turning the camera off partially reduced the effect, but it remained for a few more days with minimal effect. The camera was turned off on doys 138 2021 sometime between 9:20 AM and 9:40 AM (Swedish time). The interference could be from the way the camera was installed as the same camera is available on other stations and it doesn't cause a problem, and it also suddenly started causing a problem for 0OST. It could be the power unit located in the rack. The camera was turned back on on May 141 2021 at 10:35 Swedish time.

Table A.3: Table A.2 continued ...

Station	Affected Signals	doys since 103, 2021.	Remark
0ORK	GPS L5, GAL E5, GAL E5a, GAL E5b, BDS B2b	149-152, 156-157, 180, 184, 195-197	See section A.1.5 for more details.
0MOC	GPS L2, GPS L5, GAL E1, GAL E5, GAL E5a, GAL E5b, BDS B2a, BDS B2b, BDS B3	193-194	See section A.1.4 for more details.
0ALV	GPS L2, GLO G2	184-185, 193-194, 196-197, 205	The source is unknown. The disturbances lasted from 1 to 1:30 hours on the specified doys. The disturbances in all the doys occurred between 16:30 and 18:00 UTC.
6SUN	BDS B3	140, 148-150 153-154, 158-160,164, 168, 178, 192, 195, 206-207, 209, 216, 218, 222-224	Unknown source. The disturbances affected the BDS B3 signal only.
0NYL	GPS L2, GLO G2	150, 153-154, 157-158, 160-162, 177-178, 182-198, 206-212, 218-219	Unknown source. TPP also shows problems of solving GLO.
0AMM	GPS L2, GLO G2	154, 157, 182-186, 191	Unknown source. TPP also shows problems of solving GLO.
0ALI	All signals	141	The disturbance stayed for one hour. The source was unknown.
0HFS	GPS L1	166	The disturbance stayed for more than two hours. The source was unknown.
0NRA	BDS B1-2	246	Spectrum showed interference centered at 1558.6 MHz, which stayed for nearly an hour.
0TIV	All signals	All doys	See section 4.3 for details.
0KRI	GPS L1, GLO G1, GAL E1, BDS B1-2	243	See section A.1.6 for more details.
0NOR	GPS L5, GAL E5, GAL E5a, BDS B2a	All doys	ASH700936D.M OSOD antenna related issue. See section 4.2 for more details.
0LEK	GPS L5, GAL E5, GAL E5a, BDS B2a	All doys	The same problem as in 0NOR.
0LOV	GPS L5, GAL E5, GAL E5a, BDS B2a	All doys	The same problem as in 0NOR.
0OSK	GPS L5, GAL E5, GAL E5a, BDS B2a	All doys	The same problem as in 0NOR.
0OVE	GPS L5, GAL E5, GAL E5a, BDS B2a	All doys	The same problem as in 0NOR.
0SKE	GPS L5, GAL E5, GAL E5a, BDS B2a	All doys	The same problem as in 0NOR.
0SVE	GPS L5, GAL E5, GAL E5a, BDS B2a	All doys	The same problem as in 0NOR.
0VIL	GPS L5, GAL E5, GAL E5a, BDS B2a	All doys	The same problem as in 0NOR.

A.2.3 List of SWEPOS stations

Table A.4: List of SWEPOS stations (see map in Figure 1.1). Twenty-three more stations in Sweden which are owned by Trimble are also included.

stnid	stnmrk	stnm	type	latitude	longitude	height
0ABI	ABIS.0	Abisko	NRTK	68.354344	18.816440	433.3
0ABY	ABY_.0	Åby	NRTK	58.658908	16.179640	61.5
0AKE	AKER.0	Åkersberga	NRTK	59.481447	18.301947	44.3
0ALE	ALBA.0	Albacken	NRTK	62.780456	16.013701	273.7
0ALF	ALFT.0	Alfta	NRTK	61.344518	16.064899	143.5
0ALI	ALIN.0	Alingsås	NRTK	57.929535	12.527833	117.5
0ALM	ALMU.0	Almunge	NRTK	59.866298	18.070800	57.2
0ALS	ALST.0	Alsterbro	NRTK	56.946615	15.907181	159.6
0ALV	ALVD.0	Älvdalen	NRTK	61.230958	14.037074	280.9
0AMB	AMBJ.0	Ambjörby	NRTK	60.510247	13.151176	194.2
0AME	AMME.0	Ämmeberg	NRTK	58.870273	15.000185	144.3
0AMM	AMMA.0	Ammarnäs	NRTK	65.958198	16.205717	463.3
0AMS	AMSE.0	Åmsele	NRTK	64.532529	19.349897	250.0
0ANA	ASAR.0	Åsarna	NRTK	62.642587	14.371667	400.6
0ANG	ANGE.0	Ånge	NRTK	62.525368	15.659629	218.6
0ANS	ANSE.0	Ånäset	NRTK	64.275929	21.042970	51.6
0ARA	ARVK.0	Arvika	NRTK	59.659370	12.599998	131.8
0ARB	ARBO.0	Arboga	NRTK	59.396964	15.834570	48.1
0ARD	ARDA.0	Ardala	NRTK	58.360820	13.336819	140.4
0ARJ	ARJE.0	Arjeplog	SWEPOS klass A	66.318021	18.124868	490.3
0ART	ARJT.0	Arjeplog-C	NRTK	66.049360	17.841613	472.5
0ARV	ARVI.0	Arvidsjaur	NRTK	65.593303	19.172465	428.8
0ASD	ASDA.0	Åseda	NRTK	57.171197	15.350214	279.4
0ASE	ASEL.0	Åsele	NRTK	64.160769	17.356359	367.7
0AST	ASTO.0	Åstorp	NRTK	56.137282	12.951336	82.0
0ATR	ATRA.0	Ätran	NRTK	57.120455	12.949346	166.3
0ATT	ATTA.0	Attarp	NRTK	57.858193	14.122239	163.1
0ATV	ATVI.0	Ätvidaberg	NRTK	58.198894	16.002508	130.1
0AZ1	AZ1_.0	AstaZero1	NRTK	57.773199	12.779834	250.0
0AZ2	AZ2_.0	AstaZero2	SWEPOS klass A			
0AZ3	AZ3_.0	AstaZero3	SWEPOS klass A	57.781205	12.770483	238.9
0AZ4	AZ4_.0	AstaZero4	SWEPOS klass A	57.786725	12.767936	238.1
0BAS	BAST.0	Bastuträsk	NRTK	64.792698	20.036674	275.9
0BEB	BEBY.0	Bergsbyn	NRTK	64.720651	21.083993	37.0
0BEF	BEFO.0	Bengtsfors	NRTK	59.044662	12.228329	173.0
0BER	BERG.0	Bergsåker	NRTK	62.414164	17.229675	54.7
0BIE	BIE_.0	Bie	NRTK	59.087756	16.211649	92.4
0BIL	MBIL.0	Mobilmonitor	Monitorstation			
0BIP	BISP.0	Bispgården	NRTK	63.027251	16.625206	219.3
0BIS	BISK.0	Biskopsgården	NRTK	57.725054	11.891920	132.3
0BJA	BJAR.0	Bjärnum	NRTK	56.295968	13.705401	154.1
...						

Table header: "stnid", "stnmrk", and "stnm" indicate four character identification, marker name and full name, respectively, while "type" indicates the owner of the stations. Latitude and longitude are in degrees while height is in meters. NRTK stands for Network-RTK.

Table A.5: Table A.4 continued ...

stnid	stnmrk	stnm	type	latitude	longitude	height
0BJO	BJOR.0	Björneborg	NRTK	59.240294	14.259870	200.3
0BJU	BJUR.0	Bjuröklubb	NRTK	64.480590	21.574923	70.3
0BKI	BKIN.0	Brokind	NRTK	58.242985	15.665826	142.8
0BLA	BLAN.0	Blankaholm	NRTK	57.580371	16.515220	71.7
0BLI	BLID.0	Blidö	NRTK	59.626715	18.900368	40.1
0BMO	MON_BOD.0	Bodum_Mon	Monitorstation	63.922096	16.335012	257.7
0BOR	BORA.0	Borås	SWEPOS klass A	57.714960	12.891351	220.5
0BOS	BOTS.0	Botsmark	NRTK	64.267041	20.227327	238.5
0BRA	BRAN.0	Brände	NRTK	64.348338	20.978485	95.5
0BRO	BRO_.0	Bro	NRTK	59.513452	17.634093	54.5
0BRU	BRUN.0	Brunnsbo	NRTK	57.729982	11.972135	78.0
0BST	BSTA.0	Båstad	NRTK	56.428110	12.848312	59.4
0BTT	BOTT.0	Bottnaryd	NRTK	57.772980	13.824127	270.8
0BUE	BUEA.0	Bureå_C	NRTK	64.620919	21.204056	46.1
0BUG	BUGA.0	Bugärde	NRTK	57.666570	12.405549	203.1
0BUR	BURT.0	Burträsk	NRTK	64.517335	20.658672	120.2
0BYG	BYGD.0	Bygdeå	NRTK	64.045634	20.862599	48.5
0CHA	CHAR.0	Charlottenberg	NRTK	59.883051	12.303950	181.6
0DAJ	DAJA.0	Dala_Järna	NRTK	60.548129	14.370681	278.7
0DAL	DALB.0	Dalby	NRTK	55.668696	13.351079	129.3
0DAN	DANG.0	Dångebo	NRTK	56.514366	15.153386	177.8
0DAV	DAVA.0	Dåva	NRTK	63.870063	20.412630	72.0
0DEG	DEGB.0	Degeberga	NRTK	55.831624	14.088232	82.2
0DIL	DILE.0	Dingle	NRTK	58.526384	11.578303	66.9
0DOC	DOCK.0	Docksta	NRTK	63.056112	18.331962	55.9
0DOR	DORO.0	Dorotea	NRTK	64.263623	16.416468	367.3
0EDB	EDSB.0	Edsbruk	NRTK	58.012040	16.476769	79.6
0EDS	EDSE.0	Edsele	NRTK	63.406433	16.541467	207.7
0ED_	ED_.0	Ed	NRTK	58.908659	11.941716	207.1
0EKB	EKEB.0	Ekeby	NRTK	56.004000	12.967418	127.6
0EKE	EKET.0	Eketorp	NRTK	56.266268	16.478759	43.7
0ENS	ENST.0	Enstaberga	NRTK	58.767525	16.860180	82.4
0ENV	ENVI.0	Enviken	NRTK	60.808797	15.766500	191.8
0ERS	ERSB.0	Ersboda	NRTK	63.857650	20.335509	81.4
0ESK	ESKI.0	Eskilstuna	NRTK	59.368258	16.510563	61.5
0ESL	ESLO.0	Eslöv	NRTK	55.838659	13.310307	119.7
0ESN	ESND.0	Eksund	NRTK	58.587242	16.096169	70.3
0FAF	FAFO.0	Fällfors	NRTK	65.125200	20.786579	209.3
0FAL	FALK.0	Falköping	NRTK	58.169940	13.556089	260.9
0FAR	FARO.0	Fårö	NRTK	57.919007	19.139117	36.9
0FIL	FILI.0	Filipstad	NRTK	59.714670	14.162139	190.8
0FIN	FINN.0	Finnbacka	NRTK	61.051850	15.571575	474.0
0FLR	FLUR.0	Flurkmark	NRTK	63.983570	20.236156	105.2
0FLU	FALU.0	Falun	NRTK	60.624482	15.622793	163.6
0FOT	FOTO.0	Fotö	Monitorstation	57.671245	11.657857	64.8
0FRB	FRBG.0	Fredriksberg	NRTK	60.141094	14.370970	347.6
0FRE	FRED.0	Fredrika	NRTK	64.077467	18.402726	339.7
0FRI	FRIG.0	Friggesund	NRTK	61.897278	16.555054	95.3
0FRL	FROL.0	Frölunda	NRTK	57.650253	11.912194	113.4
0FUN	FUNA.0	Funäsdalen	NRTK	62.519392	12.601074	635.5
...						

Table A.6: Table A.4 continued ...

stnid	stnmrk	stnm	type	latitude	longitude	height
0FUR	FURD.0	Furudal	NRTK	61.168418	15.142244	251.2
0GAD	GADD.0	Gäddede	NRTK	64.504192	14.138839	383.3
0GAL	GALL.0	Gällö	NRTK	62.914157	15.236426	345.5
0GAM	GAMM.0	Gammelsta	NRTK	58.755183	16.614917	77.2
0GEB	GEBB.0	Grebbestad	NRTK	58.691908	11.261072	55.2
0GIS	GRIS.0	Grisslehamn	NRTK	60.101890	18.801116	31.6
0GLO	GLOM.0	Glommersträsk	NRTK	65.261471	19.623535	395.5
0GMA	GMAR.0	Gräsmark	NRTK	59.946054	12.909577	150.6
0GMO	MON_GBG.0	Göteborg_Mon	Monitorstation	57.711988	11.983710	65.4
0GNA	GRNN.0	Gränna	NRTK	58.023974	14.461349	139.7
0GRA	GRAN.0	Grängesberg	NRTK	60.071437	14.979908	357.9
0GRI	GRIL.0	Grillby	NRTK	59.625396	17.251100	53.0
0GRN	GRAF.0	Gräftåvallen	NRTK	63.041444	13.967878	607.2
0GRO	GROV.0	Grövelsjön	NRTK	62.060333	12.317260	728.7
0GRS	GRAS.0	Grästorps	NRTK	58.330816	12.677041	103.3
0GST	GSTO.0	Gamla_Storbäcken	NRTK	64.149386	20.784573	80.3
0GUL	GULL.0	Gullspång	NRTK	58.981153	14.109701	125.8
0GUM	GUMB.0	Gumboda	NRTK	64.234341	21.018544	62.5
0GUN	GUNN.0	Gunnarsbyn	NRTK	66.087466	21.800487	76.7
0GVA	GVAR.0	Gällivare	NRTK	67.136630	20.666690	405.5
0GVG	GVBG.0	Gustavsberg	NRTK	59.325066	18.390115	65.9
0HAD	HALM.0	Halmstad	NRTK	56.668845	12.876700	60.6
0HAE	HAVE.0	Haverö	NRTK	62.387956	15.131996	334.9
0HAF	HAFO.0	Hasselfors	NRTK	59.085599	14.653159	122.9
0HAM	HAMR.0	Hamra	NRTK	61.655112	15.000550	495.3
0HAP	HAPA.0	Haparanda	NRTK	65.828063	24.131668	49.8
0HAS	HASS.0	Hässleholm	SWEPOS klass A	56.092219	13.718080	114.5
0HAV	HAVD.0	Haverdal	NRTK	56.729339	12.667444	59.8
0HDA	HDAL.0	Hammerdal	NRTK	63.582817	15.352245	354.4
0HDG	HUDD.0	Huddinge	NRTK	59.221727	17.934078	108.2
0HED	HEDE.0	Hede	NRTK	62.419459	13.513212	471.2
0HEM	HEMA.0	Hemavan	NRTK	65.820465	15.080997	517.7
0HEN	HENN.0	Hennan	NRTK	62.026520	15.909952	255.6
0HFS	HALE.0	Hällefors	NRTK	59.784355	14.520441	236.8
0HIL	HILL.0	Hillerstorp	NRTK	57.316996	13.887355	213.4
0HJO	HJO_.0	Hjo	NRTK	58.301326	14.286516	141.2
0HJV	HJVA.0	Hjältevad	NRTK	57.629444	15.343358	210.5
0HLL	HLLS.0	Hällestad	NRTK	58.741697	15.571916	95.2
0HLM	HOON.0	Holmön	NRTK	63.806898	20.864672	31.8
0HLO	HOLO.0	Hölö	NRTK	59.022796	17.543804	78.1
0HLV	HALV.0	Hällevik	NRTK	56.013665	14.690544	73.3
0HMS	HEMS.0	Hemse	NRTK	57.239707	18.382321	63.7
0HNA	HNAS.0	Hällnäs	NRTK	60.534898	17.880047	42.3
0HOA	HOL_.0	Hol	NRTK	57.967681	12.693490	200.7
0HOB	HOBU.0	Hoburgen	NRTK	56.921748	18.151059	86.5
0HOJ	HOSJ.0	Holmsjö	NRTK	56.444053	15.655163	142.9
0HOO	HOOR.0	Höör	NRTK	55.932596	13.542740	123.2
0HOR	HORN.0	Horndal	NRTK	60.290428	16.403292	164.3
0HOS	HOLM.0	Holmsund	NRTK	63.672849	20.388650	33.3
0HOT	HOTA.0	Hotagen	NRTK	63.973894	14.166823	363.1
0HRN	HRNE.0	Hörnefors	NRTK	63.621116	19.909812	43.0
...						

Table A.7: Table A.4 continued ...

stnid	stnmrk	stnm	type	latitude	longitude	height
0HRO	HROR.0	Hasslerör	NRTK	58.749048	13.937713	98.7
0HSA	HSSA.0	Hassela	NRTK	62.108193	16.711682	181.8
0HST	HSTA.0	Herrestad	NRTK	58.350224	11.840190	60.2
0HSU	HSUN.0	Hedesunda	NRTK	60.394197	17.010368	110.4
0HUD	HUDI.0	Hudiksvall	NRTK	61.725218	17.139747	56.8
0HVI	HVIK.0	Hällsvik	NRTK	57.702947	11.737393	47.8
0HYB	HYBO.0	Hybo	NRTK	61.795445	16.208878	176.6
0JAK	JAKK.0	Jäckvik	NRTK	66.387502	16.965912	473.9
0JAM	JAMJ.0	Jämjö	NRTK	56.188431	15.827831	63.3
0JAR	JARP.0	Järpen	NRTK	63.352762	13.449093	375.0
0JAT	JATT.0	Jättendal	NRTK	61.974512	17.257016	64.5
0JAV	JAVR.0	Jävre	NRTK	65.156013	21.486057	61.2
0JFA	JFAA.0	Järfälla	NRTK	59.424177	17.834401	92.2
0JNA	JONA.0	Jönåker	NRTK	58.743184	16.734910	63.4
0JOK	JOKK.0	Jokkmokk	NRTK	66.605020	19.832376	297.5
0JON	JONK.0	Jönköping	SWEPOS klass A	57.745474	14.059612	260.5
0JOR	JORN.0	Jörn	NRTK	65.055716	20.043299	302.0
0JTP	JONS.0	Jonstorp	NRTK	56.229668	12.676233	55.4
0JUN	JUNS.0	Junsele	NRTK	63.694698	16.887961	252.2
0JUO	JUNO.0	Junosuando	NRTK	67.430508	22.500827	255.5
0KAB	KABD.0	Kåbdalis	NRTK	66.148787	19.989184	388.2
0KAL	KALL.0	Kållandsö	NRTK	58.663630	13.192507	90.8
0KAR	KARL.0	Karlstad	SWEPOS klass A	59.444023	13.505629	114.7
0KAS	KASE.0	Kallsedet	NRTK	63.701250	12.958857	436.8
0KAT	KATT.0	Katthammarsvik	NRTK	57.426512	18.837714	56.8
0KBO	KABO.0	Karlsborg	NRTK	58.530567	14.511340	136.4
0KEB	KEBN.0	Kebnekaise	NRTK	67.868027	18.622716	711.0
0KIC	KIRC.0	Kiruna-C	NRTK	67.859873	20.234974	619.1
0KIE	KIRE.0	Kiruna-E	NRTK	67.847129	20.380154	461.2
0KIR	KIRU.0	Kiruna	SWEPOS klass A	67.877579	21.060243	498.8
0KIV	KIRV.0	Kiruna_V	NRTK	67.794203	20.229159	548.0
0KLI	KLIN.0	Klintehamn	NRTK	57.386388	18.211911	43.9
0KNA	KNAR.0	Knäred	NRTK	56.521575	13.318439	114.8
0KOB	KOBB.0	Kobben	SWEPOS klass A	60.409641	18.230205	29.8
0KOL	KOLS.0	Kolsva	NRTK	59.594185	15.854123	89.4
0KOP	KOPP.0	Koppom	NRTK	59.716464	12.161074	169.8
0KOR	KORP.0	Korpilombolo	NRTK	66.847889	23.055540	209.3
0KOT	KORT.0	Kortedala	NRTK	57.762174	12.037666	170.9
0KOV	KOVI.0	Köpingsvik	NRTK	56.880955	16.724522	52.7
0KRA	KRAM.0	Kramfors	NRTK	62.875454	17.927672	152.4
0KRB	KARB.0	Kårböle	NRTK	61.982736	15.314870	285.9
0KRE	KREK.0	Krokek	NRTK	58.673751	16.338135	123.6
0KRI	KRIS.0	Kristianstad	NRTK	56.031334	14.182577	53.0
0KRO	KROK.0	Krokslätt	NRTK	57.680228	11.984511	128.1
0KST	KSTA.0	Kosta	NRTK	56.841300	15.394697	268.4
0KTH	KTHL.0	KTH	NRTK	59.349920	18.069379	76.6
0KUM	KUML.0	Kumla	NRTK	59.132766	15.139727	96.6
...						

Table A.8: Table A.4 continued ...

stnid	stnmrk	stnm	type	latitude	longitude	height
OKUN	KUNG.0	Kungsholmsfort	NRTK	56.104241	15.589039	35.9
OKVI	KVIK.0	Kvikkjokk	NRTK	66.942495	17.739060	363.9
OLAD	LAND.0	Landskrona	NRTK	55.870266	12.841875	47.3
OLAJ	LANS.0	Lansjärv	NRTK	66.655231	22.191937	134.7
OLAK	LAKA.0	Lakaträsk	NRTK	66.278519	21.128713	218.1
OLAN	LANG.0	Långshyttan	NRTK	60.457602	16.029462	156.0
OLAR	LARU.0	Långserud	NRTK	59.271629	12.655928	128.1
OLAS	LAST.0	Lästringe	NRTK	58.902423	17.313252	61.5
OLBH	LBYH.0	Ljungbyhed	NRTK	56.078051	13.242950	90.8
OLDA	LDAL.0	Ljungdalen	NRTK	62.850714	12.790872	651.5
OLED	LEDE.0	Lilla Edet	NRTK	58.114024	12.140627	110.6
OLEK	LEKS.0	Leksand	SWEPOS klass A	60.722147	14.877010	478.7
OLEN	LENN.0	Lennartsfors	NRTK	59.319826	11.915603	154.0
OLFT	LFTA.0	Loftahammar	NRTK	57.905685	16.698703	48.5
OLHE	LHEM.0	Linghem	NRTK	58.437442	15.796434	125.3
OLIC	LINC.0	Linköping_C	NRTK	58.416796	15.626534	86.6
OLIE	LIEL.0	Linsell	NRTK	62.157542	13.891294	452.8
OLIH	LIHU.0	Lidhult	NRTK	56.829844	13.449193	215.4
OLIL	LILL.0	Lillhärdal	NRTK	61.853276	14.066764	492.8
OLIN	LIND.0	Lindesnäs	NRTK	60.328041	14.531437	297.1
OLIO	LIDO.0	Lidingö	NRTK	59.365656	18.126947	87.6
OLKB	LKBB.0	Lillkobben	SWEPOS klass A	60.404671	18.197556	28.2
OLKO	LIDK.0	Lidköping	NRTK	58.502074	13.128938	92.4
OLMO	MON_LIN.0	Linköping_Mon	Monitorstation	58.432233	15.693055	85.1
OLNC	LNDC.0	Landvetter_C	NRTK	57.683846	12.209661	109.1
OLND	LNDV.0	Landvetter	NRTK	57.666058	12.296745	204.1
OLOB	LOBE.0	Löberöd	NRTK	55.778319	13.514904	172.1
OLOD	LODD.0	Löddeköpinge	NRTK	55.766946	12.995750	57.1
OLOF	LOFS.0	Lofsdalen	NRTK	62.132114	13.275473	863.3
OLOV	LOVO.0	Lovö	SWEPOS klass A	59.337804	17.828919	80.7
OLSE	LASE.0	Långele	NRTK	63.183357	17.065308	139.3
OLUL	LULE.0	Luleå	NRTK	65.555295	22.215316	49.9
OLUM	LUMS.0	Lumsheden	NRTK	60.709689	16.250822	235.5
OLVA	LOVA.0	Lövånger	NRTK	64.371110	21.313163	48.4
OMAK	MARK.0	Markaryd	NRTK	56.457345	13.591877	149.7
OMAN	MANS.0	Månsarp	NRTK	57.662319	14.076181	285.5
OMAT	MATF.0	Matfors	NRTK	62.366046	16.979289	117.0
OMED	MEDL.0	Medle	NRTK	64.738265	20.673750	114.2
OMGV	MORG.0	Morgongåva	NRTK	59.931391	16.953550	102.6
OMJO	MJOL.0	Mjölby	NRTK	58.324796	15.124951	160.8
OMKO	MOLK.0	Molkom	NRTK	59.598594	13.725946	120.0
OMLA	MALA.0	Malå	NRTK	65.188144	18.758617	360.3
OMLE	MOLE.0	Mölle	NRTK	56.281864	12.499114	59.7
OMLK	MALK.0	Malmköping	NRTK	59.136439	16.720863	90.6
OMLL	MLLR.0	Mellerud	NRTK	58.703188	12.455302	104.7
OMLM	MALB.0	Malmberget	NRTK	67.194137	20.698021	527.7
OMLU	MALU.0	Malung	NRTK	60.686421	13.725471	349.9
...						

Table A.9: Table A.4 continued ...

stnid	stnmrk	stnm	type	latitude	longitude	height
0MLY	MOLN.0	Mölnlycke	NRTK	57.660256	12.114652	102.0
0MOA	MOAS.0	Mönsterås	NRTK	57.044583	16.438558	49.8
0MOB	MOBY.0	Mörbylånga	NRTK	56.526640	16.378670	43.4
0MOC	MOCK.0	Mockfjärd	NRTK	60.508696	14.966837	221.7
0MOR	MORA.0	Mora	NRTK	61.012040	14.564276	211.3
0MOS	MOSE.0	Mosebacke	NRTK	59.318428	18.074214	92.4
0MRJ	MRJA.0	Morjärv	NRTK	66.069082	22.701763	71.4
0MRS	MRST.0	Märsta	NRTK	59.625915	17.859881	56.1
0MSE	MSEL.0	Moskosel	NRTK	65.875041	19.457591	373.1
0MUF	MUFO.0	Munkfors	NRTK	59.834479	13.542243	138.1
0MUN	MUNK.0	Munka-Ljungby	NRTK	56.256303	12.916553	59.6
0NAS	NASS.0	Nässjö	NRTK	57.656300	14.697671	352.4
0NAT	NATT.0	Nattavaara	NRTK	66.756576	20.955047	361.9
0NBA	NOBA.0	Norrback	NRTK	64.715447	17.678678	490.5
0NBG	NORB.0	Norberg	NRTK	60.062514	15.920665	177.2
0NBI	NBIO.0	Norra Biotesten	SWEPOS klass A	60.436536	18.188592	29.2
0NBR	NBRO.0	Nybro	NRTK	56.745944	15.908976	132.0
0NBY	NOLB.0	Nolbykullen	NRTK	62.300237	17.363858	208.2
0NHL	NHLM.0	Norsholm	NRTK	58.509281	15.975599	73.1
0NIK	NIKK.0	Nikkala	NRTK	65.805362	23.914782	38.4
0NMN	MON_NYK.0	Nyköping_Mon	Monitorstation	58.760177	16.995231	94.5
0NMO	MON_NOR.0	Norrköping_Mon	Monitorstation	58.616753	16.178274	43.4
0NOA	NOAS.0	Nornäs	NRTK	61.431923	13.240214	500.3
0NOF	NOFO.0	Norrfors	NRTK	63.767816	18.995382	184.8
0NOR	NORR.0	Norrköping	SWEPOS klass A	58.590233	16.246386	40.9
0NOS	NOSJ.0	Norsjö	NRTK	64.910618	19.481710	341.1
0NRA	NRRA.0	Norråker	NRTK	64.435913	15.591757	315.6
0NUN	NUNN.0	N Unnaryd	NRTK	57.595876	13.724798	264.5
0NYB	NYBO.0	Nyborg	NRTK	65.795919	23.170031	39.4
0NYK	NYKO.0	Nyköping	NRTK	58.770007	16.977573	67.7
0NYL	NYLI.0	Nyliden	NRTK	63.717295	18.496596	261.3
0NYN	NYNA.0	Nynäshamn	NRTK	58.902974	17.944234	67.8
0OCK	OCKE.0	Ockelbo	NRTK	60.890542	16.716662	124.6
0ODE	ODES.0	Ödeshög	NRTK	58.226563	14.651592	184.0
0OKC	OSKC.0	Oskarshamn_C	NRTK	57.251938	16.465361	53.6
0OML	OMLM.0	Öster-Malma	NRTK	58.950972	17.159267	69.9
0ONS	ONSA.0	Onsala	SWEPOS klass A	57.395301	11.925520	45.9
0OPP	OPPE.0	Oppeby	NRTK	58.034329	15.806890	143.4
0ORK	ORKE.0	Örkelljunga	NRTK	56.286138	13.275060	142.7
0ORN	ORNS.0	Örnsköldsvik	NRTK	63.290325	18.717835	57.4
0ORR	ORRE.0	Orrefors	NRTK	56.839518	15.744904	210.6
0ORS	ORSJ.0	Örsjö	NRTK	56.701173	15.752736	160.1
0OSA	OSAM.0	Oskarström	NRTK	56.801593	12.978549	76.3
0OSC	OSTC.0	Östersund C	NRTK	63.169407	14.672945	393.4
0OSK	OSKA.0	Oskarshamn	SWEPOS klass A	57.065640	15.996813	149.7
0OSM	OSMO.0	Österbymo	NRTK	57.825157	15.276632	230.1
0OST	OSTE.0	Östersund	SWEPOS klass A	63.442796	14.858073	490.8
...						

Table A.10: Table A.4 continued ...

stnid	stnmrk	stnm	type	latitude	longitude	height
0OTM	OSTM.0	Östmark	NRTK	60.283998	12.757712	151.7
0OVE	OVER.0	Överkalix	SWEPOS klass A	66.317861	22.773376	223.4
0OVT	OVET.0	Övertorneå	NRTK	66.385723	23.658710	101.7
0OXE	OXEL.0	Oxelösund	NRTK	58.670957	17.107042	48.2
0PAU	PAUL.0	Pauliström	NRTK	57.466411	15.510571	201.3
0PJU	PJUS.0	Porjus	NRTK	66.958596	19.818077	431.8
0RAD	RADD.0	Råddeby	NRTK	57.680872	12.714155	235.9
0RAM	RAMS.0	Ramsjö	NRTK	62.182308	15.649528	257.3
0RAT	RATA.0	Ratan	NRTK	63.985593	20.895574	32.5
0RAU	RAUT.0	Rautas	NRTK	67.994351	19.894740	508.8
0RAV	RAVL.0	Rävlanda	NRTK	57.649597	12.490869	112.0
0REJ	REJM.0	Rejmyre	NRTK	58.825421	15.930152	95.0
0REN	RENG.0	Rengsjö	NRTK	61.364766	16.617279	122.3
0RIB	RIBY.0	Rinkabyholm	NRTK	56.651224	16.248682	49.5
0RIN	RING.0	Ringarum	NRTK	58.334613	16.448994	86.5
0ROB	ROBY.0	Ronneby	NRTK	56.207882	15.272202	68.2
0ROC	ROCK.0	Rockneby	NRTK	56.801587	16.346522	47.6
0ROE	ROSE.0	Rosenlund	NRTK	57.779408	14.213936	152.8
0ROM	ROMA.0	Roma	NRTK	57.511279	18.448325	69.3
0ROR	RORO.0	Rörö	NRTK	57.776957	11.615816	52.2
0ROS	ROSV.0	Rosvik	NRTK	65.427033	21.690800	44.0
0ROT	ROTT.0	Rottne	NRTK	57.023104	14.890460	225.7
0RUN	RUNS.0	Runsten	NRTK	56.697653	16.692491	55.4
0RYF	RYFO.0	Ryfors	NRTK	56.563160	13.932188	175.2
0SAA	SAAR.0	Sävar	NRTK	63.900446	20.556078	52.8
0SAF	SAFF.0	Säffle	NRTK	59.135873	12.934679	115.1
0SAK	SAVT.0	Sävträsk	NRTK	63.969117	20.709372	68.8
0SAL	SALE.0	Sälen	NRTK	61.154237	13.266085	399.6
0SAN	SAND.0	Sandarne	NRTK	61.266207	17.153916	54.0
0SAR	SARN.0	Särna	NRTK	61.693845	13.148247	483.1
0SAT	SATE.0	Säter	NRTK	60.346493	15.745006	201.8
0SAV	SAVA.0	Sävast	NRTK	65.769786	21.738447	50.8
0SAX	SAXN.0	Saxnäs	NRTK	64.971772	15.347458	623.4
0SBA	SBAR.0	Söderbärke	NRTK	60.071677	15.557111	163.5
0SBR	SBRU.0	Sundsbruk	NRTK	62.459597	17.356957	86.5
0SBY	SKBY.0	Skogsby	NRTK	56.631007	16.512855	83.2
0SDE	SODT.0	Södertälje	NRTK	59.189568	17.608090	108.6
0SIB	SIBB.0	Sibbhult	NRTK	56.264205	14.197376	116.4
0SJO	SJOS.0	Sjösa	NRTK	58.783483	17.101527	45.5
0SKC	SKEC.0	Skellefteå_C	NRTK	64.754256	20.921454	54.2
0SKE	SKEL.0	Skellefteå	SWEPOS klass A	64.879200	21.048293	81.7
0SKH	SKEH.0	Skelleftehamn	NRTK	64.688597	21.230457	39.4
0SKL	SKIL.0	Skillinge	NRTK	55.474885	14.279363	58.8
0SKN	SKAN.0	Skanör	NRTK	55.413764	12.857947	49.4
0SKO	SKOR.0	Skorped	NRTK	63.378213	17.883636	200.7
0SKR	SKRS.0	Skärstad	NRTK	57.887235	14.364162	205.0
0SKY	SKYT.0	Skyttorp	NRTK	60.074573	17.744299	68.3
...						

Table A.11: Table A.4 continued ...

stnid	stnmrk	stnm	type	latitude	longitude	height
OSLI	SLIT.0	Slite	NRTK	57.706494	18.798241	39.7
OSLU	SLUS.0	Slussfors	NRTK	65.431555	16.245431	410.0
OSMA	SMAL.0	Smålandsstenar	NRTK	57.161340	13.405089	193.4
OSMO	SMOG.0	Smögen	NRTK	58.353465	11.217932	46.0
OSMY	SMYG.0	Smygehamn	NRTK	55.345701	13.369854	50.8
OSNA	SNAS.0	Strömsnäs	NRTK	63.173453	15.859849	276.0
OSNE	SKEN.0	Skene	NRTK	57.492756	12.647394	115.2
OSNG	SANG.0	Sangis	Monitorstation	65.858886	23.494013	42.9
OSOA	SOAK.0	Söderåkra	NRTK	56.449196	16.071765	69.2
OSOD	SODE.0	Söderboda	NRTK	60.437296	18.416321	41.5
OSOL	SOLL.0	Sollentuna	NRTK	59.444372	17.952935	48.3
OSOP	SOPP.0	Övre Soppero	NRTK	68.090869	21.691855	409.6
OSOR	SORS.0	Sorsele	NRTK	65.535242	17.539905	392.0
OSOV	SOVI.0	Södra_Vi	NRTK	57.740637	15.799870	169.9
OSSK	SSKA.0	Storskäret	NRTK	60.376036	18.246397	41.2
OSTA	STAV.0	Stavsnäs	NRTK	59.308865	18.693262	36.7
OSTD	STDE.0	Stöde	NRTK	62.407975	16.569396	115.5
OSTF	STFO.0	Storfors	NRTK	59.532402	14.272816	170.6
OSTI	STIP.0	Stripa	NRTK	59.706398	15.096706	187.6
OSTJ	STJO.0	Stavsjö	NRTK	58.730062	16.410703	116.0
OSTL	STLI.0	Storlien	NRTK	63.301673	12.121829	684.7
OSTN	STRA.0	Strängnäs	NRTK	59.375644	17.021520	55.3
OSTO	STOC.0	Stockaryd	NRTK	57.315613	14.594701	266.2
OSTR	STRO.0	Strömstad	NRTK	58.936640	11.181333	79.1
OSTS	STSU.0	Strömsund	NRTK	63.852397	15.561214	340.8
OSTU	STOR.0	Storuman	NRTK	65.092544	17.105140	403.1
OSTY	STYR.0	Styrsö	NRTK	57.618616	11.760428	44.7
OSUM	MON_SUM.0	Sundsvall Mon	Monitorstation	62.383081	17.334132	63.4
OSUN	SUND.0	Sundsvall	SWEPOS klass A	62.232479	17.659893	32.1
OSUR	SURT.0	Surte	NRTK	57.830990	12.017255	90.2
OSVA	SVAR.0	Svartnäs	NRTK	60.913021	16.140203	336.0
OSVD	SVED.0	Svedala	NRTK	55.510047	13.235139	109.4
OSVE	SVEG.0	Sveg	SWEPOS klass A	62.017416	14.700015	491.5
OSVI	SVIK.0	Sandvik	NRTK	57.077023	16.860593	42.7
OSVL	SVAL.0	Svalöv	NRTK	55.920181	13.110948	106.4
OSVP	SVAP.0	Svappavaara	NRTK	67.649135	21.055342	382.7
OSVS	SVST.0	Svängsta	NRTK	56.261570	14.769498	104.1
OSVT	SVTJ.0	Svarttjärn	NRTK	64.512020	21.061627	116.1
OSYS	SYSS.0	Sysslebäck	NRTK	60.710313	12.885720	198.6
OTAV	TAVE.0	Tavelsjö	NRTK	64.037358	20.046157	163.8
OTEG	TEG_.0	Teg	NRTK	63.819583	20.244283	49.1
OTEN	TENH.0	Tenhult	NRTK	57.704754	14.324342	282.9
OTIV	TIVE.0	Tived	NRTK	58.780595	14.536832	176.7
OTJU	TJUR.0	Tjurholmen	NRTK	57.964671	12.112167	59.0
OTNN	TRON.0	Trönninge	NRTK	57.137620	12.276478	57.3
OTOC	TOCK.0	Töcksfors	NRTK	59.508378	11.833523	171.8
OTOK	TORE.0	Torekov	NRTK	56.412758	12.624983	47.6
...						

Table A.12: Table A.4 continued ...

stnid	stnmrk	stnm	type	latitude	longitude	height
0TOR	TORP.0	Torpsbruk	NRTK	57.033426	14.571745	224.9
0TOS	TOSS.0	Tösse	NRTK	58.973871	12.635296	106.1
0TOU	TOUP.0	Torup	NRTK	56.960249	13.074027	138.6
0TRE	TREK.0	Trekanten	NRTK	56.696565	16.120857	78.2
0TRL	TRAL.0	Träslövsläge	NRTK	57.057362	12.312840	68.7
0TRN	TRAS.0	Tranås	NRTK	58.028507	14.992058	198.6
0TRO	TROL.0	Trollhättan	NRTK	58.252280	12.280127	130.1
0TUA	TUNA.0	Tuna	NRTK	57.574814	16.109921	159.0
0TUH	TUHA.0	Tuna_Hästberg	NRTK	60.336690	15.194008	344.6
0TUN	TUNG.0	Tungelsta	NRTK	59.106567	18.043866	68.6
0TVS	TVSK.0	Tvärskog	NRTK	56.624263	16.043343	89.1
0TYJ	TYSJ.0	Tyngsjö	NRTK	60.292424	13.870202	390.8
0TYR	TYRE.0	Tyresö	NRTK	59.221951	18.205594	72.2
0TYS	TYST.0	Tystberga	NRTK	58.847566	17.233368	73.4
0ULL	ULLA.0	Ullatti	NRTK	67.013301	21.815226	253.4
0UME	UMEA.0	Umeå	SWEPOS klass A	63.578141	19.509602	54.7
0UMO	MON_UME.0	Umeå_Mon	Monitorstation	63.835092	20.269148	47.8
0UPP	UPPS.0	Uppsala	NRTK	59.865152	17.590168	58.1
0UPV	UPVY.0	Upplands Väsby	NRTK	59.522508	17.909484	49.1
0VAD	VADA.0	Värgårda	NRTK	58.032884	12.818135	155.0
0VAF	Vafa.0	Västerfärnebo	NRTK	59.944244	16.276398	113.8
0VAG	VAGN.0	Vagnhärad	NRTK	58.945625	17.496549	53.6
0VAN	VANE.0	Vänernborg	SWEPOS klass A	58.693129	12.035006	170.0
0VAR	VARB.0	Varberg	SWEPOS klass B	57.101267	12.257123	79.1
0VAX	VAXT.0	Våxtorp	NRTK	56.420102	13.115270	95.7
0VEB	VEBO.0	Vebomark	NRTK	64.401991	21.010290	78.3
0VED	VEDA.0	Vetlanda_C	NRTK	57.425800	15.086322	245.9
0VEI	VEIN.0	Veinge	NRTK	56.551571	13.073221	103.1
0VEN	VENJ.0	Venjan	NRTK	60.952648	13.908602	318.9
0VGG	VAGG.0	Vaggeryd	NRTK	57.499320	14.142995	242.4
0VIA	VIAR.0	Viared	NRTK	57.694642	12.818800	219.3
0VIB	VINB.0	Vinberget	NRTK	62.373817	17.427742	151.8
0VID	VIDS.0	Vidsele	NRTK	65.834270	20.510809	111.5
0VIK	VIKE.0	Viken	NRTK	56.154096	12.577840	53.0
0VIL	VILH.0	Vilhelmina	SWEPOS klass A	64.697851	16.559932	450.5
0VIN	VIND.0	Vindeln	NRTK	64.202231	19.714051	218.9
0VIS	VISB.0	Visby	SWEPOS klass A	57.653873	18.367319	79.4
0VIT	VITT.0	Vittangi	NRTK	67.683853	21.627367	284.6
0VMA	VMAS.0	Västra Måsklinten	SWEPOS klass A	60.394205	18.273106	28.5
0VMN	MON_VAR.0	Varberg_Mon	SWEPOS klass B	57.119725	12.285665	95.4
0VNG	VING.0	Vinga	NRTK	57.632347	11.604872	57.0
0VOL	VOLL.0	Vollsjö	NRTK	55.701825	13.782177	142.0
0VRE	VREN.0	Vrena	NRTK	58.861143	16.700795	74.3
0VRI	VRIM.0	Vuollerim	NRTK	66.431519	20.626224	143.3
0VSE	VASE.0	Väse	NRTK	59.385885	13.852957	97.2
0VSL	VISL.0	Vislanda	NRTK	56.786954	14.440731	206.7
0YST	YSTA.0	Ystad	NRTK	55.432646	13.836360	52.1
...						

Table A.13: Table A.4 continued ...

stnid	stnmrk	stnm	type	latitude	longitude	height
0YTT	YTTE.0	Ytterån	NRTK	63.318169	14.168364	340.6
1ALB	ALVS.1	Älvsbyn2	NRTK	65.673985	21.006945	76.8
1ANE	ANEB.1	Aneby	NRTK	57.834274	14.814636	264.5
1ARK	ARKO.1	Arkö	NRTK	58.483275	16.962659	38.2
1ASA	ASAK.1	Väne-Åsaka	NRTK	58.241713	12.423078	114.2
1BAG	BAGA.1	Bagaregården	NRTK	57.720923	12.018757	119.1
1BOD	BODA.1	Böda	NRTK	57.246952	17.058660	46.1
1BOL	BOLL.1	Bollebygd	NRTK	57.669572	12.570604	133.8
1BOS	BOTS.1	Botsmark	NRTK			
1BOT	BOTE.1	Boteå	NRTK	63.135296	17.716974	87.9
1GAT	GAVT.1	Gävle	SWEPOS klass B	60.666763	17.131648	56.7
1GIM	GIMO.1	Gimo	NRTK	60.172801	18.169956	47.4
1GRY	GRYT.1	Gryt	NRTK	58.186669	16.800864	54.6
1HAG	HAGF.1	Hagfors2	NRTK	60.035020	13.704400	215.1
1HEL	HELS.1	Helsingborg	NRTK	56.046044	12.710104	89.1
1HOL	HOLJ.1	Höljes	NRTK	60.899126	12.598610	276.6
1IDR	IDRE.1	Idre	NRTK	61.857748	12.713272	494.2
1JRN	JARN.1	Järna	NRTK	59.083786	17.556871	63.8
1LAT	LANT.1	Långträsk	NRTK	65.382515	20.339146	363.3
1LID	LIDE.1	Liden	NRTK	62.700919	16.802353	181.6
1LUG	LUGN.1	Lugnås	NRTK	58.642138	13.692649	97.2
1LYC	LYCK.1	Lycksele	NRTK	64.627276	18.667181	260.5
1MAL	MALM.1	Malmö	NRTK	55.601133	13.029830	83.0
1MOL	MOLL.1	Mollösund	NRTK	58.077796	11.483897	71.8
1MRF	MARI.1	Mariefred	NRTK	59.261469	17.225138	39.0
1OMO	MON_ORE.1	Örebro_Mon1	Monitorstation	59.280366	15.197840	70.9
1ONS	ONSA.1	Onsala_mast	NRTK	57.395335	11.924544	45.5
1OTT	OTT_.1	Onsala_TT1	SWEPOS klass A	57.394109	11.919032	46.1
1ROF	ROBF.1	Robertsfors	NRTK	64.191615	20.855989	86.3
1SKI	SKIN.1	Skinnskatteberg	NRTK	59.828515	15.689538	157.2
1SKU	SKUR.1	Skurup	NRTK	55.477192	13.502428	111.7
1SKV	SKOV.1	Skövde	NRTK	58.387281	13.840084	211.9
1SSJ	SSJO.1	Stora Sjöfallet	NRTK	67.488382	18.341318	425.3
1STV	STVI.1	Storvik	NRTK	60.595507	16.549690	118.4
1TRA	TRAN.1	Tranemo	NRTK	57.484239	13.351265	213.2
1ULR	ULRI.1	Ulricehamn	NRTK	57.790616	13.423420	283.9
1UMC	UMEC.1	Umeå_C	SWEPOS klass B	63.853164	20.307887	76.5
1VAS	VAST.1	Västerås	NRTK	59.641595	16.570945	74.0
1VMO	MON_VAX.1	Växjö_Mon1	Monitorstation	56.883754	14.816701	218.8
2ARH	ARHO.2	Arholma	NRTK	59.860717	19.125451	45.9
2FBG	FBER.2	Falkenberg	NRTK	56.898021	12.487012	60.0
2FRO	FROV.2	Frövi	NRTK	59.467379	15.363703	84.3
2HAR	HARA.2	Häradsbäck	NRTK	56.530672	14.460551	216.6
2HER	HERR.2	Herrljunga	NRTK	58.076183	13.018045	146.9
2HUS	HUSU.2	Husum	NRTK	63.329887	19.164781	57.9
2LJU	LJUN.2	Ljungby2	NRTK	56.835065	13.935049	204.7
2OSV	OVAL.2	Östervåla	NRTK	60.183001	17.174679	82.6
...						

Table A.14: Table A.4 continued ...

stnid	stnmrk	stnm	type	latitude	longitude	height
2OTT	OTT..2	Onsala_TT2	SWEPOS klass A	57.393746	11.918660	47.3
3OTT	OTT..3	Onsala_TT3	SWEPOS klass A	57.393738	11.921166	48.1
4GAV	GAVL.4	Gävle	SWEPOS klass B	60.666772	17.131684	56.6
4OTT	OTT..4	Onsala_TT4	SWEPOS klass A	57.393351	11.919138	48.2
5GAV	GAVL.5	Gävle5	NRTK	60.666525	17.132388	56.5
5OTT	OTT..5	Onsala_TT5	SWEPOS klass A	57.392993	11.920040	49.1
6ARJ	ARJE.6	Arjeplog-Mast	NRTK	66.318035	18.124977	491.1
6HAS	HASS.6	Hässleholm-Mast	NRTK	56.092177	13.718018	115.5
6JON	JONK.6	Jönköping-Mast	NRTK	57.745434	14.059708	261.7
6KAR	KARL.6	Karlstad-Mast	NRTK	59.444055	13.505621	115.4
6LEK	LEKS.6	Leksand-Mast	NRTK	60.722189	14.877138	479.6
6LOV	LOVO.6	Lovö-Mast	NRTK	59.337895	17.828926	80.9
6MAR	MART.6	Mårtsbo	SWEPOS klass A	60.595145	17.258530	76.1
6OSK	OSKA.6	Oskarshamn-Mast	NRTK	57.065676	15.996868	151.4
6OST	OSTE.6	Östersund-mast	NRTK	63.442766	14.857977	491.0
6OTT	OTT..6	Onsala_TT6	SWEPOS klass A	57.392762	11.919235	47.7
6OVE	OVER.6	Överkalix-Mast	NRTK	66.317829	22.773447	224.3
6SUN	SUND.6	Sundsvall-Mast	NRTK	62.232482	17.659792	33.8
6SVE	SVEG.6	Sveg-Mast	NRTK	62.017372	14.700087	492.6
6UME	UMEA.6	Umeå-Mast	NRTK	63.578139	19.509502	56.5
6VAN	VANE.6	Vänernborg-Mast	NRTK	58.693177	12.035093	170.7
6VIL	VILH.6	Vilhelmina-Mast	NRTK	64.697805	16.559913	451.7
6VIS	VISB.6	Visby-Mast	NRTK	57.653905	18.367367	80.6
7BOR	BORA.7	Borås_mast	NRTK	57.714910	12.891465	222.4
7MAR	MART.7	Mårtsbo-Mast	NRTK	60.595056	17.258447	76.4
7NOR	NORR.7	Norrköping-Mast	NRTK	58.590143	16.246375	42.0
8KIR	KIRU.8	Kiruna-Mast	NRTK	67.877546	21.060183	499.9
8MAR	MART.8	Mårtsbo-Mast2	SWEPOS klass A	60.595033	17.258658	75.4
8SKE	SKEL.8	Skellefteå-Mast	NRTK	64.879208	21.048155	82.7
TBJO	None	Björna	Trimble	63.547786	18.602194	185.1
TBLA	None	Blackstad	Trimble	57.796088	16.202901	125.8
TDAD	None	Danderyd	Trimble	59.415524	18.039993	64.0
TFAG	None	Fagerhult	Trimble	57.997835	14.122943	222.7
TFRA	None	Frändefors	Trimble	58.497394	12.273739	106.3
TGRU	None	Grums	Trimble	59.346570	13.099205	133.5
THAR	None	Härnösand	Trimble	62.639261	17.961760	74.9
THOR	None	Horred	Trimble	57.355650	12.470752	106.6
TING	None	Ingelstad	Trimble	56.751948	14.925356	198.4
TLIS	None	Lindsdal	Trimble	56.732920	16.285247	58.5
TMOR	None	Mörlunda	Trimble	57.317142	15.857197	138.8
TMOT	None	Motala	Trimble	58.536093	15.020524	133.9
TNAV	None	Naverstad	Trimble	58.772902	11.559981	121.7
TNOR	None	Norrundet	Trimble	60.931290	17.138162	42.6
TOST	None	Östra Frölunda	Trimble	57.343554	13.033069	184.2
TRAN	None	Råneå	Trimble	65.857404	22.284459	56.1
TRAT	None	Rättvik	Trimble	60.889891	15.109487	206.5
TRIM	None	Rimbo	Trimble	59.739524	18.361874	61.6
TROK	None	Roknäs	Trimble	65.342108	21.227721	44.1
TTAN	None	Tännö	Trimble	57.094203	14.046522	192.0
TTIE	None	Tierp	Trimble	60.339670	17.519620	61.9
TVAN	None	Vännäs	Trimble	63.905494	19.751624	128.5
TVIR	None	Virso	Trimble	59.876565	16.078039	120.1

LANTMÄTERIET



801 82 Gävle Phone 0771 - 63 63 63 E-mail lantmateriet@lm.se
Internet: www.lantmateriet.se